The relevance of myeloid-derived suppressor cells during *Litomosoides sigmodontis* infection

Dissertation

zur

Erlangung des Doktorgrades (Dr. rer. nat.)

der

Mathematisch-Naturwissenschaftlichen Fakultät

der

Rheinischen Friedrich-Wilhelms-Universität Bonn

vorgelegt von

Ruth Shalom Emilie Tamadaho

aus Benin

Bonn 2018

Angefertigt mit Genehmigung der Mathematisch-Naturwissenschaftlichen Fakultät der Rheinischen Friedrich-Wilhelms-Universität Bonn

1. Gutachter: Prof. Dr. med. Achim Hörauf

2. Gutachter: Prof. Dr. rer. nat. Irmgard Förster

Tag der Promotion: 27.04.2018

Erscheinungsjahr: 2018

Mit der Betreuung von Dr. rer. nat. Laura E. Layland

Summary

68 million people are infected with lymphatic filariasis (LF) in Sub-Saharan Africa, South-East Asia and South America, causing a major health problem with economic repercussions among the infected populations. This disease is caused by three species of filarial nematode parasites such as *Wuchereria bancrofti*, *Brugia malayi* and *Brugia timori.* In infected patients, only 50% become patent (release microfilariae, MF) and this is well represented in the laboratory BALB/c mice when naturally infected with *Litomosoides sigmodontis* (Ls). Infection with Ls has been shown to induce regulatory cell populations including Tregs, IL-10 producing cells and alternative activated macrophages (AAMs) and more importantly, $CD4^+$ T cells have been found to play a paramount role during the infection. In fact, previous observations have revealed the impairment of Ls filarial stages induced by these cells. Recently, Myeloid-Derived Suppressor Cells (MDSCs) have been characterized in cancer and other pathologies including bacterial, viral and parasitic infections. There are two subsets of MDSCs: monocytic MDSCs (Mo-MDSCs) and granulocytic or polymorphonuclear MDSCs (PMN-MDSCs) both identified in man and murine models. The hallmark of either MDSC populations is the suppression of T and B cell responses using various mechanisms which are mostly specific to the pathology or setting. For instance, there is evidence that MDSCs can suppress and accumulate through receptors such as the Interleukin 4 receptor-alpha (IL-4α), Tumor necrosis receptor 2 (TNFR2) and C-C motif chemokine receptor 2 (CCR2) or they use soluble factors such as nitric oxide (NO), reactive oxygen species (ROS) and transforming growth factor-beta (TGF-β), to function. MDSCs have been shown to interfere in host-pathogen interactions and various research studies consider those cells as a new therapeutic target to control resistance to diseases such as cancer. However, it remains unclear whether they play a role in helminth infections, especially if they could affect filarial development or filarial-specific responses and would be able to serve as tool to overcome filariasis. Thus, the current work verified the hypothesis of a possible role of MDSC populations during Ls infection in BALB/c mice by means of parasitological analyses, flow cytometry and a specifically designed *in vitro* cell culture assay to measure their suppressive activities on $CD4^+$ T cells. The results revealed that populations of MDSC subsets expanded in the thoracic cavity (TC), the site of infection, of infected mice whereas only very few MDSCs were found in naive mice. This expansion correlated positively with worm burden. Interestingly, although numbers of PMN-MDSCs in the TC were higher than amounts of Mo-MDSCs, the latter showed high suppressive abilities on the production of IL-13 and IFN-γ by Ls-specific $CD4^+$ T cells in a cell-contact independent manner. Further analyses demonstrated that Mo-MDSCs used distinct functional mechanisms such as nitric oxide (NO) and TGF-β to impair the production of IL-13 and IFN-γ, respectively. Surprisingly, comparisons of PCR array data on isolated MDSC populations from infected and naive mice displayed an overall shut-down of inflammatory pathways in both infection-derived MDSC subsets and therefore supporting filarial establishment. In conclusion, the involvement of MDSCs during Ls infection offered a favorable milieu for parasite development, impairing host immunity, and therefore targeting MDSCs may provide a therapeutic tool to fight filariasis.

Zusammenfassung

68 Millionen Menschen sind mit lymphatischer Filariose (LF) vorwiegend in Subsahara-Afrika, Südostasien und Südamerika infiziert. Die durch LF verursachten gesundheitlichen Probleme sind hierbei mit enormen wirtschaftlichen Einbußen für die infizierten Patienten verbunden. Verursacht wird LF durch die Filarienspezies *Wuchereria bancrofti*, *Brugia malayi* und *Brugia timori.* Im Falle einer Infektion kommt es nur bei ca. 50% zu einer patenten Infektion (freisetzen von Mikrofilarien, MF). Dies kann ebenfalls in BALB/c Mäusen beobachtet werden, wenn diese mit dem mausspezifischen Parasiten *Litomosoides sigmodontis* (Ls) infiziert werden. Frühere Studien haben gezeigt, dass Infektionen mit Ls die Produktion regulatorischer Zellpopulationen, einschließlich Tregs, IL-10 produzierender Zellen und alternativ aktivierter Makophagen (AAM), induzieren können und weiter, dass $CD4^+$ T-Zellen während dieser Infektion eine besonders wichtige Rolle spielen. Zum Beispiel wurde gezeigt, dass die obengennanten Zellen Ls Filarien schaden konnten. In letzter Zeit, wurden Myeloide Suppressorzellen (engl. Myeloid-Derived Suppressor Cells (MDSCs)) sowohl bei Krebserkrankungen als auch in anderen Krankheitsbildern wie in bakteriellen, viralen und parasitischen Infektionen beschrieben. Es gibt zwei Typen von MDSCs, welche sowohl im Menschen als auch in der Maus beschrieben sind, die monozytischen (Mo-MDSCs) und die granulozytischen bzw. polymorphkernigen MDSCs (PMN-MDSCs). Die Haupteigenschaft dieser Zellen ist es mittels krankheitsspezifischer Mechanismen die T- und B-Zellproliferation zu unterdrücken. Die Suppression dieser Zellen wird hierbei durch Rezeptoren wie IL-4Rα (Interleukin 4 receptor-alpha), TNFR2 (Tumor necrosis factor receptor 2) und CCR2 (C-C motif chemokine receptor 2) oder mittels löslicher Faktoren wie NO (nitric oxide), ROS (reactive oxygen species) und TGF-β (transforming growth factor-beta) vermittelt. Ebenfalls ist bekannt, dass diese Zellen einen negativen Einfluss auf die Interaktion zwischen Wirt und dem jeweiligen Krankheitserreger haben können. Somit könnten MDSCs als Zielstrukturen gegen Krankheiten, nämlich bei Krebserkrankungenstudien benutzt werden. Es ist jedoch unklar, welche Rolle MDSCs bei Helminthen-Infektionen haben. Ziel dieser Studie war es, eine mögliche Rolle von MDSCs während einer Ls-Infektion in BALB/c Mäusen zu untersuchen. Hierfür wurden parasitologische Parameter bestimmt und weiterführende Untersuchungen mittels Durchflusszytometrie und einem spezifisch entworfenen *In-vitro*-Zellkultur-Assay durchgeführt, um ihre suppressiven Aktivitäten auf $CD4^+$ T-Zellen zu messen. Hierbei konnte gezeigt werden, dass MDSC-Populationen den Infektionsort, die Thoraxhöhle (TC), der infizierten Mäuse besiedeln, wohingegen sehr wenig MDSCs in naiven Mäuse gefunden wurden. Diese Besiedelung positiv korrelierte mit der Wurmbelastung. Interessanterweise, obwohl die Anzahl von PMN-MDSCs in der TC höher war als Mo-MDSCs, weisen Mo-MDSCs eine erhöhte supprimierende Aktivität gegenüber IL-13 und IFN-γ durch Ls-spezifische $CD4^+$-T-Zellen in einer Zell-Kontakt-unabhängigen Weise auf. Mittels NO und TGF-β konnten Mo-MDSCs hierbei die IL-13 und IFN-γ Produktion beeinträchtigen. Überraschenderweise zeigten Vergleiche von PCR-Array-Daten von isolierten MDSC-Populationen infizierter und naiver Mäuse eine allgemeine Reduktion/Abschaltung von Genen, die entzündliche Pathways codieren, so dass man schlussfolgern kann, dass die MDSCs die Etablierung der Filarien fördern. Die in dieser Arbeit durchgeführten Untersuchen konnten zeigen, dass die Beteiligung von MDSCs während einer Filarieninfektion zu einer Beeinträchtigung der Immunreaktion im Wirt führen und somit zu einem günstigen Milieu für die Entwicklung der Parasiten beitragen. Ein therapeutischer Ansatz in diese Richtung könnte demnach ein neues Werkzeug für die Bekämpfung von Filarien bedeuten.

This thesis is based on the following original publications:

Tamadaho RSE, Hoerauf A, Layland LE. Immunomodulatory effects of myeloid-derived suppressor cells in diseases: role in cancer and infections. Immunobiology. 2018; 223 (4-5) 432-442.

Ritter M, **Tamadaho RSE**, Feid J, Vogel W, Wiszniewsky K, Perner S, Hoerauf A, Layland LE. IL-4/5 signalling plays an important role during *Litomosoides sigmodontis* infection influencing both immune-regulation and tissue pathology in the thoracic cavity. International Journal for Parasitology. 2017; 47 (14):951-960.

Tamadaho RSE et al., Role of myeloid-derived suppressor cells during *Litomosoides sigmodontis* infection (*manuscript in preparation*).

Aspects of this work were presented in poster format during conferences (see page 150).

Other publications:

Rodrigo MB, Schulz S, Krupp V, Ritter M, Wiszniewsky K, Arndts K, **Tamadaho RSE**, Endl E, Hoerauf A, Layland LE. Patency of *Litomosoides sigmodontis* infection depends on Toll-like receptor 4 whereas Toll-like receptor 2 signalling influences filarial-specific CD4 (+) T-cell responses**.** Immunology. 2016; 147(4):429-42.

Ritter M, Krupp V, Wiszniewsky K, Wiszniewsky A, Katawa G, **Tamadaho RSE**, Hoerauf A, Layland LE. Absence of IL-17A in *Litomosoides sigmodontis* infected mice influences worm development and drives elevated filarial-specific IFN-γ (*manuscript under review*).

List of abbreviations

Ab	Antibody
ACT buffer	Ammonium-chloride-Tris-buffer
AM	Alveolar macrophages
B	Loading buffer
B. malayi	*Brugia malayi*
B. timori	*Brugia timori*
BCP	Bromochloro propane
CCR2	C-C motif chemokine receptor 2
CML	Chronic myeloid leukemia
DAMPs	Danger-associated molecular proteins
DC	Dendritic cell
DEC	Diethylcarbamine citrate
dKO	Double knock-out
EC	Experion electrode cleaner
eNOS	Endothelial nitric oxide synthase
FDS	Filarial dance sign
G	Gel
G-CSF	Granulocyte-colony stimulating factor)
GMCSF	Granulocyte macrophage colony stimulating factor
GS	Gel-stain solution
h	Hour(s)
HBD3	Human beta-defensin 3
HDAC2	Histone deacetylase-2
HNSCC	Head and neck squamous cell carcinoma
Hsp	Heat shock protein
IAV	Influenza A virus
IDO	Indoleamine 2, 3 dioxygenase
IFN-γ	Interferon-gamma

IL	Interleukin
IL-4Rα	Interleukin 4 receptor-alpha
iNKT	Invariant NKT
iNOS	Inducible nitric oxide synthase
LF	Lymphatic filariasis
LPS	Lipopolysaccharide
LsAg	*Litomosoides sigmodontis* antigen
MCF	Macrophage colony factor)
MCP	Monocyte chemoattractant protein
M-CSF	Macrophage-colony stimulating factor
MDA	Mass drug administration
MDSCs	Myeloid-derived suppressor cells
medLN	mediastinal lymph node
MF	Microfilariae
MHC	Major Histocompatibility Complex
min	Minute(s)
Mo-MDSCs	Monocytic MDSCs
MSCs	Mesemchymal stem cells
NADPH	Nicotinamide adenine dinucleotide phosphate
Nb	*Nippostrongylus brasiliensis*
NO	Nitric oxide
NOX	(NADPH oxydase)
p.i.	Post-infection
PD-L1	Programmed death ligand 1
PGE2/COX2	Prostaglandin E2/cyclooxygenase-2
PMN-MDSCs	Polymorphonuclear MDSCs
PPARγ	Peroxisome proliferator-activated receptor-gamma
PSC	Pancreatic stellate cells
Rb	Retinoblastoma protein
RNS	Reactive nitrogen species
ROS	Reactive oxygen species

RT	Room temperature
SCC	Human squamous cell carcinomas
SDF	Stromal cell-derived factor
ST	Stain
STAT	Signal transducer and activator of transcription
TC	Thoracic cavity
TGF-β	Transforming growth factor-beta
TNF	Tumor Necrosis Factor
TNFR2	Tumor necrosis receptor 2
VEGF	Vascular endothelial growth factor
W. bancrofti	*Wuchereria bancrofti*
WHO	World health organization
WT	Wild type

Table of contents

1. INTRODUCTION

1.1 Human lymphatic filariasis

Parasitic worms known as filariae are microorganisms that cause filariasis which are considered tropical neglected diseases. They can inhabit the lymphatics or subcutaneous tissues (Chandy et al., 2011) and those that parasitize man lead to filarial infections including lymphatic filariasis, onchocerciasis, loiasis and mansonellosis (Pearlman et al., 2002). Lymphatic filariasis (LF) is a mosquito-borne filarial infection and is elicited by *Wuchereria bancrofti* (*W. bancrofti*), *Brugia malayi* (*B. malayi*) or *Brugia timori* (*B. timori*) with *Wuchereria bancrofti* responsible for over 90% of the cases. Together, they constitute a serious source of disability in endemic communities and are therefore considered major public health problems. Consequently, LF is one of many infectious diseases that have been targetted for global elimination (Cano et al., 2014). The upcoming sections will relate the current knowledge about LF focusing on its pathology, manifestations, available treatments to fight the disease, and manipulation of host immune responses.

1.1.1 Distribution

Previously, the world health organization estimated that 120 million people are infected with LF worldwide and endemic communities can be found in 81 countries including sub-Saharan Africa, south-east Asia and South America (WHO, 2015) (Figure 1.1). About 70% of infected cases are encountered in India, Nigeria, Bangladesh and Indonesia. However, due to the mass drug elimination programs (MDA) mentioned above, new data now suggests that only 67.88 million people are infected (Ramaiah and Ottesen, 2014). Interestingly, the disease is more prominent in males than females. For instance in India, the male/female ratio was reported to be 10/1 and is thought to be due to the fact that women in this country tend to cover most parts of their bodies and have therefore less exposure to potential bites (Chandy et al., 2011). Further findings have

suggested that hormonal factors make females more resistant to the infection, especially those aged 15-40 and evidence has been provided that children born from infected mothers have a higher predisposition for developing LF when compared to those born from non-infected mothers (Alexander and Grenfell, 1999; Lammie et al., 1991; Simonsen et al., 2014b). Before displaying symptoms of LF, it is necessary to be exposed intensively for long periods of time and therefore migrants from countries that are non-endemic are at a lower risk of developing the disease.

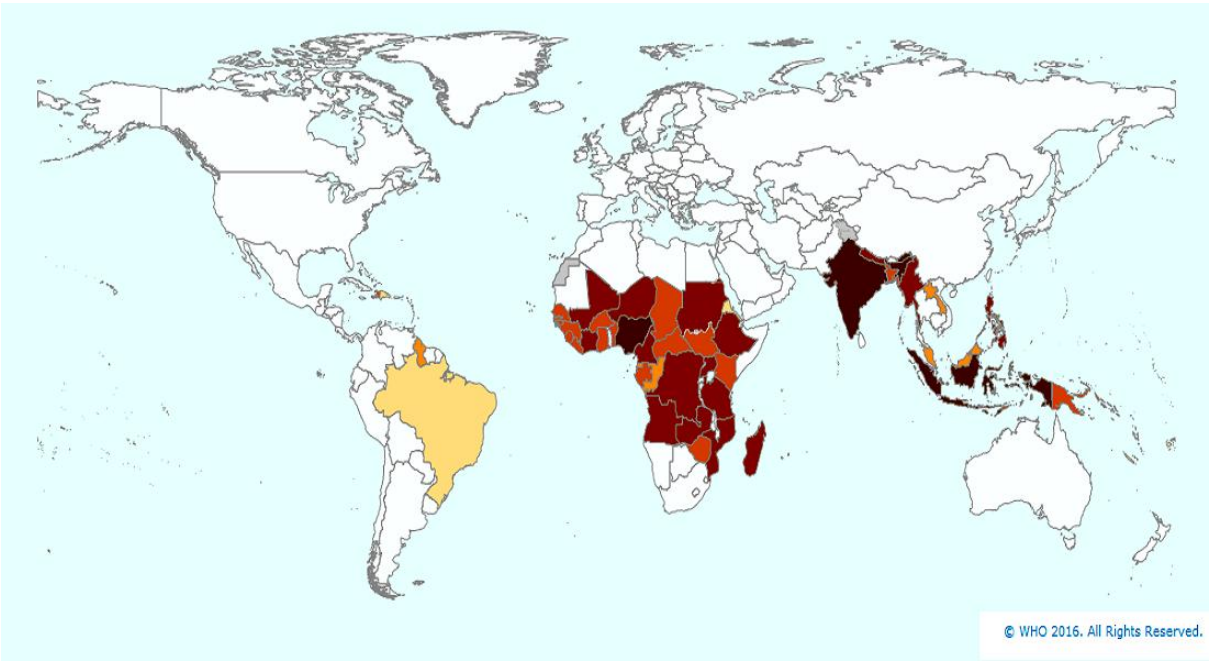

Figure 1.1: The worldwide distribution of lymphatic filariasis (Adapted from World Health Organization (WH0) 2016). The picture depicts endemic countries (in colour) that were requiring preventive chemotherapy for lymphatic filariasis in 2015. Countries in white/grey are non-endemic countries.

1.1.2 Life-cycle of lymphatic filariasis

The life-cycle of LF (see Figure 1.2) starts with the transmission of infective filariae (third-stage larvae, L3) (1500 x 20 µm) to humans by infected mosquito vectors (*Anopheles*, *Culex*, *Aedes* and *Mansonia*) during their uptake of a blood meal (Simonsen et al., 2014a; Simonsen et al., 2014b). The larvae penetrates the skin and migrates to the lymphatic vessels and after two moults develop into male (40 x 0.1 mm) or female (80-100 x 0.25 mm) adult worms; a process which

takes several weeks. Female worms that mature and become fertile release microfilariae (MF) into the peripheral blood and can do so over 20 years. In *W. bancrofti* infected individuals, MF are released in the blood after 8 months whereas in those with *B. malayi*, MF appear after only 3 months. MF measure 260 x 8 µm and are ingested by a vector during another blood meal and develop into third-stage larvae in about 10-14 days. These migrate to the mosquito's proboscis and to initiate another cycle, the developing third-stage larvae are transmitted to a new human host while taking a further blood meal. Usually, the presence and numbers of MF in peripheral blood corresponds with the biting habits of the mosquito vector which can be periodical, and thus LF is often diagnosed in night blood (Simonsen et al., 2014b; Simonsen et al., 1997).

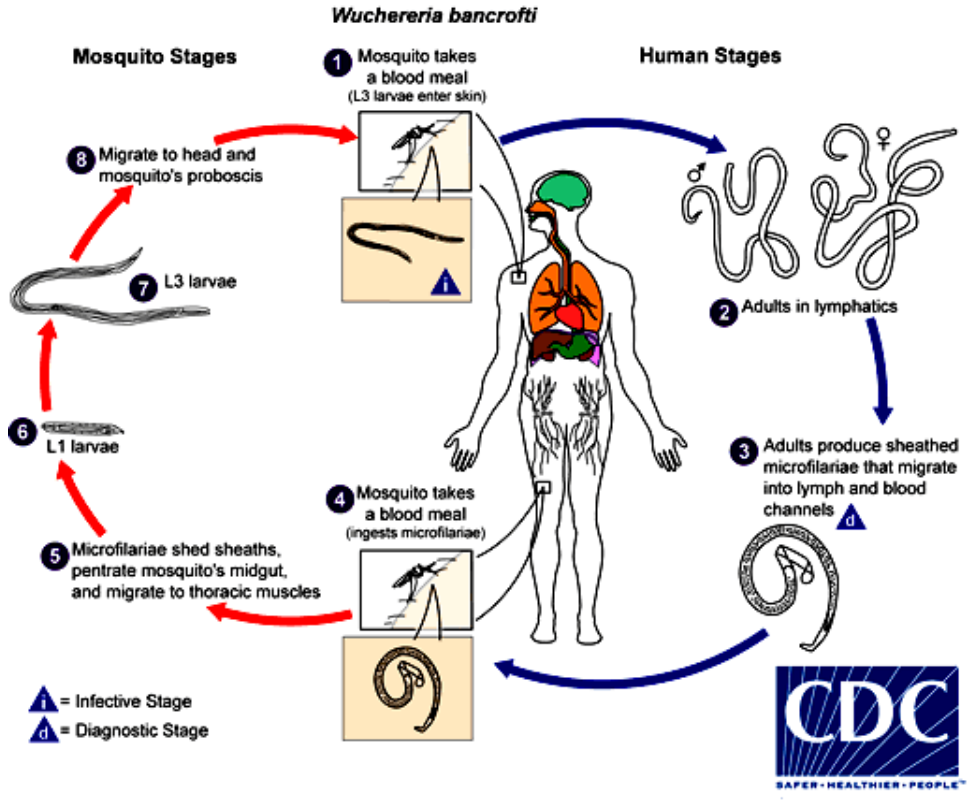

Figure 1.2: The life-cycle of the parasites causing lymphatic filariasis (*W. bancrofti*) (Adapted from Centers for Disease Control and Prevention (CDC)).

1.1.3 The role of Wolbachia

Many filarial parasites require the endosymbiotic bacteria *Wolbachia* (Figure 1.3) for fertility, reproduction, larval moulting and thus overall survival purposes (Hoerauf et al., 1999).

Investigations have suggested that *Wolbachia* originally infected the common ancestor of every filarial nematode but has been lost by some current filarial species which became *Wolbachia*-free. For instance, *Loa loa* filariae are part of this category and are the only filariae that parasitize man which are *Wolbachia*-free (Desjardins et al., 2013). *Wolbachia* are gram-negative bacteria of the order of *Rickettsiales* that are located intracellularly, within host-derived vacuoles, throughout the syncytial hypodermal cord cells of all forms of the helminth including oocystes, embryos, larval stages and adult male and female worms. Furthermore, they are transmitted vertically by adult females which is how they have become target for drug therapy (Hoerauf, 2003; Kozek, 1977; McLaren et al., 1975). Foster and colleagues have shown that while the filarial nematode *B. malayi* supplies amino acids for the growth of *Wolbachia*, the latter provides its host with essential metabolites including the coenzymes for the biosynthesis of riboflavin, flavin adenine dinucleotide. Moreover, heme constitutes another metabolite required by *B. malayi* filariae and this is provided by *Wolbachia* (Foster et al., 2005). With regards to *Wolbachia* effects on filarial models such as the rodent-specific species *Litomosoides sigmodontis* (see section 1.2), a study from Hoerauf and colleagues described a mutualistic relationship between the endobacteria and the rodent parasite. Furthermore, the authors have shown that treatment of *L. sigmodontis* with doxycycline, a tetracycline which is an antibiotic that fights gram-negative bacteria, eliminated *Wolbachia* and resulted in filarial growth retardation and infertility. In contrast, such treatment had no effect on *Acanthocheilonema viteae*, a *Wolbachia*-free filaria (Hoerauf et al., 1999). In addition, researchers have reported that *Wolbachia* have the ability to strongly induce immune responses through the activation of innate cells such as macrophages and the recruitment of neutrophils. As a result of this induction, high amounts of pro-inflammatory cytokines such as IL-6, IL-1β and TNF-α are produced which in turn lead to the activation of the vascular endothelial growth factor pathways (VEGFs), which have been

implicated in filarial pathologies (Hoerauf, 2003; Kozek, 1977; Saint Andre et al., 2002; Tamarozzi et al., 2011; Taylor et al., 2000).

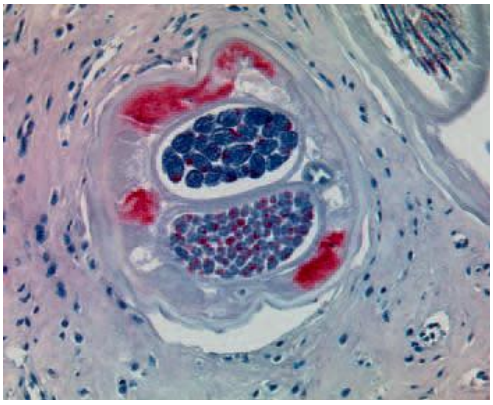

Figure 1.3: *Wolbachia*, the endosymbiont bacteria. (Adapted from (Simonsen et al., 2014b). Picture shows a cross-section of adult female *O. volvulus* worm showing *Wolbachia* endobacteria stained in red.

1.1.4 Pathology of lymphatic filariasis

1.1.4.1 Clinical aspects

In endemic areas of LF, community members show varying impacts of the infection and are classified into four groups. The first group encompasses non-infected individuals that show no evident signs of disease, even though they are constantly exposed to the infection. They are referred to as “endemic normal (EN) individuals”. The second and third groups comprise individuals that are “asymptomatic” and this state is the normal infection scenario. These people have a regulated immune response and have “worm nests” that are detectable by ultrasound (Mand et al., 2004). These groups present either patent (MF+) or latent (MF-) states and research has shown them to have unique immune profiles (Arndts et al., 2012). Individuals of the fourth group display acute or chronic manifestations of LF with few or no MF or worms (Maizels et al., 1995). Individuals with such manifestations are considered “symptomatic” and the following section describes the clinical features of this group (Simonsen et al., 2014b).

1.1.4.2 Acute and chronic manifestations

Acute phases of filariasis are marked with acute dermatolymphangioadenitis (ADLA) and acute filarial lymphangitis (AFL) (Simonsen et al., 2014b). Dilatation of lymphatic vessels, which is induced by adult worms and referred to as lymphangiectasia, diminishes the function of the lymphatics and causes ADLA and has been linked to secondary microbial infections including bacterial and fungal infections (Dreyer et al., 1999; Pfarr et al., 2009). These ADLA phases are determined by pain, tenderness, local swelling and warmth in the groin or limbs and accompanied by fever, nausea and vomiting. AFL, which is considered to be milder than ADLA episodes, is thought to be driven by filariae death which takes place spontaneously after treatment.

90% of chronic manifestations stem from acute episodes (Figure 1.4). Lymphedema, that can eventually lead to elephantiasis, is commonly encountered in the lower limb but may, in less usual cases, be found in the arms, scrotum, penis, vulva or breast (Mahalingashetti et al., 2014). The evolution of lymphedema into severe elephantiasis proceeds through 7 stages with stages 6 and 7 indicating elephantiasis (Dreyer et al., 2002). Other chronic but rare phases of LF include chyluria (presence of chyle in the urine) and tropical pulmonary eosinophilia (TPE) (Fischer et al., 2004).

Figure 1.4: Chronic manifestations of lymphatic filariasis. (Adapted from (Simonsen et al., 2014b). From the left to the right, pictures show lymphedema and elepentiasis of the rightleg and hydrocele.

1.1.5 Diagnosis of lymphatic filariasis

Ongoing LF infections are detected via the presence of MF in peripheral blood but due to the aforementioned periodic nature of MF, this serological testing has to be performed at night in areas endemic for *W. bancrofti* (Amaral et al., 1994; Anitha and Shenoy, 2001; Chandy et al., 2011). The detection of adult filarial worms by ultrasonography, the so-called filarial dance sign (FDS), can be achieved for both bancroftian and brugian filariasis and can detect latent individuals (MF-). The technique offers the benefit to locate and observe the movement of worms in infected areas; again verifying active infections. Further methods to help detect infections include the presence of filarial DNA via polymerase chain reaction (PCR) in patient blood and for vectors. With regards to the latter another less sensitive and effective method consists of dissecting mosquitoes in order to identify infective L3 larvae. In contrast, the use of PCR allows sensitivity and is comparable to the traditional detection of MF in the blood. Of high sensitivity and effectiveness is the immunochromatographic card test (ICT) for detecting circulating filarial antigen (CFA) using whole blood. Blood titres of CFA are associated with worm burden in the host and has an advantage over the examination of blood slides since the ICT method bypasses the collection of blood at night and offers the privilege of time saving (Bhumiratana et al., 1999; Cano et al., 2014; Ivoke et al., 2015; Melrose and Rahmah, 2006; Phantana et al., 1999). However ICT testing is only available for bancroftian infection although recent findings have provided evidence of cross-reactivity with *Loa loa* filariae (Wanji et al., 2015; Wanji et al., 2016). Further tests involve the detection of anti-filarial antibodies such as total IgG or filarial-specific IgG4 via ELISA but this method has no consensus among researchers and for good reason, a few patients with clinical signs were shown negative to antibody testing

(Turner et al., 1993). Finally, overt clinical manifestations (lymphodema and hydrocoele) were used as epidemiological tools to detect LF cases.

1.1.6 Treatment of lymphatic filariasis

To date a combination of albendazole with diethylcarbamine citrate (DEC) is the first choice of strategy used in mass drug administration to fight LF. In countries co-endemic with onchocerciasis, ivermectin and albendazole are given together. Using this strategy has allowed countries including Togo, Egypt, China, and Japan to eradicate the disease (Cano et al., 2014; De-Jian et al., 2013; Ramzy et al., 2006; Sodahlon et al., 2013; Tada, 2011; Webber, 1979).

DEC has been reported to be the most effective treatment for human filarial infection and has been shown to mainly kill MF in an indirect manner (Hussein et al., 2004; Simonsen et al., 2005) but it can also affect adult filarial worms. Although its mechanism of action is not yet fully understood, studies have shown that administration of 6 mg/kg body weight of DEC for 12 days leads to the decrease of acute and chronic cases of MF for at least a year (Simonsen et al., 2014b; Taylor et al., 2010). Besides its clearance of MF, the swift killing of parasites induced by DEC elicits some side effects including scrotal pain and systemic inflammation due to the release of *Wolbachia* (Taylor et al., 2010). Additionally, research has indicated severe reactions including fatal encephalopathy after DEC treatment mostly in patients with high *Loa loa* MF numbers, raising concerns in the use of the drug in areas endemic with *Loa loa* infection (Carme et al., 1991).

Findings have reported that Ivermectin has a slower rate of parasitemia clearance, leading to softer side effects compared to DEC. It is administered at doses of 100-200 µg/kg in order to reduce MF in LF (Simonsen et al., 2014b; Taylor et al., 2010). Ivermectin has also been shown to have efficacy in onchocerciasis and strongyloidiasis, ascariasis, trichuriasis, and enterobiasis. It

causes the hyperpolarisation of glutamate-sensitive channels which leads to paralysis of the MF (Geary and Moreno, 2012).

Similarly to ivermectin, albendazole is used as medicine to clear infections caused by intestinal nematode and other helminth infections such as echinococcosis and cysticercosis (Horton, 2002). It decreases MF counts within 6-12 months when given at a daily dose of 400 mg for 21 days (Simonsen et al., 2014b; Taylor et al., 2010). Albendazole is usually employed in combination with DEC or Ivermectin with success obviously due to its direct effect on gastrointestinal helminths.

As evidence has been provided that the endosymbiont *Wolbachia* is crucial for filarial growth and survival, other therapies have been developed to target *Wolbachia* for the elimination of filarial worms (Hoerauf et al., 1999). Substantiating this, studies using doxycycline a tetracycline, have demonstrated that the drug led to the decrease of adult worms in bancroftian and brugian filariasis by inducing their sterility and eventually their death (Hoerauf et al., 1999; Simonsen et al., 2014b; Taylor et al., 2010). Of note, the treatment has also been proven to ameliorate pathological manifestations of LF such as lymphedema and hydrocele and is of general use in LF endemic zones with co-endemicity with onchocerciasis. This therapy is not recommended for pregnant women and children aged under 5.

Interestingly, some findings have reported the use of herbs by ayurrveda to treat elephantiasis. These herbs include *Vitex negundo L*. (roots), *Butea monosperma L.* (roots and leaves), *Ricinus communis* L. (leaves), *Aegle marmelos Corr.* (leaves), *Canthium mannii* (Rubiaceae), *Boerhaavia diffusa L*. (whole plant) (Chandy et al., 2011; Jain and Singh, 2010; Sahare et al., 2008; Wabo Pone et al., 2010).

1.1.7 Immune responses during infection with lymphatic filariasis

Immune responses to filarial infections appear to be parasite stage-specific (Lawrence and Devaney, 2001) and need more investigations. Of note, innate defense mechanisms are initiated upon early infection with filarial nematodes, starting with the down-regulation of dendritic cells upon encounter with the L3 larvae (Hoerauf et al., 2005). Neutrophils and eosinophils are suggested to be found at the site of infection and degranulation of mast cells is induced when larvae migrate to the skin (Hise et al., 2004a; Saint Andre et al., 2002). Extracts from filariae have been demonstrated to trigger toll-like receptor (TLR) pathways and lead to the release of pro-inflammatory cytokines such as IL-6 and TNF-α. *Wolbachia* surface protein (WSP) and *Wolbachia*-derived proteins are also capable of inducing innate immune responses by inducing TLR-2, 4 and 6 (Hise et al., 2004b; Saint Andre et al., 2002; Taylor et al., 2000). Moreover, Babu *et al.* reported that stimulation of isolated NK cells of from normal individuals with MF or live L3 of *B. malayi* leads to the production of interferon gamma (IFN-γ) and TNF-α within 24 hours (Babu et al., 2007). Similarly, IFN-γ has been shown to mediate MF killing through the release of nitric oxide, in a model of *B. malayi* infection (Taylor et al., 1996). In line with this, MF+ subjects revealed decreased production of IFN-γ and IL-2 and elevated levels of IL-4 and IL-5 (Semnani and Nutman, 2004).

With regards to adaptive immunity, filarial parasites have been shown to use multiple means including the induction of regulatory cell subsets such as $Foxp3^+$ regulatory T cells (Tregs), IL-10 producing cells including Tr1 cells and also the induction of alternatively activated macrophages (AAM) (Ludwig-Portugall and Layland, 2012). PBMCs from MF+ individuals have been reported to secrete higher amounts of IL-10 when compared to those with chronic disease, indicating that MF+ subjects develop higher regulatory responses. In addition, transforming growth factor beta (TGF-β) levels were related to MF+ individuals, since neutralizing this cytokine in *in vitro* assays using PBMCs from those individuals rescued lymphocyte proliferation (King et al., 1993; Mahanty

et al., 1996; Mahanty and Nutman, 1995). The release of such immunosuppressive cytokines creates an environment that supports filarial survival. IL-10 promotes IgG4 responses whereas Th2 responses lead to elevated IgE levels as reviewed in Pfarr *et al*, and MF+ individuals presented elevated IgG4 when compared to patients with severe pathology that showed higher levels of IgE (Kurniawan et al., 1993; Pfarr et al., 2009). In addition, while the highest quantities of IgE are found in TPE patients, the lowest amounts are observed in MF+ individuals (Hussain et al., 1981) although individuals with patent infection have been reported to have higher IgE levels when compared to those with latent infection (Arndts et al., 2012). In contrast, EN individuals produce high levels of IFN-γ and IL-2 when compared to the other two groups and show elevated levels of IgG1 and IgG2 but low amounts of IgG4 when compared to MF+ subjects (Steel et al., 1996) (Steel et al., 1996).

Interestingly, patients with acute disease display strong Th1 responses (IL-6 and IL-8) and elevated Th17 responses when compared to MF+ individuals (Babu et al., 2009). However, amongst asymptomatic patients, PBMCs from MF+ individuals produced low levels of TNF-α, IL-10 and IL-5 upon filarial-specific re-stimulation when compared to those from MF- individuals (Arndts et al., 2012; Satapathy et al., 2006). Such pro-inflammatory cytokines and their receptors have been shown to be associated with the induction of VEGFs (Ristimaki et al., 1998). Furthermore, genomic hybridization can be conferred to individuals with genetic differences, such as single-nucleotide polymorphisms (SNPs), which have been associated with various disease states. Indeed, different SNPs for TGF-β have been observed in patients with severe pathology when compared to MF+ individuals (Debrah AY et al., 2011; Gershon, 2002).

1.2 The murine model of lymphatic filariasis

Litomosoides sigmodontis (*L. sigmodontis*, Ls) (described formerly as *L. carinii*) is the only rodent-specific filarial species which can complete its life-cycle (the release of MF into the periphery), in BALB/c mice, a common laboratory mouse strain. This is in contrast to C3H and C57BL/6 mouse strains which eliminate worms after a period of time (Graham et al., 2005; Hoffmann et al., 2001; Le Goff L et al., 2002; Petit et al., 1992). Its natural host is the hispid cotton rat (*Sigmodon hispidus*) and belongs to the same family as *W. bancrofti* and *Brugia species*: filariae that parasitize man. Interestingly, in humans, only 50% of asymptomatic W. *bancrofti*-infected individuals become MF+ (Turner et al., 1993). This partial development of patent infections also occurs in Ls-infected BALB/c mice (Graham et al., 2005; Hoffmann et al., 2001; Le Goff L et al., 2002; Petit et al., 1992; Rodrigo et al., 2016), indicating that Ls infection can serve as a key tool for understanding the mechanisms underlying the immunity to filarial infection in general and particularly to have deeper insights in the establishment of partial patent infections.

1.2.1 *Litomosoides* sigmodontis life-cycle in BALB/c mice

In this model of Ls infection, the mite *Ornithonyssus bacoti*, serves as an intermediate host for the helminth. During a blood meal, infective L3 larvae from the intermediate host actively migrate through the skin and into the lymphatic vessels to the thoracic cavity (TC), the site of infection in BALB/c mice after approximately 4 days. Approximately 40% of the initial L3 numbers reach the TC (Hoffmann et al., 2000). In the TC of BALB/c mice, L3 larvae moult into L4 larvae from day 8 post-infection (p.i.) and potentially develop into either female (10 cm, length) or male (1-2 cm, length) adult worms by the fourth week of infection. A proportion of adult worms then mate and MF are released by the female worms around day 49-50 p.i. The released MF (approx. 80 µm in length) which are considered the first larval stage of Ls (L1), are ingested by mites during another blood meal. Inside these mites, the L1 stage moults within 6-7 days into the L2 stage and after 10-12 days to the infectious L3 larval stage which completes the life-cycle.

Another infection takes place when the L3 stage is transmitted to the rodent upon a subsequent blood meal (Figure 1.5).

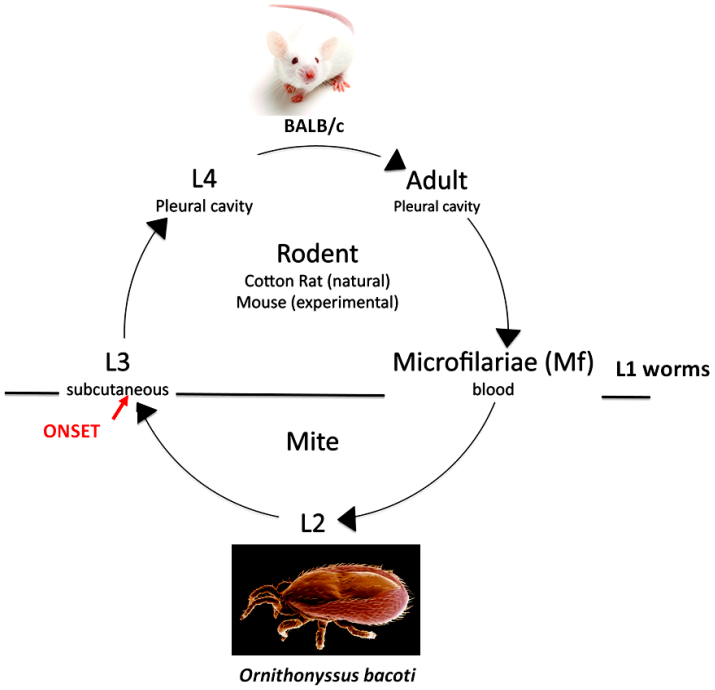

Figure 1.5: The life-cycle of *Litomosoides sigmodontis*. (Adapted from (Kochin et al., 2010). The L3 stage of the pathogen enters the vertebrate natural host (the cotton rat) by the bite of a mite where it matures via the L4 stage into adults that produce many MF (microfilariae) that are responsible for transmission. Circulating MF in the periphery are taken up by the arthropod vector and mature via the L2 stage into the L3 stage that is transmitted to the vertebrate host through the skin.

1.2.2 Immune mechanisms in the murine model of lymphatic filariasis

As mentioned above, patency during Ls infection is strain-dependent and so are the immune responses. Here, as with responses in human LF, the observed reactions are linked to the stage of the parasite, showing that diverse mechanisms are involved throughout the life-cycle. Although the detailed sequence of events involved in the early infection with Ls is not yet fully understood, a few studies have assessed the immune responses occurring at this stage. For instance, during transmission of L3 larvae into the mice, findings have shown that strong pro-inflammatory responses are induced which leads to their destruction (Bain and Babayan, 2003). Interestingly, high amounts of IL-6 and IL-5 have been measured in the lymph nodes of Ls-infected BALB/c mice 60 hours after infection (Babayan et al., 2003). In addition eosinophils accumulate early at the site of infection of Ls-infected mice in an IL-5-dependent manner; with

IL-5 being responsible for their maturation and infiltration into tissues (Al-Qaoud et al., 2000; Spencer and Weller, 2010). However, deficiencies in IFN-γ or IL-5 do not affect early parasite burden but impact worm load and MF counts at later time points (Al-Qaoud et al., 2000; Saeftel et al., 2001). Recent studies have indicated that from day 5 p.i., type 2 innate lymphoid cells (ILC2s) expand in the TC of Ls-infected mice but not in the spleen or the blood, pointing out their involvement at the early phase of the infection and their local function. Following the expansion of these cells, which peaked at the pre-patent stage, elevated amounts of IL-5 and IL-13 were produced leading to a strong Th2 response although no mention was made of the impact of ILC2s on parasite load (Boyd et al., 2015). Furthermore, investigations have reported that on day 7 p.i., elevated levels of Tregs have been found at the site of infection, which remained during the course of infection and their elimination reduced both worm burden and the MF load (Taylor et al., 2009). Expanding on other cell type with modulating effects during Ls infection at early stage, are alternatively activated macrophages (AAMs) which were found in the TC of mice a few days after infection (Jenkins and Allen, 2010) and were maintained at the site till day 60 p.i. (Ajendra et al., 2014). In the chronic phase of infection, these cells can affect $CD4^+$ T cells by making them hyporesponsive to the parasite (Taylor et al., 2006).

At later time point, $CD4^+$ T cells have been found to be essential for larval development into adults worms and Th2 responses are of great importance during Ls infection in BALB/c mice (Al-Qaoud et al., 1997). Similarly to the human filarial parasites, which induce TLRs through WSP and *Wolbachia*-derived proteins, during Ls infection, these receptors are also triggered. Indeed, a recent study has shown that while TLR4 plays a crucial role in MF release during Ls infection, $CD4^+$ T cell responses occur in a TLR2-dependent manner. Furthermore, such findings have indicated the reduced levels of Tregs in TLR2-deficient mice on days 49 and 72 p.i., which were also reduced in TLR4-deficient mice only at day 49 and both in the mediastinal lymph nodes but

no differences have been observed in the spleen (Rodrigo et al., 2016). While the paramount role of $CD4^+$ T cells in fighting Ls infection has been highlighted, a study has provided evidence that depletion of $CD8^+$ T cells did not in contrast to $CD4^+$ T cells, influence the outcome of the infection (Korten et al., 2002).

Innate cells such as neutrophils, basophils and eosinophils are highly involved in filarial infections. Interestingly, during the chronic phase of the infection, activated eosinophils release granule proteins including ribonucleases (RNASE2 and 3), Eosinophil cationic protein (ECP), Major Basic Protein (MBP) and Eosinophil Peroxidase (EPO), which together with eosinophils have been shown to favor worm growth during Ls infection using EPO and MBP BALB/c knockout mice (Specht et al., 2006). Of note, studies have demonstrated the crucial role of IL-5, which promote eosinophil maturation and infiltration, for the control of adult parasite burden in Ls-infected BALB/c mice lasting from day 60 through day 200 p.i. (Volkmann et al., 2003). However, IL-4 that is produced by basophils has been revealed to impact eosinophil count and function as well since depletion of basosphils led to reduced eosinophils and $CD4^+$ T cells proliferation during Ls infection. Such findings suggest that basophils do not reduce parasite burden themselves but strengthen anti-filarial responses (Torrero et al., 2010). Neutrophils have also been shown to function towards the killing of adult worms through the formation of inflammatory nodules around adult worms and to accumulate at the TC, in an IL-5 dependent manner. In this study, the authors have additionally reported G-CSF, a neutrophil-chemotactic cytokine, to be necessary for the formation of nodules (Al-Qaoud et al., 2000). Further findings also provided evidence that IFN-γ is responsible for neutrophil migration and used in the encapsulation process to control nodule formation and worm burden (Saeftel et al., 2001). Interestingly, Attout and colleagues have observed in Ls-infected BALB/c mice, the formation of 2 types of granulomas with distinct cellular composition. Indeed, in the pre-patent phase, eosinophils have been reported to be the

major component of granulomas whereas in the late time point, granulomas composed mainly of neutrophils, have been found around adult worms. Of interest, the authors have described in these later granulomas, the presence of only altered as well as altered though cell-free worms and the proportions of the latter decreased with time, indicating that the alteration of the filarial worms was a requirement for cell recruitment and granuloma formation (Attout et al., 2008).

When considering adaptive cells, depletion of natural killer (NK) cells indicated increased worm burden although higher numbers of the cells only accumulated a few weeks after infection (Korten et al., 2002). Few data are available on the impact of B cells in Ls infection. However, µMT mice which lack mature B cells, showed no circulating MF during Ls infection, inferring that antibodies may interfere in the stimulation of embryogenesis in adult worms (Martin C et al., 2001). Using B1 cell-deficient mice BALB.Xid, Al-Qaoud and colleagues have previously shown the influence of B1 cells during Ls infection as lack of these cells led to increase worm burden and MF load (Al-Qaoud et al., 1998). More investigations are needed to understand the role of B cell responses against Ls parasites. With regards to Tregs, Rodrigo and colleagues, when comparing immune responses in MF+ versus MF- Ls-infected BALB/c mice have recently noted no change in the numbers of Tregs in the two groups on days 35, 49 and 72 p.i., both in the spleen and the mediastinal lymph nodes (Rodrigo et al., 2016). Interestingly, a study has shown that Ls-infected NOD mice failed to develop type 1 diabetes due to a shift towards Th2 responses and Tregs expansion (Hubner et al., 2009), suggesting that Ls worms can prevent the development of type 1 diabetes in NOD mice. Similarly, previous data have shown that the promotion of Tregs, based on TGF-β induction, dampened reactions to airway inflammation (Dittrich et al., 2008).

With regards to MF load, BALB/c mice deficient for IL-4 or IL-5 have shown exponentially high numbers of MF compared to WT mice, demonstrating the importance of those cytokines in MF

control (Volkmann et al., 2003) and similar results have been noted in BALB/c mice deficient for both IL-4Rα and IL-5 (Ritter et al., 2017). Furthermore, recent findings have reported higher levels of IL-5 in cultures of splenic or mediastinal lymph node cells from MF+ Ls-infected BALB/c mice when compared to those from MF- Ls-infected BALB/c mice and as mentioned above, the control of MF production by Ls-infected mice involves a TLR4-dependent pathway since lack of TLR4 permitted all mice to develop patency (Rodrigo et al., 2016).

When considering the resistant strain C57BL/6, the migration of L3 larvae to the lymphatic system as well as the filarial recovery rates were similar in BALB/c and C57BL/6 mice although the collected adult worms from C57BL/6 mice were smaller when compared to those from BALB/c mice (Babayan et al., 2003). Interestingly, low immune responses have been observed in the early stages of infection whereas strong Th1/Th2 responses have been reported on day 30 p.i. (Babayan et al., 2003). In the skin of C3H/HeN mice on day 10 p.i., the degranulation of mast cells is induced by *Wolbachia* in a TLR2-dependent manner and vascular permeability is impaired through the chemokine C-C motif ligand 17 (CCL17) which is released by DC upon microbial challenge (Specht et al., 2011). Granzyme A has also been suggested to play a role in the early phase of the infection as increased counts of L4 were reported in C57BL/6 mice lacking granzyme A when compared to wild type (WT) mice (Hartmann et al., 2011). The formation of granulomas has also been observed in C57BL/6 mice with the exception that in these mice, additional granulomas have been described around young adults worms (Attout et al., 2008). More recent data using C57BL/6 wildtype and Rag2IL-2Rγ deficient C57BL/6 mice, have demonstrated that absence of T, B and NK cells regardless of the semi-patency of the mouse strain, was associated with dramatically high both worm burden and MF load on day 72 after Ls infection in Rag2IL-2Rγ deficient C57BL/6 mice (Layland et al., 2015). Here eosinophils were reported to be lowered in such setting.

Furthermore, IL-10$^{-/-}$ C57BL/6 mice were able to clear worm burden and MF load faster than C57BL/6 wildtype mice whereas overexpression of IL-10 lead to their higher numbers in Ls-infected mice, suggesting a crucial role for IL-10 in controlling worm burden and MF load in such settings (Specht et al., 2012; Specht et al., 2004). While comparing the effect of IL-10 originating from either T or B cells, using deficient C57BL/6 mice, Haben and colleagues have also shown that T cell-derived IL-10 successfully suppressed Th1 and Th2-mediated responses during Ls infection whereas B cell-derived IL-10 had no noticeable impact (Haben et al., 2013). Recently, Hartmann and colleagues have described that TGF-β and IL-10 participate in the suppression of IgG response to DNP-KLH vaccination (Hartmann et al., 2015). The immune responses during Ls infection are summarized in Figure 1.6.

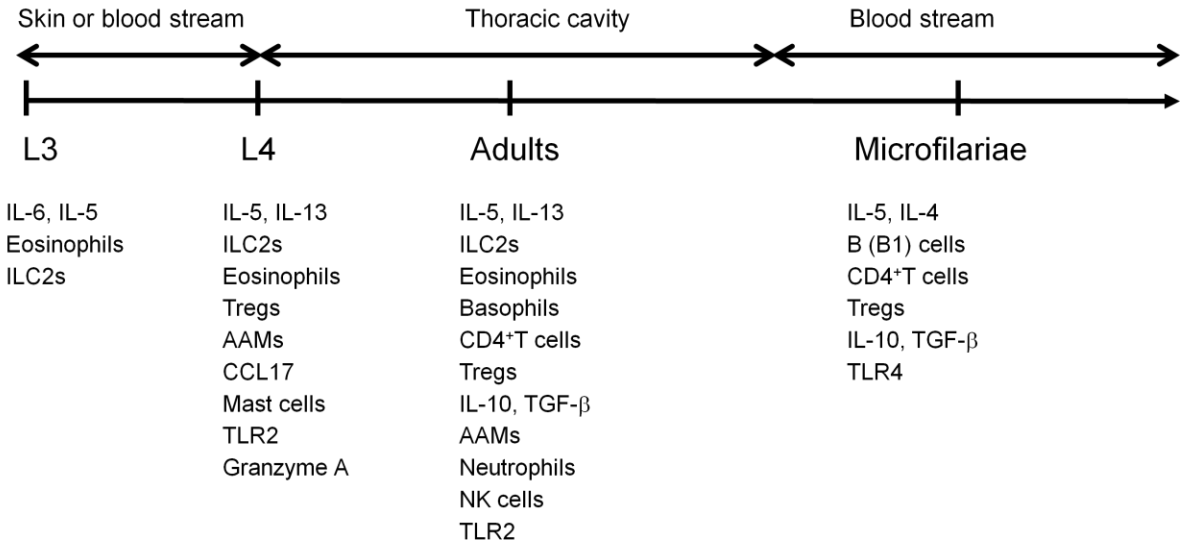

Figure 1.6: Immune responses during *L. sigmodontis* infection. The scheme pictures the developmental stages of the parasite with their location as well as the immune responses that are induced.

In view of the above, Th2 responses constitute a hallmark of Ls infection during which, depending on the filarial stage or the time point of the infection regulatory players are also evolved. Interestingly, a new population of modulatory cells, MDSCs (Myeloid-Derived Suppressor Cells), has emerged and has recently been shown to be influenced by Tregs in a murine model of disease, indicating the existence of interactions between these two cell-types

(Lee, 2016). However, to date, no studies have investigated whether these cells play a role in filarial infection. The next section will describe the current understanding about MDSCs, what they are, their function and association with other immune cells.

1.3 MDSCs as suppressors of adaptive immunity

1.3.1 Etiology and phenotype of MDSCs

Myeloid-Derived Suppressor Cells (MDSCs) comprise subsets of immune cells that have a myeloid origin and immunosuppressive abilities and may develop into dendritic cells (DC), macrophages and/or granulocytes, under steady state conditions (Gabrilovich et al., 2007). Cells with suppressive abilities were initially identified more than three decades ago and were originally termed natural suppressor cells. Pak and colleagues were the first to report that $CD34^+$ cells suppressed IL-2 production by intratumoral T cells in patients with head and neck cancer (Pak et al., 1995). This was followed by many other studies which aimed to characterize these newly discovered cells. Finally, the term MDSCs has been introduced to classify their origin and function (Haile et al., 2010; Jiang et al., 2014) and segregate them from mesenchymal stem cells (Gabrilovich et al., 2007). Since their identification and characterization has been mainly determined using cancer models, MDSCs have been observed in blood, lymph nodes, bone marrow and tumor sites. They are generally identified by the co-expression of two surface markers: CD11b and Gr-1 (Gabrilovich et al., 2007; Ostrand-Rosenberg and Sinha, 2009) and it is now well accepted that there are two distinct subsets: monocytic MDSCs (Mo-MDSCs) and granulocytic or polymorphonuclear MDSCs (PMN-MDSCs). These two subsets are becoming well defined in human and rodent model settings.

Generally, MDSCs are referred to as $CD33^+HLA\text{-}DR^-$ cells in cancer patients and different combinations of markers including CD33, CD11b, HLA-DR, Lin, CD14 and CD15 have been used to

investigate human MDSCs. For human MDSC populations, Mo-MDSCs refer to $CD14^+$ cells whereas PMN-MDSCs are $CD15^+$ cells (Gabrilovich and Nagaraj, 2009; Goedegebuure et al., 2011; Keskinov and Shurin, 2015). Diseased tissues have been proven to impact the phenotypes of the cells in human cancer. For example, MDSCs with a monocytic phenotype ($CD14^+$HLA-DR^-) are predominantly found in individuals with melanoma, as reviewed by Solito *et al.*, (Solito et al., 2014). Similarly, there was a trend for Mo-MDSC predominance in brain, ovarian, prostate cancers as well as in lung and hepatocellular carcinoma (Ho et al., 2015; Huang et al., 2013; Idorn et al., 2014; Kohanbash et al., 2013; Obermajer et al., 2011) whereas granulocytic MDSCs were dominant in head and neck cancer (Brandau et al., 2011). In contrast, haematological malignancies and gastrointestinal cancers led to the generation of both monocytic and granulocytic subsets (Brimnes et al., 2010; Gallina et al., 2006; Gorgun et al., 2013; Mundy-Bosse et al., 2011). Using whole blood from patients with colon cancer, research has also proposed S100A9 as a marker of human monocytic MDSCs (Zhao et al., 2012). In this setting, populations of $CD14^+$HLA-$DR^{-/lo}$ MDSCs, or Mo-MDSCs corresponded to $CD14^+S100A9^{hi}$ MDSCs. Previously, other authors using different conditions, have suggested CD49d and IL-4Rα as subsequent markers for Mo-MDSCs as well. Both potential markers were claimed to be associated with the suppressive activity of these cells and therefore, PMN-MDSCs were either $CD49d^-$ or IL-4Rα^{lo} and poorly limit T cell responses (Gallina et al., 2006; Haile et al., 2010; Mandruzzato et al., 2009).

In laboratory mouse strains, MDSCs were first characterized by the expression levels of CD11b and Gr1 and in addition immature markers such as CD31 (Hegde et al., 2013). Interestingly, MDSC subsets have also been shown to express F4/80, MHC I (Ostrand-Rosenberg and Sinha, 2009), CD115 (Huang et al., 2006), CD80 (Mencacci et al., 2002) and CD16 (Marshall et al., 2001) which have been linked to their suppressive actions. Rose *et al.*, further suggested the utilization of Ly6C (Mo-MDSCs) and Ly6G (PMN-MDSCs), as markers for the specific differentiation of

splenic myeloid cells (Rose et al., 2012), especially when these populations appear to have different functions in cancer infection or autoimmunity (Almand et al., 2000; Young et al., 2001; Young et al., 1997). Further investigations are needed before one can make this suggestion for all MDSCs in every setting. Currently, the primary marker is CD11b and within the $CD11b^+$ population, cells are further classified as Mo-MDSCs, $CD11b^+Ly6C^+Ly6G^-$ or PMN-MDSCs, $CD11b^+Ly6C^{int/lo}Ly6G^+$ (Ostrand-Rosenberg and Sinha, 2009; Youn et al., 2008). In terms of proportion, the frequencies of PMN-MDSCs are usually higher in tumor-bearing hosts than Mo-MDSCs although the latter have a higher reported immunosuppressive activity (Dolcetti et al., 2010; Peranzoni et al., 2010). Paradoxically, recent data provided evidence that PMN-MDSCs were better at impairing proliferation and expression of effector molecules on activated T cells when compared to Mo-MDSCs at the tumor site of several tumor models including lung carcinoma and melanoma (Raber et al., 2014). However, another group suggested the possibility that in cancer, Mo-MDSCs could change phenotypically into PMN-MDSCs with high production of ROS after stimulation with GM-CSF *in vitro* and through Histone deacetylase-2 (HDAC-2) mediated silencing of Retinoblastoma protein 1 (Rb1). Such plasticity may explain the large proportion of that subset found in cancer (Youn et al., 2013). MDSC populations in mice have been identified in the lymphatic organs of mice upon infection (Marshall et al., 2001; Mencacci et al., 2002), graft versus host reaction (Bobe et al., 1999) or even stress-associated situations such as exposure to staphylococcus endotoxin A (Cauley et al., 2000).

1.3.2 Mechanisms involved in MDSC suppressive activity

1.3.2.1 Soluble factor-dependent mechanisms

Over the years, research has supported the idea that Mo-MDSCs and PMN-MDSCs use different mechanisms to suppress immune responses. Indeed, there is strong evidence that the inhibitory pathways used by these cells lead to either the starvation of arginine via metabolism of this

amino acid by Arg-1 or the production of NO by inducible nitric oxide synthase (iNOS). Further research has shown that MDSCs inhibit T cells through the generation of ROS via nicotinamide adenine dinucleotide phosphate (NADPH) oxidase 2 (NOX2) ($gp91^{phox}$) or the formation of peroxynitrites (PNT) released from NO and superoxide anion (O_2^-). PMN-MDSCs have also been shown to curtail T cell responses by producing PNT from endothelial nitric oxide synthase (eNOS) and $gp91^{phox}$ whilst iNOS-induced NO was responsible for Mo-MDSCs suppression (Raber et al., 2014) (Figure 1.7 B). Some studies indicated that iNOS expression in MDSCs was indispensable for their suppression of $CD4^+$ T cells and amelioration of Concanavalin (Con) A-induced liver injury (Cripps et al., 2010; Fiorucci et al., 2000; Ignarro et al., 2002; Zhu et al., 2014). Increased levels of ROS, primarily produced by NOX2, in MDSCs have been reported in cells isolated from various murine models of tumor diseases and from patients with cancer too (Corzo et al., 2009). Moreover, inactivation of ROS reverses the immunosuppressive capacity of MDSCs on T cell responses. In MDSCs from tumor-bearing mice, up-regulation of NOX2 activity and ROS release lead to the enhancement of several NOX2 subunits and their stimulation causes abnormally large amounts of ROS to be released. This happens for example when MDSCs enter into contact with activated T cells (Corzo et al., 2009; Huang et al., 2013). During such interaction, ROS, together with peroxynitrite, which are both produced by MDSCs, induces the nitration of amino acids exposed at the surface of the T cells. For instance, the nitration of tyrosine on the T cell receptor or CD8 molecules changes the conformation of the TCR abolishing antigen-specific recognition (Gabrilovich and Nagaraj, 2009; Nagaraj et al., 2007). As indicated above, it has been recently suggested that the two subsets of MDSCs function via NO but use different synthetases. Further mechanisms of T cell inhibition mediated by MDSCs include the findings from the Ostrand-Rosenberg's group who demonstrated that MDSCs depleted the availability of cysteine in the microenvironment which is needed during antigen presentation (Srivastava et al., 2010). MDSCs

also facilitate the down-regulation of L-selectin (CD26L) thus reducing the migration of naive T cells to lymph nodes and therefore limiting the number of T cells responding to the presented antigen (Hanson et al., 2009). New investigations have indicated that not only iNOS, ROS or cysteine was essential for Mo-MDSC suppressive activity but TGF-β was also able to induce such function in Mo-MDSCs against B cell responses in a murine model of acquired immune deficiency syndrome (AIDS) (Rastad and Green, 2016). Furthermore using TNF humanized (hTNF KI) mice, Atretkhany and colleagues have shown that blocking TNF activity ameliorates fibroblastic sarcoma growth and led to a decreased MDSC accumulation (Atretkhany et al., 2016).

1.3.2.2 Receptor-mediated suppression pathways

Some studies have indicated that MDSCs suppress T cell activity through their IL-4Rα, a receptor that binds the Th2 related cytokines IL-4 and IL-13, which regulate IgE production by B cells. Research from Mandruzzato *et al.,* showed that both monocytic and polymorphonuclear MDSCs express IL-4Rα, but that its presence is only associated with the suppressive activity of Mo-MDSCs in melanoma and colon carcinomas (Mandruzzato et al., 2009). On the other hand, research has also provided evidence that the Th1-related cytokine IFN-γ, plays an essential role in both MDSC development and activity. Gallina and colleagues showed for example that IFN-γ producing T cells from mice with tumors induced suppressive activities in MDSCs and made them responsive to IL-13 (Gallina et al., 2006). However, Sinha *et al.,* used IFN-γ-deficient, IFN-γR-deficient and IL-4Rα-deficient BALB/c and C57BL/6 mice in various experimental models and revealed that neither receptor was involved in MDSC activity (Sinha et al., 2012). Recently, Hu and colleagues provided evidence for the requirement of the tumor necrosis factor receptor 2 (TNFR2) for MDSCs suppressive activity. This work further suggested that NF-kB and p38 signalling pathways were involved in MDSCs suppressive activities (Hu et al., 2014) (Figure 1.7 C). Substantiating these findings is the work from Polz *et al.,* which demonstrated that TNFR2

expression is required for the generation and function of Mo-MDSCs *in vitro* (Polz et al., 2014). In support, findings in both mouse and man have implicated TNFR2 in the suppressive activity of MDSCs in diverse types of cancer (Ham et al., 2015). MDSCs also express CD274 or programmed death ligand 1 (PD-L1) which when engaged with its receptor PD-1 on T cells, can inhibit proliferation and TCR-mediated activation of IL-2. Interestingly, a recent study on *Pneumocystis* infection suggested that during infection, *Pneumocystis*-derived components such as beta-glucans interact with TLR2 and trigger pro-inflammatory responses leading to the accumulation of MDSCs. These MDSCs interact with the residing alveolar macrophages (AMs) that express PD-1 through PD-1/PD-L1 ligation, causing suppressive histone modification and DNA methylation on the PU.1 gene. The down-regulation of the PU.1 gene led AMs to be defective in phagocytosis (Lei et al., 2015). Recently, Song and colleagues using a model of pancreactic cancer, have demonstrated that the pancreatic adenocarcinoma up-regulated factor (PAUF) could directly bind to MDSCs and then rendered them capable of releasing Arg-1, NO or ROS, factors involved in MDSC suppressive activity, as mentioned above (Song et al., 2016).

1.3.2.3 STAT-pathways are critical for MSDC suppression

Mo-MDSC and PMN-MDSC suppressive activities are thought to further diverge in the expression and phosphorylation of STATs. PMN-MDSC suppressive functions are thought to be mainly mediated by STAT3 phosphorylation, whilst STAT1 seems to play a main role in Mo-MDSC suppressive biology (Albeituni et al., 2013). In confirmation, the inhibitory activity of Mo-MDSCs was decreased when IFN-γ or STAT1 signalling was removed (Movahedi et al., 2008). As a result, in $STAT1^{-/-}$ mice, lung-residing PMN-MDSCs dramatically increased in response to bacterial infection (Poe et al., 2013). STAT3 is a crucial transcription factor involved in inflammation since Janus kinase 2 (Jak2)/STAT3 signalling is critical for tumor-associated MDSC development and IL-6-induced STAT3 signalling, downstream of heat shock protein 72 (HSP 72)/TLR2, was shown to

be involved in MDSC inhibitory (Chalmin et al., 2010; Condamine and Gabrilovich, 2011). In murine models, phosphorylated STAT3 has been shown to regulate the expansion of myeloid progenitors as well as MDSCs (Panni et al., 2014). MDSCs can accumulate via PGE2 and it has been shown that PGE2 and STAT3 are potential mechanisms involved in MDSC activity (Mao et al., 2013). Pancreatic stellate cells (PSCs) produce IL-6, VEGF, macrophage-colony stimulating factor (M-CSF) and chemokines such as SDF (stromal cell-derived factor)-1 and MCP (monocyte chemoattractant protein)-1. Co-cultures of PBMCs from healthy individuals with PSC–culture supernatants induced STAT3 phosphorylation which further correlated with elevated IL-6 and MDSC differentiation (Mace et al., 2013). Studies have also shown that the production of ROS occurs through STAT3 phosphorylation as well. Interestingly, MDSCs isolated from HNSCC (head and neck squamous cell carcinoma) patients secreted Arg-1 in a STAT3-dependent manner (Corzo et al., 2009).

Moreover, using CpG oligonucleotide-mediated delivery of STAT3 siRNA into $TLR9^{+}$ PMN-MDSC, Hossain *et al.*, provided evidence of the association between Arg-1 and STAT3 activities of these cells in the prostate (Hossain et al., 2015). MDSCs induced by lipopolysaccharide (LPS) in the lung secrete IL-6 and GM-CSF which respectively activate STAT3 and STAT5 and the activation of the latter promotes MDSC survival, broadening the repertoire of STAT family members that MDSCs employ (Condamine and Gabrilovich, 2011). More recently, a study described the crucial role of estrogen in MDSC accumulation. Of note, the STAT3 pathway has been activated in human and mouse bone marrow myeloid precursors by estrogen, which leads to the enhancement of JAK2 and SRC activity (Svoronos et al., 2016). Furthermore, IL-6-dependent phosphorylation of STAT3 and activation of the Notch signalling pathway induced by MDSCs, have recently been suggested as suppressive mechanisms used by the cells in breast cancer (Peng et al., 2016). The involvement of STAT3 has also been shown in the interaction of MDSCs with activated T cells.

Interestingly, upon STAT3 phosphorylation, the suppressive activity of MDSCs has been induced through ARG-1 and Indoleamine 2, 3 dioxygenase-1 (IDO) expression (Pinton et al., 2016). In conclusion, the various mechanisms by MDSCs which suppress T cell responses have not been determined using the same setting, suggesting that they do not work at the same time.

1.3.3 Accumulation/activation of MDSCs

As mentioned above, Mo-MDSCs and PMN-MDSCs can be induced by the presence of diverse factors including GM-CSF, VEGF, prostaglandin E2/cyclooxygenase-2 (PGE2/COX2), IFN-γ and may use the STAT1 or STAT3 signalling pathways (see section 1.3.2.3). Factors responsible for MDSC accumulation include growth factors, cytokines, chemokines and others molecules such as HSP 72 (Chalmin et al., 2010) or complement anaphylatoxin C5a, which facilitates MDSC infiltration into tumors and enhances their suppressive abilities through ROS and reactive nitrogen species (RNS) pathways (Markiewski et al., 2008). Cytokines such as TGF-β, IL-1, IL-6, IL-3 and GM-CSF can also induce ROS production in MDSCs (Sauer et al., 2001). GM-CSF was the first growth factor to be associated with MDSC accumulation and in individuals with head and neck cancer, those with recurring disease presented higher levels of $CD34^+$ cells secreting GM-CSF (Young et al., 1997). Studies have suggested that whereas Mo-MDSCs require GM-CSF for accumulation/generation, PMN-MDSCs are more influenced by Granulocyte-colony stimulating factor (G-CSF) (Dolcetti et al., 2010; Youn et al., 2013). VEGF levels in plasma have also been linked to the presence of MDSCs in breast, head and neck and lung cancer. These investigations showed that MDSC frequencies at the tumor site decreased when the tumor has been removed or when patients with lung cancer received anti-VEGF therapy (Young et al., 2001). Wu and colleagues also demonstrated that the anti-inflammatory molecule peroxisome proliferator-activated receptor-gamma (PPARγ) was also crucial for MDSC expansion extending the

repertoire of molecules and pathways involved in MDSC expansion to include lipid-related factors (Wu et al., 2012).

Rudolf *et al.*, reported that $CD11b^{+}CD33^{+}CD14^{+}HLA\text{-}DR^{lo}$ MDSCs were elevated in PBMCs at the onset of melanoma malignancies and interestingly, frequencies remained comparable regardless of enhanced tumor burden or the progression of the disease. Using serum from patients, they further reported that IL-8 levels also remained constant (Rudolph et al., 2014), even though several chemokines including IL-8 and cytokines (IL-10, IL-13, IL-6) have also been associated with MDSC accumulation in various cancer scenarios (Arihara et al., 2013; Gabitass et al., 2011; Rudolph et al., 2014). For instance, individuals with hepatocellular carcinoma presented increased concentrations of IL-10, IL-13 and VEGF and concentrations correlated with levels of $CD14^{+}HLA\text{-}DR^{-/lo}$ MDSCs (Arihara et al., 2013). Furthermore, Gabitass *et al.*, found that patients with pancreatic, esophageal or gastric cancer had higher IL-13 levels when compared to healthy subjects and this was also reflected in levels of Arg-1 (Gabitass et al., 2011). Th1 cytokines can also lead to the accumulation of MDSCs: IFN-γ was shown to participate in the inhibitory activity of MDSCs through NO production since neutralizing IFN-γ abrogated MDSCs-mediated suppression in $TGF\beta1^{-/-}$ mice (Cripps et al., 2010). Moreover, Tu *et al.*, also showed that high levels of IL-1β leads to the mobilization and the recruitment of MDSCs. MDSC activation by IL-1β for example was shown to be dependent on NF-κB and the activated MDSCs contributed to the development of gastric inflammation and initiation of carcinogenesis in mice (Tu et al., 2008). The PGE2/COX2 pathway, which have a key role in influencing colorectal cancer development (Greenhough et al., 2009), has also been shown to factor into Mo-MDSCs accumulation in the following manner: the exposure of monocytes to PGE2, IL-1β, IFN-γ or LPS, all inducers of COX2, leads monocytes to produce COX2 which in turn blocks the differentiation of mature $CD1a^{+}$ dendritic cells and drives MDSC development *in vitro*. Thereafter, endogenous PGE2, IDO, IL-

4Rα, NOX 2 and IL-10 were produced, all factors associated with MDSCs suppressive function (Mao et al., 2013; Obermajer et al., 2011).

Further related markers of MDSC accumulation include S100A8 heterodimeric proteins which act as danger-associated molecular proteins (DAMPs). These calcium-binding proteins are released by neutrophils, activated monocytes and tumor cells and can engage TLR4 or other TLRs which are involved in MDSC accumulation or function (Gebhardt et al., 2006). Indeed, when compared to healthy volunteers, levels of MDSCs were shown to correlate with the constitutive expression of S100A8/9 proteins in plasma samples from gastric cancer patients, and therefore, it is suggested that MDSCs require these proteins for their expansion (Wang et al., 2013). Such hypotheses have also been proposed by another research group suggesting that these proteins could be markers for MDSCs (Zhao et al., 2012). High PMN-MDSCs accumulation has also been associated with increased levels of Chemokine C-X-C motif ligand 8 (CXCL8) and advanced or late-stage tumors. Of note, this subset was reported to be cryosensitive and therefore preservation methods need much attention for studies using PMN-MDSCs (Trellakis et al., 2013).

As mentioned above, GM-CSF promotes the expansion of Mo-MDSC populations that are expressing CD11b and the C-C motif chemokine receptor 2 (CCR2) which recognises C-C motif chemokine ligand 2 (CCL2) and human β-defensin 3 (HBD3). Utilizing a toxin-mediated ablation strategy to target CCR2-expressing cells, it was shown that Mo-MDSCs regulate the entry of activated $CD8^+$ T cells into the tumor site, thereby limiting the efficacy of immunotherapy and suggesting CCR2 as a chemokine receptor involved in MDSCs accumulation (Lesokhin et al., 2012). In support of this, MDSCs found in human squamous cell carcinomas (SCC) produced NO, TGF-β and Arg-1 and inhibited E-selectin *in vitro*. Interestingly, they expressed CCR2 and since HBD3 is present in tumors, the interaction of CCR2/HBD3 could also play a role in the recruitment of MDSCs (Gehad et al., 2012).

It is generally accepted that inflammation enhances tumor growth and IL-1β has been shown to increase the accumulation of elevated levels of MDSCs (Bunt et al., 2006). On this basis, Bunt and colleagues suggested that the effect of inflammation in tumor growth occurs through MDSCs. Using tumor secreting IL-1β cells versus normal tumor cells, they found that IL-1β-induced inflammation-activated MDSCs through TLR4/CD14 pathway. The activation of this pathway in MDSCs enhances the cross-talk between MDSC and macrophages where after macrophages up-regulate IL-10 production by MDSCs and in turn MDSCs down-regulate macrophage production of IL-12 (Bunt et al., 2009) (Figure 1.7 A). It is intriguing how MDSCs suppress through TLR4/CD14 pathway when the activation of this pathway generally promotes pro-inflammatory responses. In the lung, tissue resident Arg-1-expressing MDSCs ($CD11b^{+}Ly6G^{int}Ly6C^{lo/-}F480^{+}CD80^{+}$) are induced in response to LPS or bacterial infection and can phagocytose apoptotic neutrophils during bacterial pneumonia (Ray et al., 2013). The removal of these apoptotic cells (efferocytosis) by MDSCs occurs late in infection so as to not hinder bacterial clearance by neutrophils; hence MDSC do not accumulate rapidly in this setting. Their secretion of IL-10 also dampens Th2 effector responses elicited during allergic airway inflammation (Arora et al., 2010).

1.3.4 MDSCs in diverse pathological conditions

1.3.4.1 Cancer and autoimmune diseases

As mentioned above, the majority of studies on MDSCs have focused on cancer and have reported that MDSCs have suppressive activities on $CD8^{+}$ T cells including reduced proliferation and a suppressed release of IFN-γ and IL-2 production by T cells (Brandau et al., 2011; Cui et al., 2013; Schilling et al., 2013). Indeed, Brandau *et al.,* reported that PMN-MDSCs were responsible for the suppression of $CD8^{+}$ T cell proliferation and IFN-γ production in cancer patients (Brandau et al., 2011). Similar results were also revealed by Schilling *et al.,* when studying patients with

advanced melanoma but those studies showed that both subsets of MDSCs were capable of suppressing $CD8^+$ T cell proliferation (Schilling et al., 2013). In addition, Cui *et al.,* using flow cytometry, noted the suppression of IL-2 and IFN-γ production by $CD4^+$ T cells as well as granzyme B production by $CD8^+$ T cells in ovarian cancer patients (Cui et al., 2013). In the context of sepsis, MDSC were shown to be generated by acute phase proteins and were shown to be crucial for the control of systemic inflammation and sepsis (Sander et al., 2010). In a few studies, MDSCs have also been identified in autoimmune models. For example, Kurkó *et al.,* reported the presence of PMN-MDSCs in the synovial fluid of patients with rheumatoid arthritis and in an experimental autoimmune arthritis mouse model (Egelston et al., 2012; Kurko et al., 2014). MDSCs derived from the synovial fluid dampened both DC maturation and T cell proliferation. Crook *et al.,* also showed for the first time that Mo-MDSCs inhibited T and B cell function in a collagen-induced arthritis model of autoimmune disease. Of interest, Mo-MDSCs limited autologous B cell proliferation and antibody production in an NO and PGE_2-dependent manner and required cell-cell contact (Crook et al., 2015). Another example of MDSCs identification in autoimmune diseases appeared in a study from Zhang *et al.,* which revealed that the levels of $CD11b^+CD33^+$ MDSCs were increased in PBMCs from children at the onset of asthma. These authors have further demonstrated using a murine model of airway allergic inflammation, that levels of MDSCs correlated with high amounts of IL-10 and low levels of IL-12 in bronchoalveolar fluid (Zhang et al., 2013). Interestingly, Höchst and colleagues showed that whereas a noted suppressive capacity in kidney fibrosis was restricted to $Ly6G^+$ MDSC populations, in a model of liver inflammation, $Ly6C^+$ cells were exclusively suppressive (Hochst et al., 2015). Interestingly, transmigration of monocytes via liver sinusoidal endothelial cells (LSECs) can drive MDSC differentiation and since MDSCs are thought to be activated in acute phases they potentially contribute to immunoregulation in the liver (Robinson et al., 2016).

1.3.4.2 MDSCs in parasitic and others pathologies

Although cancer pathologies have had the monopoly on MDSC research for a long time, a few studies are now emerging about the activities of MDSCs in other infectious conditions. For example, MDSCs, defined as $CD11b^+GR1^+$, have been shown to steadily increase during infections with *Echinnococcus granulosus* and in acute toxoplasmosis, these cells were shown to accumulate in the lung and had NO-dependent immunoregulatory properties (Pan et al., 2013; Voisin et al., 2004). Interestingly, Schmid *et al.,* using an experimental model of leishmaniasis, showed that *in vitro* generated-MDSCs derived from C57BL/6 mice suppressed *Leishmania major*-primed $CD4^+$ T and $CD8^+$ T cells whereas BALB/c-derived MDSCs suppressed only $CD4^+$ T cells. In these studies, the authors revealed an impaired generation of Mo-MDSCs in BALB/c mice when compared to C57BL/6 mice revealing a strain-dependent activity of MDSCs and perhaps an indication to the different susceptibility of these strains to leishmania infection (Schmid et al., 2014). Studies with *Trypanosoma cruzi (T. Cruzi)* also indicated that the genetic background plays a role in the level of infection. $\gamma\delta$ T cells in BALB/c mice for example produced IL-17 and no IFN-γ and studies have shown that IL-17-producing $\gamma\delta$ T cells modulate MDSC numbers which are considered vital for controlling the acute phase of *T. cruzi* infection (Cardillo et al., 2015). In *T. brucei brucei* infections $CD11b^+Ly6C^+$ monocytes were shown to accumulate in spleen, liver and lymph nodes and many presented an inflammatory DC phenotype (TNF/iNOS-producing DC) and this was dependent on IL-10 (Guilliams et al., 2009). Recently, higher levels of MDSC with the potential to reduce T cell population, have been observed in mice after infections with the liver-affecting *Schistosoma japonicum* (Pan et al., 2014). In nematode infections caused by *Heligmosomoides polygyrus bakeri*, isolated $CD11c^-CD11b^+Gr1^+$ cells suppressed OVA-specific $CD4^+$ T cell proliferation in an NO-dependent manner and nematode specific IL-4 responses *in*

vitro. Moreover, an adoptive transfer of these cells resulted in higher parasite burden indicating that these cells promoted chronic infection (Valanparambil et al., 2017).

With regards to bacterial infections, a study has noted the relevance of pulmonary-residing MDSCs in a murine model of tuberculosis (TB). Here, MDSCs were shown to phagocytose *Mycobacterium tuberculosis* and consequently release IL-10, IL-6 and IL-1α. In addition, higher numbers of MDSCs correlated with elevated expression levels of IL-4Rα and targeted depletion of MDSCs, using anti-Gr-1 antibodies or all-trans-retinoic acid (ATRA), ameliorated the state of the disease (Knaul et al., 2014). MDSCs have also been documented in individuals with chronic HIV infection. The authors noted that *in vitro*, PMN-MDSCs from HIV-infected individuals impaired the proliferative activity of $CD8^+$ T cells of healthy donors and of Gag/Nef-specific $CD8^+$ T cells (which are non-specific $CD8^+$ T cells for HIV peptides) from HIV-patients under highly active antiretroviral treatment. Furthermore, the levels of MDSCs in PBMCs correlated positively with viral titres and Treg numbers but inversely with the number of $CD4^+$ T (Vollbrecht et al., 2012). More recently, studies in C57BL/6 mice using LP-BM5 retroviral infection indicated that Mo-MDSCs could inhibit both B and T cell responses (Green et al., 2013; Rastad and Green, 2016). Furthermore, studies in C57BL/6 mice using influenza A virus infection demonstrated that the absence of invariant NKT (iNKT) cells induced the suppressive effect of Gr-$1^+CD11b^+CD11c^-$ MDSCs on $CD8^+$ T cell proliferation which increased viral titre and mortality. In addition, using CD40- and CD40L-deficient mice, the authors further demonstrated that the interaction of iNKT cells and MDSCs through CD40/CD40L caused MDSCs to down-regulate Arg-1 and NOS2 but released IL-12p40 allowing $CD8^+$ T cells to proliferate and control viral infection (de Santo et al., 2008) (Figure 1.7 D).Collectively, these initial studies indicate the relevance of MDSCs in varying chronic diseases and further research is needed to decipher the significance of MDSC populations in such scenarios.

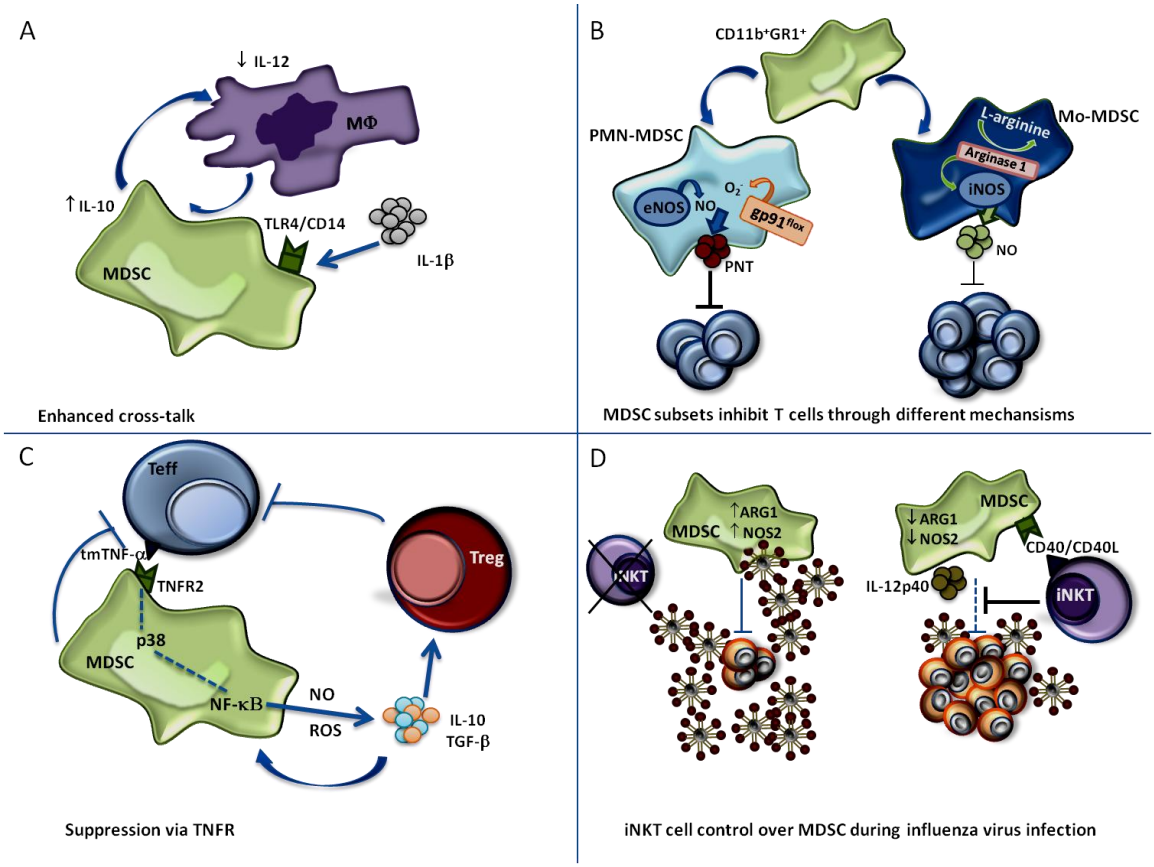

Figure 1.7: Mechanisms of MDSCs activity. The scheme shows the A) Cross-talk of MDSCs with macrophages; B) Inhibition of T cells through the release of PNT and by PMN-MDSCs and Mo-MDSCs respectively; C) Interaction of MDSCs with Tregs and suppression of T cells via TNFR and D) Interaction of MDSCs with iNKT cells during influenza virus infection.

1.4 Aims of the study

As described in section 1.3, MDSCs evolve during pathologies and intervene in host-pathogen reactions leading to immunomodulation and doing so, have either beneficial or detrimental effects on the host. Studies have addressed their role in cancer, bacterial, viral and parasitic infections but whether they play a role in filarial infections is unclear. One study has reported that MDSC levels were inversely associated with T cell population in *Schistosoma japonicum* infection (Pan et al., 2014). Interestingly, Ls serves a model for filarial infections in mice and research has shown that during Ls infection, there is an expansion of cells with modulatory/suppressive effects including Tregs, AAMs and IL-10-producing cells (see section 1.2). Of note, no investigations have so far assessed the impact of MDSCs in Ls infection or if

targeting these cells could help in the development of new therapies to fight filariasis. Thus, the current project proposed to study the relevance of MDSCs in filariasis using the Ls model, as the life-cycle of Ls is well established at the Institute of Medical Microbiology, Immunology and Parasitology (IMMIP). The thesis aimed to: a) identify MDSC populations in Ls-infected BALB/c mice as the life-cycle of the rodent filariae is fully completed in this mouse strain; b) develop an *in vitro* based co-culture assay system to determine whether MDSCs display a suppressive function on filarial-specific $CD4^+$ T cells that arise during infection; c) decipher the mechanism(s) underlying MDSC activity in the disease. This includes the establishment of gene profiles of Mo-MDSCs and PMN-MDSCs.

2. MATERIALS AND METHODS

2.1 Materials

2.1.1 Ethics statement

Wildtype (WT) and IL-4Rα/IL-5$^{-/-}$ BALB/c mice were kept under SPF conditions at the Institute of Medical Microbiology, Immunology and Parasitology (IMMIP), University Clinic Bonn, Germany and were bred in accordance with German animal protection laws and the EU guidelines 2010/63/E4. Furthermore, all the mice experiments were approved by and conducted in accordance with guidelines of the appropriate committee (Landesamt für Natur, Umwelt und Verbraucherschutz, NRW, Germany).

2.1.2 Mice

IL-4Rα/IL-5$^{-/-}$ BALB/c mice were kindly provided by Prof. Dr. Klaus Matthaei, Australia National University College of Medicine, Biology and Environment, Canberra, Australia. WT BALB/c mice obtained from Janvier Labs (Le Genest Saint Isle, France).

2.1.3 Plastic and glassware

All plastic and glassware equipment were purchased at Eppendorf (Hamburg, Germany), Becton Dickinson (Heidelberg, Germany), Nunc (Roskilde, Denmark) or Greiner (Frickenhausen, Germany) (see details in appendix).

2.1.4 Antibodies and microbeads

Name	Conjugate	Producer	Method
Alexa fluor 488 anti-mouse/human CD11b (clone M1/70)	Alexa Fluor 488	BioLegend	FACS

Alexa fluor 647 anti-mouse CD11c (clone N418)	AF647	BioLegend	FACS
Anti MHC Class II Micro Beads		Miltenyi	MACS
anti-mIL-10 purified Rat monoclonal IgG1 (clone JES052A5)	-	RD	*in vitro* blocking
anti-mIL-6 purified Rat monoclonal IgG1 (clone MP520F3)	-	RD	*in vitro* blocking
anti-mouse CD16/32 purified (clone 93)		Thermo Fisher Scientific	*in vitro* stimuli
anti-mouse CD25 PE (clone PC61.5)	PE	Thermo Fisher Scientific	FACS
anti-mouse CD25 PE-Cy7 (clone PC61.5)	PE-Cy7	Thermo Fisher Scientific	FACS
anti-mouse CD28 purified (Clone 37.51)	-	Thermo Fisher Scientific	*in vitro* stimuli
anti-mouse CD3 purified (clone 17A2)	-	Thermo Fisher Scientific	*in vitro* stimuli
anti-mouse CD4 APC (clone RM4-5)	APC		FACS
anti-mouse CD4 FITC (clone RM4-5)	FITC	Thermo Fisher Scientific	FACS
anti-mouse CD4 PE (clone GK1.5)	PE	Thermo Fisher Scientific	
anti-mouse IFN gamma APC (clone XMG1.2)	APC	Thermo Fisher Scientific	FACS

anti-mouse IL-13 FITC (clone eBio13A)	FITC	Thermo Fisher Scientific	FACS
anti-mouse/rat Foxp3 PE (clone FJK-16s)	PE	Thermo Fisher Scientific	FACS
anti-mTNF-a/TNFSF1A purified Rat monoclonal IgG1 (clone MP6-XT22)	-	RD	*in vitro* blocking
APC/Cy7 anti-mouse Ly-6C (clone HK1.4)	APC-Cy7	BioLegend	FACS
aTGF Iso MOPC-21		BioXcell	*in vitro* blocking
aTGFb 1D11.16.8		BioXcell	*in vitro* blocking
Biotin Rat Anti Mouse IL-10		BD	ELISA
Biotin Rat Anti Mouse IL-5		BD	ELISA
IgG1 Isotype control purified Rat monoclonal IgG1 (clone 43414)		RD	*in vitro* blocking
IgG2B Isotype control purified Rat monoclonal IgG2B (clone 141945)		RD	*in vitro* blocking
MC-21 (anti-mCCR2	-	Kindly provided by Prof. Mack	*in vitro* blocking
Monomethyl-L-arginine, monoacetate salt (L-NMMA)	-	abcam Biochemicals	*in vitro* stimuli
Mouse IFN-γ DuoSet ELISA		RD	ELISA
Mouse IL-10 DuoSet ELISA		RD	ELISA
Mouse IL-13 DuoSet ELISA		RD	ELISA

Mouse IL-17A (homodimer) ELISA Ready-SET-Go		RD	
Mouse IL-6 DuoSet ELISA		RD	ELISA
Mouse TNF DuoSet elisa		RD	ELISA
near-IR fluorescent reactive dye (liva/dead APC Cy7)	APC-Cy7	Life technologies	FACS
PE anti-mouse CD3e (clone 145-2C11)	PE	BioLegend	FACS
PE anti-mouse Ly-6G (clone 1A8)	PE		FACS
PerCP/Cy5.5 anti-mouse CD45 (clone 30-F11)	PerCP-Cy5.5	BioLegend	FACS
PerCP/Cy5.5 anti-mouse Ly-6C (clone HK1.4)	PerCP-Cy5.5	BioLegend	FACS
Recombinant Mouse IL-10		BD	ELISA
Recombinant Mouse IL-5		BD	ELISA

2.2 Methods

2.2.1 Parasitology assessments

2.2.1.1 *Litomosoides sigmodontis* infection

BALB/c mice were infected with *Litomosoides sigmodontis* (Ls) parasite with *Ornithonyssus bacoti* mites serving as intermediate vectors. For the life cycle of the parasite to be completed, Ls was maintained by passage in cotton rats (*Sigmodon hispidus*). Mites were kept in animal bedding at 28°C and 80 % humidity in the dark and fed with murine neonates at least twice a week. Passage of MF (L1) was performed by an overnight blood meal on microfilaraemic (≥ 1,000 MF / µl peripheral blood) cotton rats as final host. The mites subsequently take up MF (L1) during their blood meal and can then be used for infection using the bedding. Bedding was collected in an Erlenmeyer-flask and closed with polyamide gauze and placed at 28°C and 80 %

humidity in the dark, for twelve days allowing development of MF (L1) into infective L3. Prior to infection, mites were checked for L3 content under the binocular. BALB/c mice were naturally infected overnight with the infective L3 containing bedding twelve days after MF passage. To ensure comparability of infection load, mice were always exposed to the same population of mites. The following day, the bedding was removed and mice stayed without bedding overnight. Then, clean bedding was provided every day for five successive days. Finally seven days after infection, mice were transferred to suitable room until required for experiments.

2.2.1.2 Murine autopsy and pleural lavage

In order to collect organs for cell preparation, mice were euthanized using overdose of Isoflurane (>5 Vol.%) (1-cloro-2, 2, 2-trifluoroethyldifluoro-methylether; Forene, Abbolt, Wiesbaden). Thereafter, mice were disinfected with 70 % ethanol and fixed on a Styrofoam board dorsally. Using sterile surgical instruments, the spleen was taken out by opening the lower right side of the mouse without damaging either the pleural cavity or diaphragm. The spleen was transferred in 24 well plate which contained 1 ml sterile PBS (Life Technologies Corporation, Grand Island, NY, USA) per well and stored on ice. Then the abdomen was opened and the liver carefully separated from the diaphragm. A little hole was made into the upper part of the diaphragm and the thoracic cavity (TC) was washed first with 500 µl and further with 10 ml of cold PBS (Life Technologies Corporation, Grand Island, NY, USA) using a Pasteur pipette. When required, the supernatant of this first 500 µl of TC fluid would serve for cytokine measurements. The pellet was added to the 10 ml TC fluid to entirely collect the TC cells. In case of the autopsy of an infected mouse, the TC fluid was filtered using a gauze containing filter in order to collect the worms. Afterwards, the whole thorax was opened by cutting along the sternum and the

draining lymph nodes were taken out and transferred in 96 well plate containing 2-3 drops of sterile PBS (Life Technologies Corporation, Grand Island, NY, USA).

2.2.1.3 Determination of worm burden, gender, length and developmental stage

To assess worm burden, the thoracic cavity of infected mice was washed with PBS (Life Technologies Corporation, Grand Island, NY, USA). The thoracic wash was filtered using sterile 41µm gaze filter which retained the worms and the solution was collected in a sterile 15ml Falcon tubes (Becton Dickinson Labware, Franklin Lakes, NJ. USA). Worms are then placed in a small Petri dish (VWR, Langenfeld, Germany) and counted immediately or stored at 4°C until counting. For further analysis, worms were measured (length), distinguished between males and females and the stage was determined using a microscope (Leica Microsystems GmbH, Wetzlar, Germany), if necessary. Also, developmental stage was defined microscopically by analysis of the anterior buccal capsule and designation of male spiculae and female vulva (see Figure 2.1).

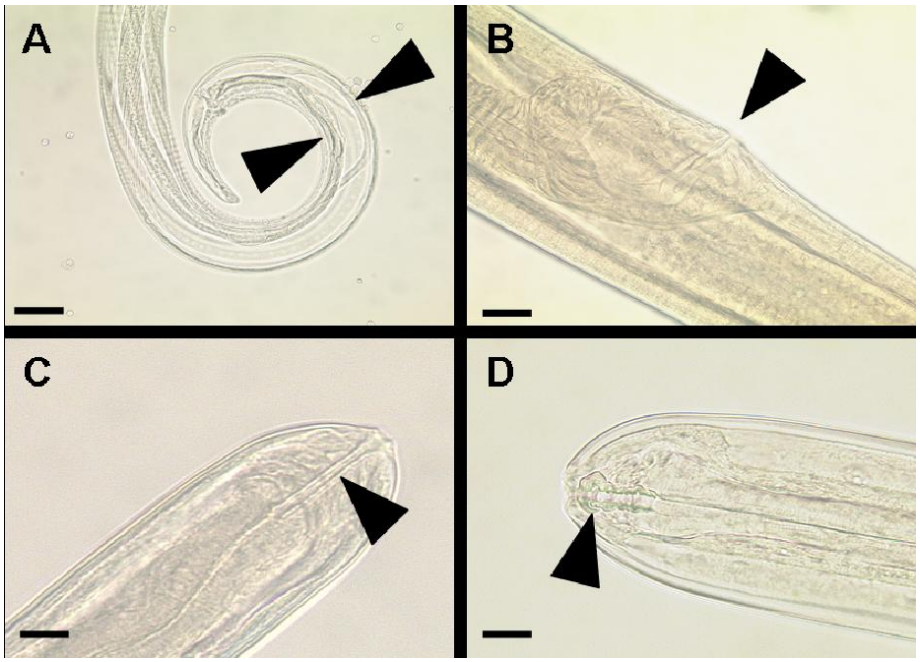

Figure 2.1: Anatomical characteristics to determine *L. sigmodontis* stages and gender. (A) Male genital structure with spiculae (arrows). (B) Female genital structure with vulva (arrow). (C) L4 stage: anterior end with buccal capsule (arrow). (D) Adult stage: anterior end with buccal capsule (arrow). Light microscope pictures, 40-fold magnification, micron bars 50 µm.

2.2.1.4 Determination of MF load

MF load was determined using Hinkelmann solution (see appendix). 50 µl of blood from individual infected mouse were placed in 300 µl Hinkelmann solution. After incubation at RT during 20-30 min, the suspension was centrifuged (Multifuge 4KR, Heraeus Holding GmbH, Hanau, Germany) at 1800 rpm, 5 min and the SN was discarded. MF were counted in the pellet, using a microscope (Leica Microsystems GmbH, Wetzlar, Germany).

2.2.2 Preparation of Litomosoides sigmodontis *antigen (LsAg)*

Litomosoides sigmodontis antigen (LsAg) was prepared on ice under sterile conditions using worms which were isolated from the TC of infected cotton rats (*Sigmodon hispidus*). Thus, Ls worms were isolated (see section 2.2.1.2) and crushed/disrupted using glass homogenizer (VWR, Langenfeld, Germany). The resulting solution was centrifuged (Multifuge 4KR, Heraeus Holding GmbH, Hanau, Germany) at 300 g for 10 min at 4°C. Protein concentrations of the extract were determined using Bradford protein assay and quantified at 590 nm using a plate reader SpectraMax 340 Pc (Molecular Devices). Thereafter, LsAg was plated on MAcconckey and blood aggar to test contamination and an endotoxin assay was performed. Aliquots of sterile and contamination-free LsAg were frozen at -80°C until when needed.

2.2.3 Cell preparation

For *in-vitro* analysis, DC, spleen and mesenteric lymph node cells (mLN) as well as TC cells were prepared as detailed in sections 2.2.3.1-2 and 2.2.1.2. In general, mice experiments during which cells were prepared, were performed as depicted in Figure 2.2 using Ls-infected mice.

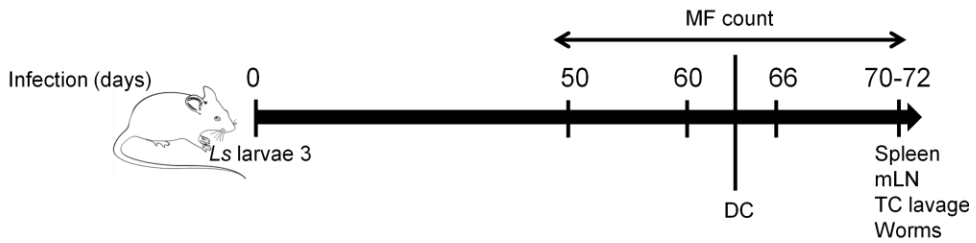

Figure 2.2: Scheme of data assessment protocol. BALB/c mice were infected for 70-72 days with Ls larvae 3. Thereafter, on the day of analysis (day 70-72), cells from the spleen, mesenteric lymph node cells (mLN), thoracic cavity (TC, site of infection) were prepared and analysed and worms were collected. 7 days prior to analysis, dendritic cells (DC) were prepared. MF count was assessed on days 50, 60, 66 and 70-72 p.i.

2.2.3.1 Preparation of spleen and mesenteric lymph node cells (mLN)

To obtain single spleen cells, spleen was crushed through a sieve in a petri dish with sterile PBS (Life Technologies Corporation, Grand Island, NY, USA). Cell preparations were depleted of erythrocytes with ammonium-chloride-Tris-buffer (ACT buffer) and resuspended in appropriate media and counted as described in section 2.2.4. The same procedure was used for mesenteric lymph nodes (mLN) except that no depletion of erythrocytes was usually needed.

2.2.1.2 Preparation of bone marrow derived dendritic cells (BMDCs)

Bone marrow was obtained by rinsing the hind legs of WT BALB/c mice with PBS solution (Life Technologies Corporation, Grand Island, NY, USA). Cell preparations were depleted of erythrocytes with ammonium-chloride-Tris-buffer (ACT buffer) and counted as described in section 2.2.4. Then $1x10^7$ cells were differentiated on Petri dish over seven days in 10 ml of IMDM medium supplemented with 10% FCS, 1% Pen/Strep, 1% L-Glutamine, 1% non-essential AA, 1% Sodium-pyruvate, 1% Sodium-bicarbonate (all from Thermo Fisher Scientific) and 20 ng/ml GMCSF (Peprotech, USA) at 37 °C. On day 3, cells were fed: 10 ml of supplemented IMDM medium and 20 ng/ml GMCSF were added and on day 6, cells were refreshed: cells were washed in PBS (Life Technologies Corporation, Grand Island, NY, USA) and thereafter, 10 ml of supplemented IMDM medium and 20 ng/ml GMCSF were added.

2.2.4 Cell viability and counting

The count of living cells was determined using the trypan blue (Sigma-Aldrich, Munich, Germany). In brief, cells were 1/10 diluted in 0.4% trypan blue (Sigma-Aldrich GmbH, Munich, Germany) solution. Thereafter, 10 µl of cell suspension were transferred to a cell counting Neubauer chamber or hemocytometer (LO Laboroptik GmbH, Bad Homburg, Germany) and living cells (non-coloured) were counted. The cell number per ml was ascertained using the formula: number of cell counted x 10 (dilution) x 10^4 (factor).

2.2.5 Flow cytometry

2.2.5.1 Surface marker staining

All reagents were obtained from Biolegend (Fell, Germany). To ascertain the frequency of MDSC subsets in Ls-infected BALB/c mice, cells collected from the thoracic cavity were resuspended in 50 µl FACS buffer (see appendix) and blocked with 0.1 µl anti-CD16/32 (Thermo Fisher Scientific, Inc., Waltham, MA, USA) and incubated at 4°C for 15 min. Thereafter, cells were washed with FACS buffer (see appendix): cells were centrifuged at 1200 rpm at 4°C and the supernatant was discarded and stained with 0.1 µl surface marker Abs (CD11b-AF488, CD45-PerCP-Cy5.5, Ly6C-APC-Cy7 and Ly6G-PE) incubated at 4°C for 20 min. Afterwards, cells were washed as previously described with FACS buffer (see appendix), resuspended and acquired on a FACS Canto (BD, Heidelberg, Germany).

2.2.5.2 Intracellular staining (ICS)

For the intracellular staining of IL-13 and IFN-γ on T cells, cells were stimulated or not with PMA (plus inhibitor) (Thermo Fisher Scientific, Inc., Waltham, MA, USA) or LsAg in 200µl RPMI medium supplemented with 10% FCS, 1% Pen/Strep, 1% L-Glutamine and 500 µl Gentamycin for

4h. Then washed with FACS buffer (see appendix) and permeabilized with 100 µl fixation/permeabilization buffer (see appendix) at RT for 30 min. Then cells were washed as described in section 2.2.5.1 using permeabilization buffer (see appendix) and resuspended in 50 µl master mix containing the antibodies for intracellular and surface marker staining (CD4-PE, CD25-PE Cy7, IFN-γ-APC and IL-13-FITC) at 4°C for 30 min. Then, cells were washed with permeabilization buffer (see appendix) and resuspended in 200 µl FACS buffer and acquired on a FACS Canto (BD, Heidelberg, Germany).

2.2.5.3 Sorting of cell populations

For the sorting of $CD4^+$ T cells and $CD4^+CD25^{hi}$ Tregs, spleen and mLN cells were stained with CD4-APC and CD25-PE (Thermo Fisher Scientific, Inc., Waltham, MA, USA) as described above. Prior to the sorting, antigen presenting cells (APCs) were depleted from spleen plus mLN using MHC class II beads (see section 2.2.5.4) and the negative suspension was used for sorting. In addition, cells collected from the TC were stained with CD11b-AF488, Ly6C-PerCP-Cy5.5 and Ly6G-PE for the sorting of MDSC subsets. Cells were sorted using BD FACS Aria III Cell Sorter (BD Biosciences, Heidelberg, Germany), in the Flow Cytometry Core Facility (FCCF), Bonn.

2.2.5.4 Depletion of MHC class II^+ cells

MHC class II^+ cells (APC) were depleted from the spleen and mLN cells using the anti-MHC class II microbeads from Miltenyi (Miltenyi Biotech GmbH, Bergisch Gladbach, Germany) according to the manufacturer's protocol. In brief, 1 x 10^7 PBMCs were resuspended in 90 µl of autoMACS running buffer (Miltenyi, Bergisch Gladbach, Germany). Afterwards, 10 µl of anti-MHC class II microbeads were added to the cells, mixed and incubated for 15 minutes inside the refrigerator (2-8°C). Cells were washed with 2 ml of running buffer and centrifuged for 10 minutes at 400 x g

(4°C). Supernatants were discarded and labelled cells were resuspended in 500 µl of running buffer. Cells were separated using a suitable MACS separator (Miltenyi Biotech, Bergisch Gladbach, Germany). The suspension depleted from MHC class II^+ cells (negative suspension) were checked for their purity by flow cytometry. Purity of isolated MHC class II^+ -depleted cells was routinely >95%.

2.2.6 In vitro *co-culture assays*

In order to assess the ability of filarial-induced MDSCs to suppress filarial-specific $CD4^+$ T cells, a co-culture assay was performed as shown in Figure 2.3. In brief, spleen and mLN cells and TC fluid from infected BALB/c mice were isolated and $CD4^+$ T cells and MDSCs were sorted according to the descriptions above (section 2.2.5). $1x10^5$ $CD4^+$ T cells were then co-cultured with $5x10^4$ GM-CSF-derived DC (section 2.2.3.2) in the presence or absence of $1x10^5$ $Ly6C^+$ or $Ly6G^+$ MDSCs and stimulated with 50 µg/ml LsAg. Upon 72h incubation at 37°C, supernatants were collected and analysed for cytokine levels using ELISA technique (see section 2.2.7). For neutralization/inhibition assays, neutralizing antibodies or inhibitors were added at least 30 min before Ls stimulation. The neutralizing antibodies included anti-CCR2, anti-IL-10, anti-IL-6, anti-TGF-β and anti-TNF-α and their isotype controls and L-NMMA served as inhibitor of NOS. Following titration assays, it was decided to use L-NMMA at a concentration of 5 µM/well and supernatants were screening after 72 hours because the highest amount of nitric oxide was produced at that time by Ls-infected $CD4^+$ T cells upon LsAg re-stimulation (see Figure 2.4 A and B). Anti-IL-6 and TNF-α were used at a concentration of 10 and 0.5 µg/mL, respectively (see Figure 2.4 C and D). Prof.Dr. Matthias Mack (University of Regensburg) and Dr. Marc Hübner have provided the anti-mCCR2 and anti-TGF-β antibodies, respectively and the concentration of these antibodies were decided upon following discussion with their providers: anti-mCCR2 (20

µg/mL) and anti-TGF-β (10 µg/mL). In transwell experiments, culture conditions remained the same except that MDSC subsets were cultured in an insert (0.4 µM pore size; Corning), permeable to soluble factors but not allowing physical cell-cell contact.

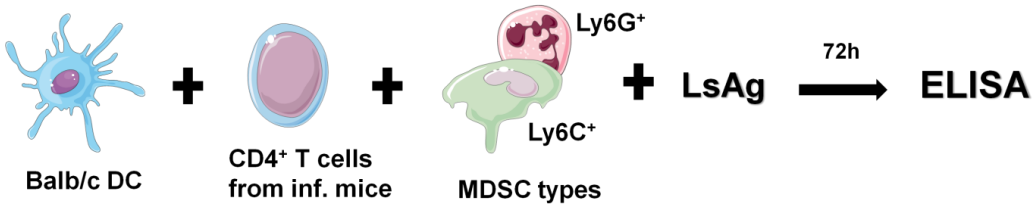

Figure 2.3: Experimental set-up for co-culture assay. In a sterile U-bottom 96 well plate, $CD4^+$ splenic T cells ($1x10^5$) were cultured with GM-CSF-derived DC ($5x10^4$) and LsAg (50 µg/ml) in the presence or absence of $Ly6C^+$ or $Ly6G^+$ MDSCs ($1x10^5$) for 72h and then screening supernatants for cytokines by ELISA.

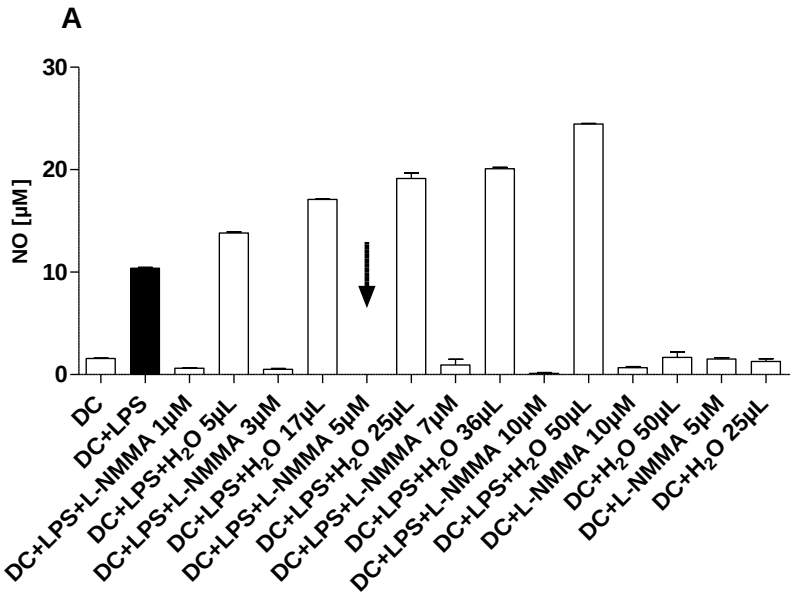
A
NO [µM]
30
20
10
0
DC
DC+LPS
DC+LPS+L-NMMA 1µM
DC+LPS+H2O 5µL
DC+LPS+L-NMMA 3µM
DC+LPS+H2O 17µL
DC+LPS+L-NMMA 5µM
DC+LPS+H2O 25µL
DC+LPS+L-NMMA 7µM
DC+LPS+H2O 36µL
DC+LPS+L-NMMA 10µM
DC+LPS+H2O 50µL
DC+L-NMMA 10µM
DC+H2O 50µL
DC+L-NMMA 5µM
DC+H2O 25µL

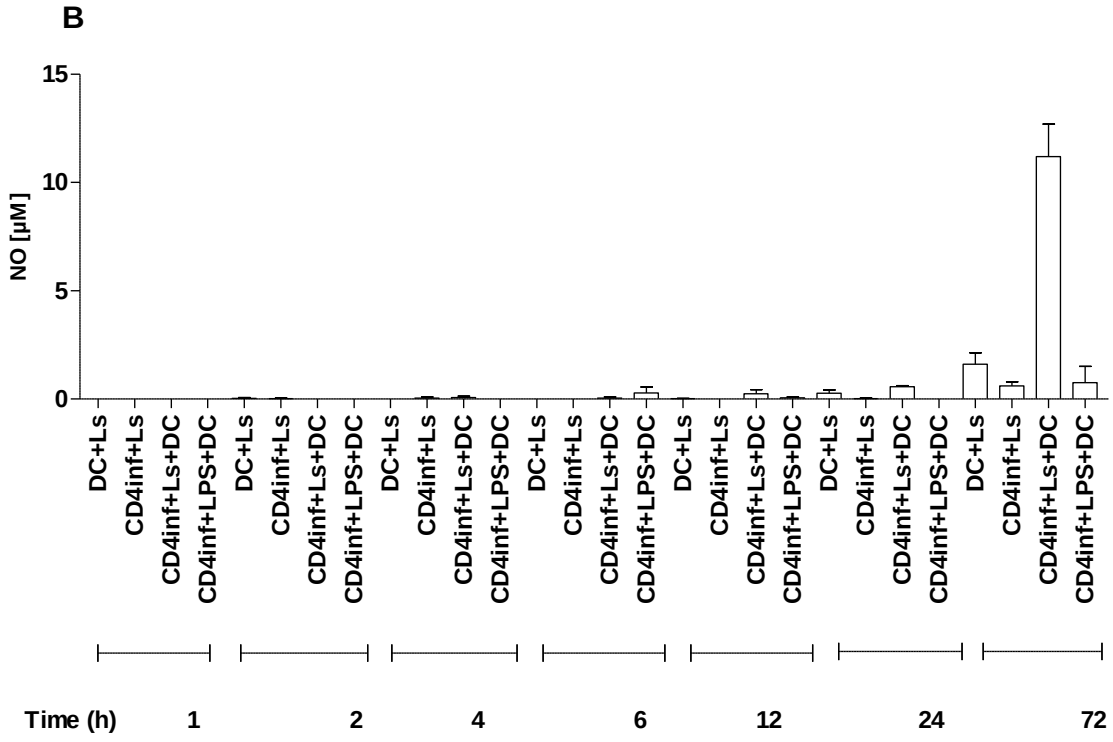
B
NO [µM]
15
10
5
0
DC+Ls
CD4inf+Ls
CD4inf+Ls+DC
CD4inf+LPS+DC
Time (h)
1
2
4
6
12
24
72

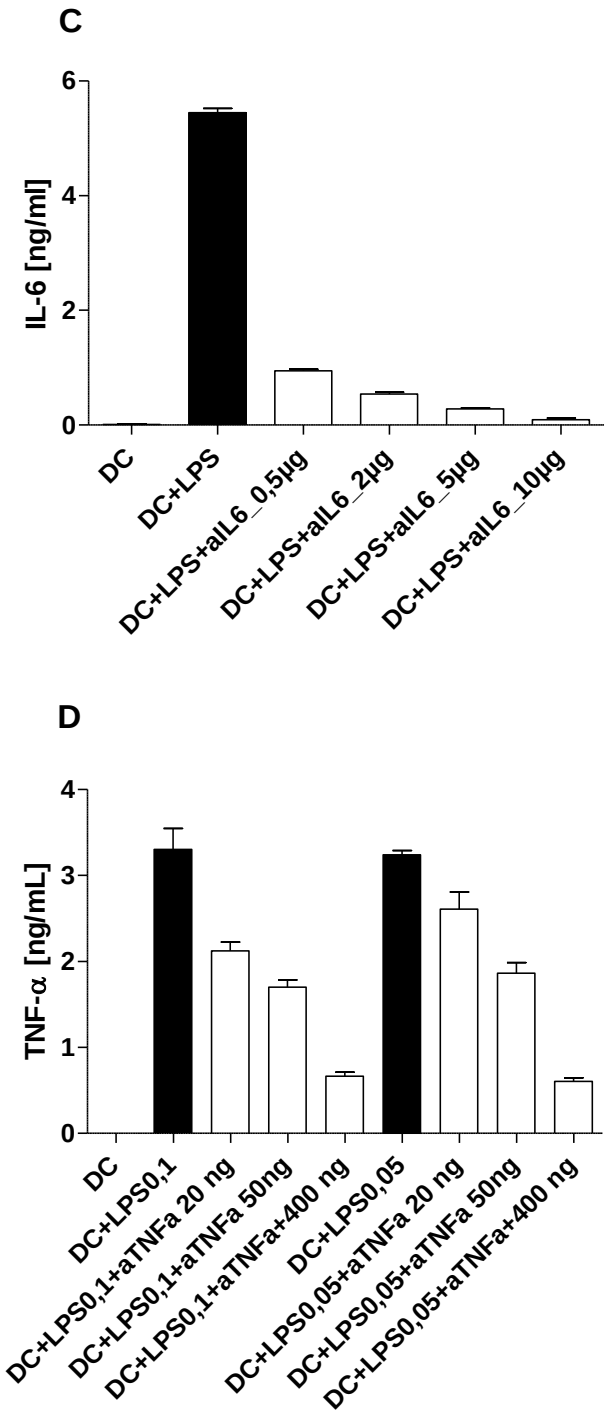

Figure 2.4: Titration assays. In a sterile U-bottom 96 well plate, GM-CSF-derived DC ($5x10^4$) were cultured with or without $CD4^+$ splenic T cells ($1x10^5$) and LsAg (50 µg/ml) or LPS (0.1 or 0.05 µg/mL) and with or without L-NMMA (5 mM), IL-6 (10 µg/ml) or TNF-α (0.5 µg/ml). Supernatants were collected after A) 72h or B) as indicated or C) and D) 24h and then screened for cytokines by ELISA.

2.2.7 Enzyme-linked immunosorbent assay (ELISA)

ELISA is a plate-based assay technique designed for detecting and quantifying substances such as peptides, proteins (in the case of this work, cytokines), antibodies and hormones. In the ELISA technique used for this work, a first antibody must be immobilized to a solid surface and then complexed with a second antibody that is linked to an enzyme. Detection is accomplished by assessing the conjugated enzyme activity via incubation with a substrate to produce a measureable product. Diverse ELISA kits have been used to measure cytokines levels in supernatants, as described below.

2.2.7.1 Ready-Set-Go ELISA kits (Thermo Fisher Scientific)

ELISA plate was coated with 50 µl of capture antibody (Ab) diluted with coating Buffer (see appendix) per well. The plate was covered and incubated overnight at 4°C. Thereafter, it was washed five times with washing buffer (see appendix) and blocked with 200 µl of 1x Assay Diluent (see appendix) and incubated at RT for 1 h, to remove unspecific bindings. Plate was washed five times with washing buffer and the standard and samples were diluted in 1x Assay Diluent. A 2-fold serial dilution of the standard was performed in the standard wells and 50 µl of 1x Assay Diluent were added to the blank wells. Then, 50 µl of the diluted samples were added per well. The plate was covered and incubated at RT for 2 h or at 4°C overnight. Thereafter, it was washed five times with washing buffer and 50 µl of detection Ab diluted in 1x Assay Diluent (see appendix), were added per well. The plate was covered and incubated at RT for 1h; then washed five times with washing buffer and 50 µl of avidin-horseradish peroxidase (HRP) diluted in 1x Assay Diluent (see appendix), were added per well. The plate was covered and incubated at RT for 30 minutes and thereafter, washed seven times with washing buffer. And for the revelation, 50 µl of the provided tetramethylbenzidine (TMB) (see appendix) were added per

well and the plate was incubated at RT for around 15 minutes and the reaction was stopped by adding 50 µl of stop solution (see appendix) per well. The plate was read at 450 nm against 570 nm using a spectrometer (Spectra Max 340pc384, Molecular Devices, Sunnyvale, USA).

2.2.7.2 Duo Set ELISA kits (R&D)

ELISA plate was coated with 50 µl of capture Ab diluted with 1 % PBS (see appendix) per well. The plate was covered and incubated overnight at 4°C. Thereafter, it was washed three times with washing buffer (see appendix) and blocked with 150 µl of 1 % PBS /1 % BSA (see appendix) and incubated at RT for 2 h, to remove unspecific bindings. Plate was washed three times with washing buffer and the standard and samples were diluted in 1 % PBS /1 % BSA. A 2-fold serial dilution of the standard was performed in the standard wells and 50 µl of 1 % PBS /1 % BSA were added to the blank wells. Then, 50 µl of the diluted samples were added per well. The plate was covered and incubated at RT for 2 h. Thereafter, it was washed five times with washing buffer and 50 µl of detection Ab diluted in 1 % PBS /1 % BSA (see appendix), were added per well. The plate was covered and incubated at RT for 2 h; then washed five times with washing buffer and 50 µl of streptavidin-horseradish peroxidase (HRP) diluted in 1 % PBS /1 % BSA (see appendix) were added per well. The plate was covered and incubated at RT for 45 minutes and thereafter, washed five times with washing buffer. And for the revelation, 50 µl of the substrate solution (see appendix) were added per well and the reaction was stopped by adding 50 µl of stop solution (see appendix) per well. The plate was read at 450 nm against 570 nm using a spectrometer (Spectra Max 340pc384, Molecular Devices, Sunnyvale, USA).

2.2.7.3 BD ELISA

ELISA plate was coated with 50 µl of capture Ab diluted with coating buffer (see appendix) per well. The plate was covered and incubated overnight at 4°C. Thereafter, it was washed four times with washing buffer (see appendix) and blocked with 150 µl of 1 % PBS /1 % BSA (see appendix) and incubated at RT for 2 h, to remove unspecific bindings. Plate was washed three times with washing buffer and the standard and samples were diluted in 1 % PBS /1 % BSA. A 2-fold serial dilution of the standard was performed in the standard wells and 50 µl of 1 % PBS /1 % BSA were added to the blank wells. Then, 50 µl of the diluted samples were added per well. The plate was covered and incubated overnight at 4°C. Thereafter, it was washed five times with washing buffer and 50 µl of detection Ab diluted in 1 % PBS /1 % BSA (see appendix), were added per well. The plate was covered and incubated at RT for 1 h; then washed five times with washing buffer and 50 µl of streptavidin-peroxidase (POD) diluted in 1 % PBS /1 % BSA (see appendix) were added per well. The plate was covered and incubated at RT for 45 min and thereafter, washed five times with washing buffer. And for the revelation, 50 µl of the substrate solution (see appendix) were added per well and the reaction was stopped by adding 50 µl of stop solution (see appendix) per well. The plate was read at 450 nm against 570 nm using a spectrometer (Spectra Max 340pc384, Molecular Devices, Sunnyvale, USA).

2.2.8 Griess assay

Nitric oxide (NO) is an important physiological messenger and effector molecule in many biological systems, including immune responses and one way to investigate nitric oxide formation is to measure nitrite (NO_2^-) which is one of two primary, stable and nonvolatile breakdown products of NO. Thus, to measure NO_2^- (and indirectly NO) release, Griess reagent kit (Molecular Probes, Inc., Oregon, USA) was used according to the manufactures's instructions. In

brief, Griess reagent was prepared by mixing equal volumes of components A (N-(1-naphthyl) ethylenedi-amine) and B (sulfanilic acid). 10 µl of freshly prepared Griess reagent was then mixed with 75 µl of sample/Aqua dest. (Blank)/standard (serial dilution 10 - 1 µM) and 65 µl of Aqua dest., to have a total volume of 150 µl. The mix was incubated for 30 min in the dark. NO production was then quantified by the colour change at 548nm using a spectrometer (Spectra Max 340pc384, Molecular Devices, Sunnyvale, USA).

2.2.9 Gene expression analysis

2.2.9.1 RNA extraction and quantification

RNA was extracted from isolated MDSCs using a combination of Trizol (Invitrogen) and RNeasy Mini kit (Qiagen, Hilden, Germany). In brief, trizol-preserved samples were incubated at 15-30°C for 5 min, to allow complete dissociation of nucleoproteins complexes and mixed with 0.1 ml of cool 1-Bromo-3-chloropropane (BCP, Sigma-Aldrich GmbH, Munich, Germany) per 1ml Trizol. The mixture was shaken vigorously for 15 seconds, incubated at RT for 2-3 minutes and centrifuged for 15 min at 12,000 g at 4 °C using Eppendorf 5417R (Eppendorf AG, Hamburg, German). Thereafter the upper aqueous phase containing the RNA was removed carefully in new tube and 1 volume of 70% EtOH was added, mixed and 700 µl of the mixture were transferred to the column placed in a 2 ml collection tube (Qiagen, Hilden, Germany). This was followed by a centrifugation step, 16,000 g for 3 min at RT and the flow-through was discarded. Then 700 µl of buffer RW1 were added to the column and centrifuged at 16,000 g for 20 seconds at RT. The flow-through was discarded and 500 µl of buffer RPE were added to the column and centrifuged as described above. This step was repeated with 700 µl RPE buffer except centrifugation for 2min, before the column was placed in a new 2 ml collection tube and centrifuged at 16,000 g for 1 min at RT in order to dry the membrane, which contained the RNA. The 2 ml collection tube

was discarded and the column was placed in a new 1.5 ml collection tube. Finally, 30 µl RNAse-free water were added to the membrane and centrifuged at 16,000 g for 1 min at RT and RNA solution was kept on ice followed by a DNase digestion using DNA-free kit (Applied Biosystems) according to the manufacturer's instructions. In short, 0.1 volume of 10X DNAse I buffer and 1 µl of rDNAse I were gently mixed with the RNA solution and incubated at 37 °C for 20-30 min using a heater (Eppendorf AG, Hamburg, Germany). Thereafter, 0.1 volume of DNAse inactivation reagent was added, incubated for 2min at RT and centrifuged at 10,000 g for 2 min. Finally, the RNA containing supernatant was transferred into a new tube and the concentration of RNA was measured using NanoVue (GE Lifescience, Chalfont St Giles, Great Britain). RNA with a $A_{260/280}$ ratio of nearly 2 was considered pure (of good quality).

To further analyze the quality of the RNA, Experion RNA StdSens Analysis kit (BioRad, Hercules, USA) was used according to the manual instruction. In brief, 2 µl of ladder and sample were incubated at 70°C for 2 min (denaturation), vortexed and kept on ice. The electrodes were cleaned by placing 800 µl of Experion electrode cleaner (EC) on the EC cleaning chip and letting it run in the Experion electrophoresis station for 2 min. Then 800 µl of Milli-Q water were placed on the DEPC cleaning chip and let run for 5 min; this was repeated once again. Thereafter, the lid of the machine was kept opened for 1 min then closed. A gel-stain solution (GS) was prepared by mixing 65 µl gel (G) and 1 µl stain (ST). The mixture was vortexed and briefly centrifuged. Next, the chip was primed by adding 9 µl of GS to gel priming well and letting it run in the prime station and then was removed. 9 µl of GS and 9 µl of G were loaded into the second GS well and G well respectively. Then, 5 µl of loading buffer (B) were placed into each sample well and into well L. 1 µl of denatured RNA ladder and 1 µl of denatured sample were loaded into well L and sample wells respectively. Caution was taken to fill unused sample wells with 1 µl Milli-Q water. The chip was placed in the Experion vortex station and vortexed for 1min and let run in the

Experion electrophoresis station within 5 min of loading. After the run was completed, the used chip was removed and discarded and the cleaning process described above, repeated.

2.2.9.2 cDNA synthesis

In order to obtain the first-strand cDNA, good quality RNA (see section 2.2.9.1) was used and genomic DNA elimination and reverse-transcription mixes were prepared as shown in Table 1 and 2, respectively. Genomic DNA elimination mix was incubated at 42 °C for 5 min and placed on ice for at least 1 min. Then 10 µl of genomic DNA elimination mix and 10 µl of reverse-transcription mix were mixed and incubated at 42 °C for 30 min and the reaction was immediately stopped, at 95°C for 5 min. For the preamplification procedure (this is to obtain enough material for PCR array, see section below), preamplification mix was prepared as depicted in Table 3. Then, 5 µl first-strand cDNA synthesis reaction were added to 20 µl preamplification mix and cycling performed as indicated in Table 4.

Table 1: Genomic DNA elimination mix

Component	**Amount for one sample**
RNA	1 ng -100 ng
Buffer GE	2 µl
Rnase-free water	variable
Total volume	**10 µl**

Table 2: Reverse-transcription mix

Component	**volume for 1 reaction (µl)**
5x Buffer BC3	4
Control P2	1
cDNA synthesis Enzyme Mix	1
RNA Inhibitor	1
Rnase-free water	3
Total volume (µl)	**10**

Table 3: Preamplification mix

Component	**volume for 1 sample (µl)**
RT^2 PreAMP PCR Mastermix	12,5
RT2 PreAMP Pathway Primer Mix	7,5
Total volume (µl)	**20**

Table 4: Cycling conditions for preamplification of cDNA (from fresh/frozen samples)

Cycles	**Duration**	**Temperature**
1	10 min	95°C
12	15 s	95°C
	2 min	60°C
Hold		4°C

2.2.9.3 PCR array

PCR Array using the RT2 SYBR Green Mastermix kit (Qiagen, Hilden, Germany) and RT2 Profiler PCR Array Mouse Innate and Adaptive Immune Responses kit (Qiagen, Hilden, Germany) were used in order to evaluate the differences between the two subsets of MDSC populations isolated

from Ls-infected BALB/c mice. These two subsets were also isolated from naive mice to serve as controls. The customized array consists of 84 genes related to innate and adaptive responses in mouse including: a) Pattern Recognition Receptors (PRRs) (DDX58 [RIG-I], NLRP3, NOD1 (CARD4), NOD2, TLR1, TLR2, TLR3, TLR4, TLR5, TLR6, TLR7, TLR8, TLR9), b) cytokines (CCL12, CCL5 [RANTES], CSF2 [GM-CSF], IFN-α2, IFN-β1, IL18, IL1α, IL1β, IL2, TNF, CXCL10 [INP10], IFN-γ, IL10, IL13, IL17A, IL23A, IL4, IL5, IL6), c) Th markers (CCR5, CXCR3, SLC11A1, STAT4, TBX21, GATA3, STAT6, CCR6, RORC, STAT3, CCR4, CCR8, FOXP3), d) T cell activation (CD80, CD86, ICAM1) and e) other genes (APCS, C3, C5AR1, CASP1 [ICE], CD14, CD4, CD40 [TNFRSF5], CD40LG [TNFSF5], CD8A, CRP, H2-Q10, H2-T23, IL1R1, IRAK1, IRF3, IRF7, ITGAM, LY96 [MD-2], LYZ2, MAPK1 [ERK2], MAPK8 [JNK1], MBL2, MPO, MX1, MYD88, NFKB1, NFKBIA [IKBALPHA/MAD3], STAT1, TICAM1 [TRIF], TRAF6, IFNAR1, IFNGR1, JAK2, RAG1, TYK2, FasL [TNFSF6]) (see full names of genes as well as the number of sorted cells in Appendix).

To perform the array, PCR components mix was prepared as shown in Table 5. Then, 20 µl PCR components mix were added to each well of the RT2 Profiler PCR Array using Qiagility device (Qiagen, Hilden, Germany). This was followed by cycling (Table 6) using a Rotor Gene Q (Qiagen, Hilden, Germany). Data were analysed using the online RT2 Profiler PCR Array Data analysis 3.5 software at the sabiociences.com website (Qiagen) and gene expression was normalized to Actine beta (Actb).

Table 5: PCR components mix

Array format R (Rotor-Disc 100)	**Components volume (µl)**
2x RT2 SYBR Green Mastermix	1150
Preamplification reaction	102
RNase-free water	1048
Total volume (µl)	**2300**

Table 6: Cycling conditions for Rotor-gene cyclers

Cycles	Duration	Temperature
1	10 min	95°C
40	15 s	95°C
	30 s	60°C

2.3 Statistics

Statistical analyses were performed using the software PRISM 5.02 (GraphPad Software, Inc., La Jolla, USA). Statistical differences between three or more than three groups were observed using a Kruskal-Wallis test (non parametric distribution) or ANOVA (parametric distribution) and when necessary, a Mann-Whitney-U test (non parametric distribution) or Student's t test (parametric distribution) for a further comparison of two groups. p-value of 0.05 or less were considered significant (*p<0. 05, **p<0.01 and ***p<0.001).

2.4 Citations' management

The citations in this document were made using the EndNote X7 bibliography software (Thomson Reuters, New York, USA), licensed for the Institute of Medical Microbiology, Immunology and Parasitology of the University Hospital Bonn.

2.5 Funding

I was supported by a fellowship awarded by the German Academic Exchange Committee (DAAD) and the work received support from intramural funding by the University Hospital of Bonn (BONFOR). Funders had no role in the study design, data collection and analysis performed for this work.

3. RESULTS

This chapter describes the findings of this thesis that show the significance of MDSCs during Ls infection. MDSCs display an immunomodulatory character which can have beneficial or detrimental effects on the outcome of pathologies and here, the first section demonstrates that both Mo-MDSCs and PMN-MDSCs expand in Ls-infected BALB/c mice. Since it is known that $CD4^+$ T cells are critical for controlling immune responses during Ls infection, the second section provides evidence for the ability of Mo-MDSCs but not PMN-MDSCs to suppress the *in vitro* production of IL-13 and IFN-γ by Ls-specific $CD4^+$ T cells. The assessment of the mechanisms underlying such capacities in Ls infection-derived Mo-MDSCs is described in sections three and four and shows that Mo-MDSCs in this setting, function independently on IL-4Rα but require NO and TGF-β to impair the production of IL-13 and IFN-γ by Ls-specific $CD4^+$ T cells, respectively. The last section informs on gene regulation in Ls infection-derived Mo-MDSCs and PMN-MDSCs.

3.1. MDSCs and *Litomosoides sigmodontis* infection

MDSCs have been identified and characterized mainly in cancer models and have thus been observed in blood, lymph nodes, bone marrow and tumor sites. They are generally identified by the co-expression of two surface markers: CD11b and Gr-1 (Gabrilovich et al., 2007; Ostrand-Rosenberg and Sinha, 2009). In addition, within the $CD11b^+$ population, MDSCs are further classified as monocytic (Mo-MDSCs, $CD11b^+Ly6C^+Ly6G^-$) or polymorphonuclear (PMN-MDSCs, $CD11b^+Ly6C^{int/lo}Ly6G^+$) (Ostrand-Rosenberg and Sinha, 2009; Youn et al., 2008) (see section 1.3.3). Although the role of MDSCs has been documented in other pathological conditions including bacterial and viral infections, little research has focused on deciphering the relevance of MDSCs in helminth infections. Investigating this could serve as basis for new therapeutics and therefore the current study aimed at assessing the impact of MDSCs during *Litomosoides sigmodontis* (Ls) infection which is an established model for filariasis (more detail in section 1.2).

Since *L. sigmodontis* worms can complete a full life-cycle in BALB/c mice, the study began with an initial comparison of the number of expanding and infiltrating MDSCs in naive versus Ls-infected BALB/c mice as well as the proportion of the infiltrating subsets. Furthermore, the analysis was expanded to cover the kinetics of systemic-residing MDSC subsets and those found at the site of infection, the thoracic cavity (TC). Correlations between MDSC subsets and parasitological parameters including worm burden and MF count were also investigated.

3.1.1 *MDSCs infiltrate the site of infection in Litomosoides sigmodontis infected mice*

In order to look whether MDSC populations infiltrate the thoracic cavity and to distinguish between monocytic (Mo-MDSCs) and polymorphonuclear MDSCs (PMN-MDSCs), cells were collected from the thoracic cavity of naive mice or Ls-infected WT BALB/c mice and analyzed by FACS/Flow cytometry using CD11b, CD45, Ly6C and Ly6G antibodies (adapted from (Schumak et al., 2015)) (see Figure 3.1).

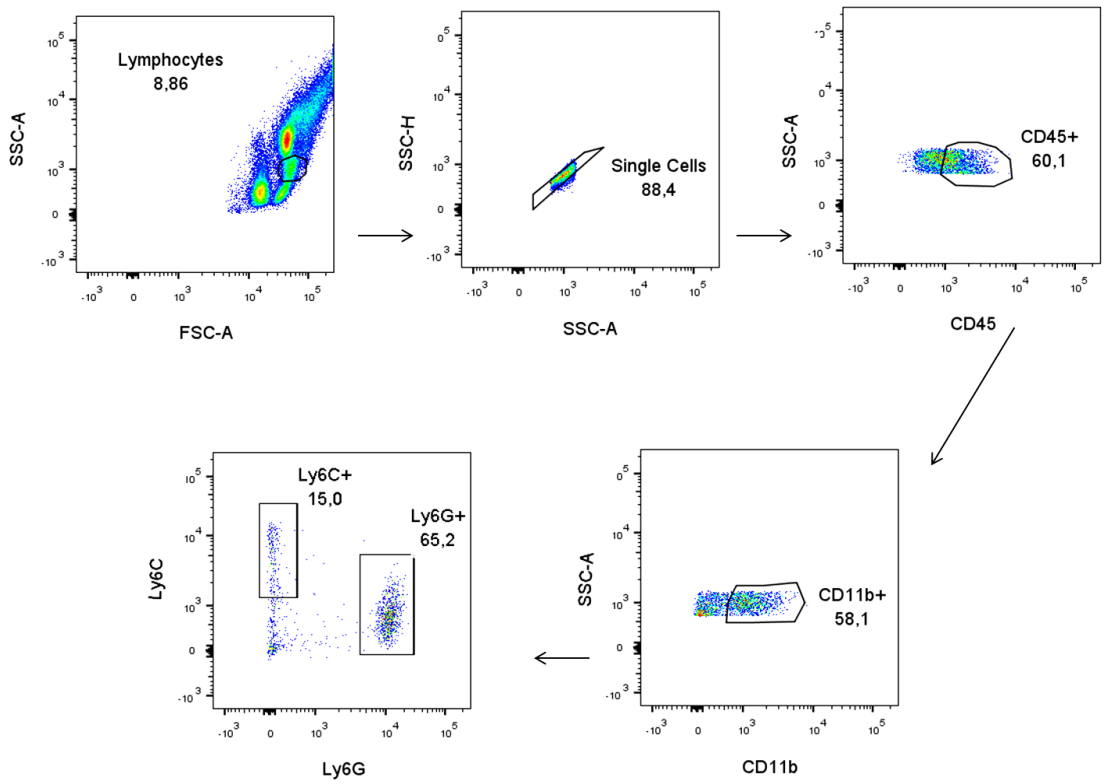

Figure 3.1: Gating strategy to identify MDSC populations. Cells were isolated from the thoracic cavity and stained with a combination of CD45, CD11b, Ly6C and Ly6G antibodies to distinguish between monocytic ($CD11b^{+}Ly6C^{+}Ly6G^{-}$, Mo-MDSCs or Ly6C) and polymorphonuclear ($CD11b^{+}Ly6C^{int/lo}Ly6G^{+}$, PMN-MDSCs or Ly6G) MDSC populations by flow cytometry. Images show flow cytometry data from a day 72 Ls-infected BALB/c mouse.

The amounts of infiltrating MDSCs in naive or day 42 p.i. Ls-infected mice (there all worms are adults) are depicted in Figure 3.2. Interestingly, very few Mo-MDSCs were present in the TC of naive mice whereas there was a substantial proportion in the TC fluid of Ls-infected mice ($p<0.01$, Figure 3.2 A). Similarly, there was only a nominal amount of PMN-MDSCs in the TC of naive mice when compared to Ls-infected BALB/c mice ($p<0.01$, Figure 3.2 B). Collectively these data show for the first time that MDSC populations infiltrate the site of infection in Ls-infected BALB/c mice whereas naive mice display very few MDSCs.

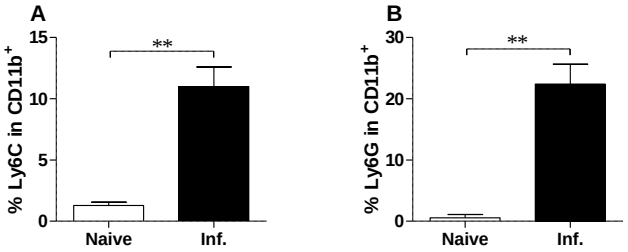

Figure 3.2: Higher levels of MDSC subsets in the thoracic cavity of Ls-infected mice when compared to uninfected mice. Wildtype (WT) BALB/c mice were left uninfected or naturally infected with Ls. On day 42 p.i., cells were isolated from the thoracic cavity and stained with a combination of CD45, CD11b, Ly6C and Ly6G antibodies to differentiate monocytic ($CD11b^{+}Ly6C^{+}Ly6G^{-}$, Mo-MDSCs or Ly6C) and polymorphonuclear ($CD11b^{+}Ly6C^{int/lo}Ly6G^{+}$, PMN-MDSCs or Ly6G) MDSC populations. Graphs show percentage of A) Mo-MDSCs and B) PMN-MDSCs within the $CD11b^{+}$ population in uninfected (white bars) and in day 42 p.i. Ls-infected (black bars). Graphs show mean ± SEM of 4 infection studies using 3-5 mice. Asterisks indicate significant differences (Mann-Whitney test) between the groups indicated by the brackets (**p<0.01).

3.1.2 *PMN-MDSC accumulate to a higher extent when compared to Mo-MDSCs*

As mentioned in section 1.2, Ls infection in BALB/c mice allows the release of MF into the periphery (patency). Indeed, in a parallel study, after screening the blood of Ls-infected mice from day 45 p.i. until day 120 p.i., it could be determined that MF production began around day 49 p.i. and peaked around day 70-72 p.i (Figure 3.3) (Petit et al., 1992; Rodrigo et al., 2016). This pointed out that the time frame day 70-72 p.i. was critical during the chronic phase of Ls infection especially in terms of patency and therefore further experiments were performed at such time points to address immune responses during chronic Ls infections.

Since researchers found in a cancer setting that PMN-MDSCs accumulated to a higher extent when compared to Mo-MDSCs (Youn et al., 2008) and having observed the infiltration of MDSC subsets at the site of infection and their higher numbers in Ls-infected mice when compared to uninfected controls, the next step compared the frequencies of the two subsets of MDSCs at the peak of patency (days 70-72 p.i.).

Interestingly, although both MDSC subsets infiltrated the TC (Figure 3.2), the frequencies ($p<0.001$, Figure 3.4 A) and absolute cell numbers ($p<0.05$, Figure 3.4 B) of PMN-MDSCs were higher when compared to Mo-MDSCs on day 72 p.i. Thus, PMN-MDSCs infiltrated the thoracic cavity of Ls-infected BALB/c mice to a higher degree than Mo-MDSCs.

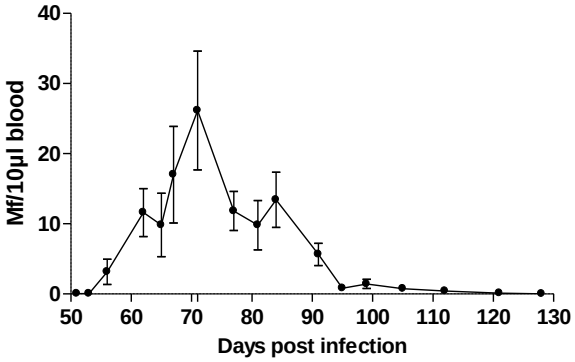

Figure 3.3: MF release during Ls infection. Wild-type BALB/c female mice were naturally infected with *L. sigmodontis*. From day 45 to 120 p.i. individual mice were screened for the number of MF in blood. Symbols represent mean ± SEM of infected mice from six independent infection experiments (n = 20 Mf+ mice). Taken from Rodrigo et al., 2016.

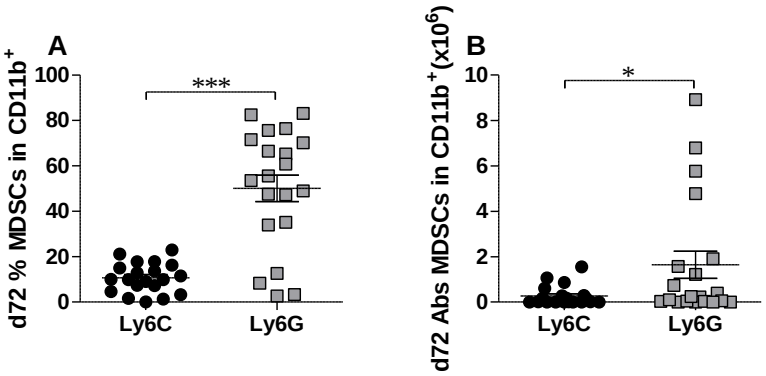

Figure 3.4: Increased frequencies of PMN-MDSCs when compared to Mo-MDSCs during Ls infection. Wildtype BALB/c mice were naturally infected with Ls. On day 72 p.i., cells were isolated from the thoracic cavity and stained with a combination of CD45, CD11b, Ly6C and Ly6G antibodies to differentiate monocytic ($CD11b^+Ly6C^+Ly6G^-$, Mo-MDSCs or Ly6C) and polymorphonuclear ($CD11b^+Ly6C^{int/lo}Ly6G^+$, PMN-MDSCs or Ly6G) MDSC populations. Comparison of MDSCs within the $CD11b^+$ compartment of day 72 infected mice as A) percentage or B) absolute cell number. Symbols show values from individual mice (n=20) from 2 independent infection studies. Asterisks indicate significant differences (Mann-Whitney test) between the groups indicated by the brackets (*p<0.05, ***p<0.001).

3.1.3 *Differential accumulation of Mo-MDSCs and PMN-MDSCs during Ls infection in the thoracic cavity and blood*

MDSCs accumulate at different levels and stages and the kinetics of this accumulation and their development have been suggested to affect the outcome of cancer, especially in diverse murine models of hepatocellular carcinoma (Kapanadze et al., 2013). To observe whether such effects also occur in Ls model, the frequencies of MDSCs in the thoracic cavity was compared to that in blood of Ls-infected WT BALB/c mice.

At the site of infection, PMN-MDSC numbers increased dramatically at the stage of final molting around day 30 p.i. (from 1% to 37%) whereas, Mo-MDSC numbers only showed a slight augmentation throughout the entire infection period (3-15%) (Figure 3.5 A). In contrast, MDSC subsets showed different accumulation rates in blood (Figure 3.5 B). In detail, Mo-MDSC levels were high at the very beginning of the infection whereas PMN-MDSC levels were low (32.5% and 0.2% respectively). Then from day 4 p.i., levels of PMN-MDSCs went up exponentially to over 80% and only slightly dropped down again around day 72 p.i. During that same time, Mo-MDSC numbers decreased from 55% to between 5% and 30% until day 72 p.i.

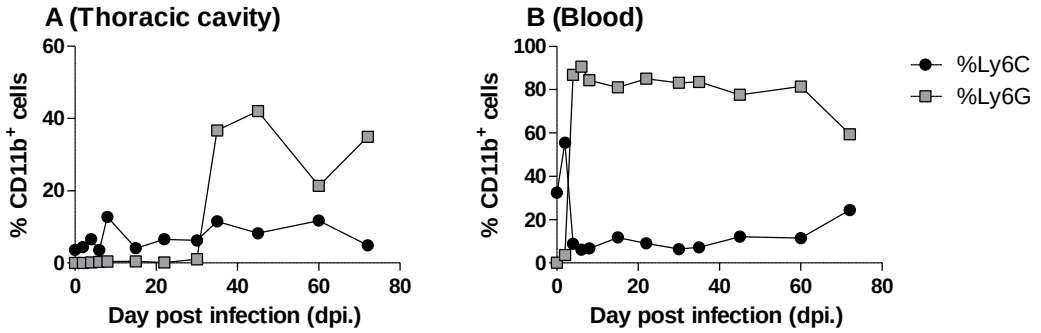

Figure 3.5: MDSC subsets activity during Ls infection. Wild-type BALB/c mice were naturally infected with *L. sigmodontis*. From day 0 to 72 p.i., cells were isolated from the thoracic cavity or blood and stained with a combination of CD45, CD11b, Ly6C and Ly6G antibodies to differentiate monocytic ($CD11b^+Ly6C^+Ly6G^-$, Mo-MDSCs or Ly6C) and polymorphonuclear ($CD11b^+Ly6C^{int/lo}Ly6G^+$, PMN-MDSCs or Ly6G) MDSC populations. Percentage of MDSCs subsets within the $CD11b^+$ cell compartment in A) the thoracic cavity or B) blood were determined by flow cytometry. Symbols show the percentage of cells in infected (n=3-5 per time point {n=50 in total}) mice from one infection.

3.1.4 *MDSC infiltration positively correlates with worm burden*

Findings have suggested that MDSC levels were associated with the level and evolution of pathology especially in cancer (Almand et al., 2000; Arihara et al., 2013). This led to the speculation that MDSC infiltration could be associated with parasite parameters including worm burden and MF counts. To test this hypothesis, a correlation analysis was performed between the numbers of MDSC subsets and either worm burden or MF count at day 70-72 p.i.

Interestingly, levels of both Mo-MDSCs and PMN-MDSCs positively correlated with worm burden ($r=0.8377$; $p<0.0001$ and $r=0.7777$, $p<0.0001$, respectively) (Figure 3.5 A). However an opposite

outcome was displayed in the correlation between MDSC levels and MF count when assessing systemic MF numbers or MF numbers in the TC. Indeed, the systemic MF counts showed no correlation with any of the two MDSC subsets (r=0.0967; p= 0.6312 and r=0.1900, p=0.3426) (Figure 3.6 C). In contrast, MF at the site of infection showed a slight positive correlation with MDSC populations (r=0.4660; p=0.0143 and r=0.4381, p=0.0223) (Figure 3.6 B), although this correlation was not as strong as the one observed between the same populations and worm burden. Ultimately, these data demonstrated that MDSC frequencies positively correlated with worm burden during Ls infection.

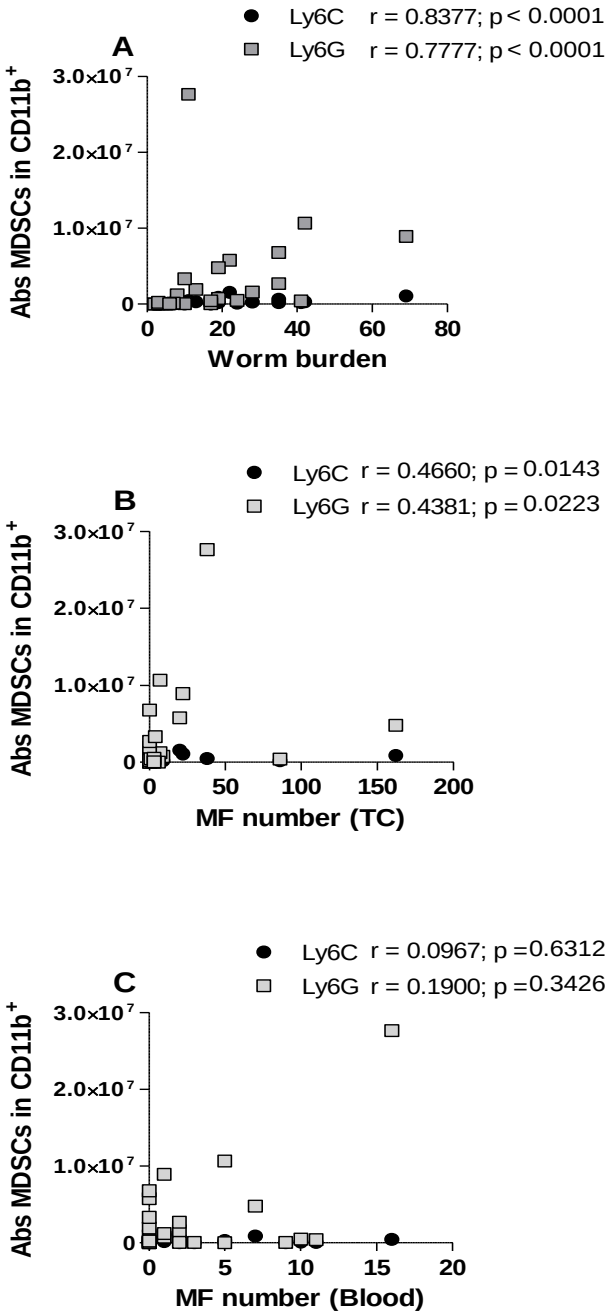

Figure 3.6: Positive correlation between MDSCs frequency and worm burden. On day 71 p.i., worms were isolated from the thoracic cavity of individual mice and counted and MF release was quantified. Cells were also isolated from the thoracic cavity and stained with a combination of CD45, CD11b, Ly6C and Ly6G antibodies to differentiate monocytic ($CD11b^+Ly6C^+Ly6G^-$, Mo-MDSCs or Ly6C) and polymorphonuclear ($CD11b^+Ly6C^{int/lo}Ly6G^+$, PMN-MDSCs or Ly6G) MDSC populations. Plots show spearman correlations between the number of MDSCs subsets and A) worm burden, B) MF number in thoracic cavity (TC) and C) MF number in blood. Data are from infected mice (n=27) from 3 independent infection studies. P-values show significant differences between worm burden and each of the two subsets and r the coefficient of correlation.

3.2 Characterization of MDSC-mediated suppression of Ls-specific $CD4^+$ T cell responses

The hallmark of MDSCs is their ability to suppress T cell responses (Gabrilovich et al., 2007). This has been shown in several cancer scenarios (Solito et al., 2014) and many other pathological conditions including bacterial, viral and parasitic infections but not in helminths (as reviewed in (Tamadaho et al., 2018)). In the previous section (section 3.1) it was demonstrated that there

was an expansion of MDSC subsets inthe thoracic cavity of Ls-infected BALB/c mice and that there was a higher frequency of the PMN-MDSC subset when compared to the Mo-MDSCs. In addition, a statistically strong positive correlation was shown between MDSC subsets and worm burden. Here, the ability of the two MDSCs subsets to suppress Ls-specific $CD4^+$ T cells and its association with parasitic parameters were evaluated.

3.2.1 *Mo-MDSCs suppress Ls-specific $CD4^+$ T cell responses*

As described above, MDSC populations share the capacity to suppress T and even B cells responses (as reviewed in (Tamadaho et al., 2018)). Therefore, to test the suppressive property of Mo-MDSCs and PMN-MDSCs that arose during Ls infection, an *in vitro* co-culture assay was developed (see Figure 2.1). In brief, $CD4^+$ T cells were isolated from the spleen and medLN of Ls-infected mice on day 72 p.i. Cells were then activated *in vitro* over 72 hours with LsAg, an extract prepared from adult Ls worms in the presence of GM-CSF derived DC from BALB/c mice. Suppression of cytokine release was then measured after co-culturing isolated Mo-MDSCs or PMN-MDSCs with $CD4^+$ T cells in a 1:1 ratio. Of interest, as noted in other helminth infections $CD4^+$ T cells from uninfected mice do not respond to Ls-antigen during *in vitro* recall assays. Therefore, no co-cultures were performed using $CD4^+$ T cells isolated from uninfected mice (Figure 3.7 A and B). In addition, when compared to the main controls (DC+$CD4^+$+LsAg or DC+$CD4^+$+CD3/28), other controls had negligible levels of IL-13 and IFN-γ (Figure 3.7 C and D, respectively).

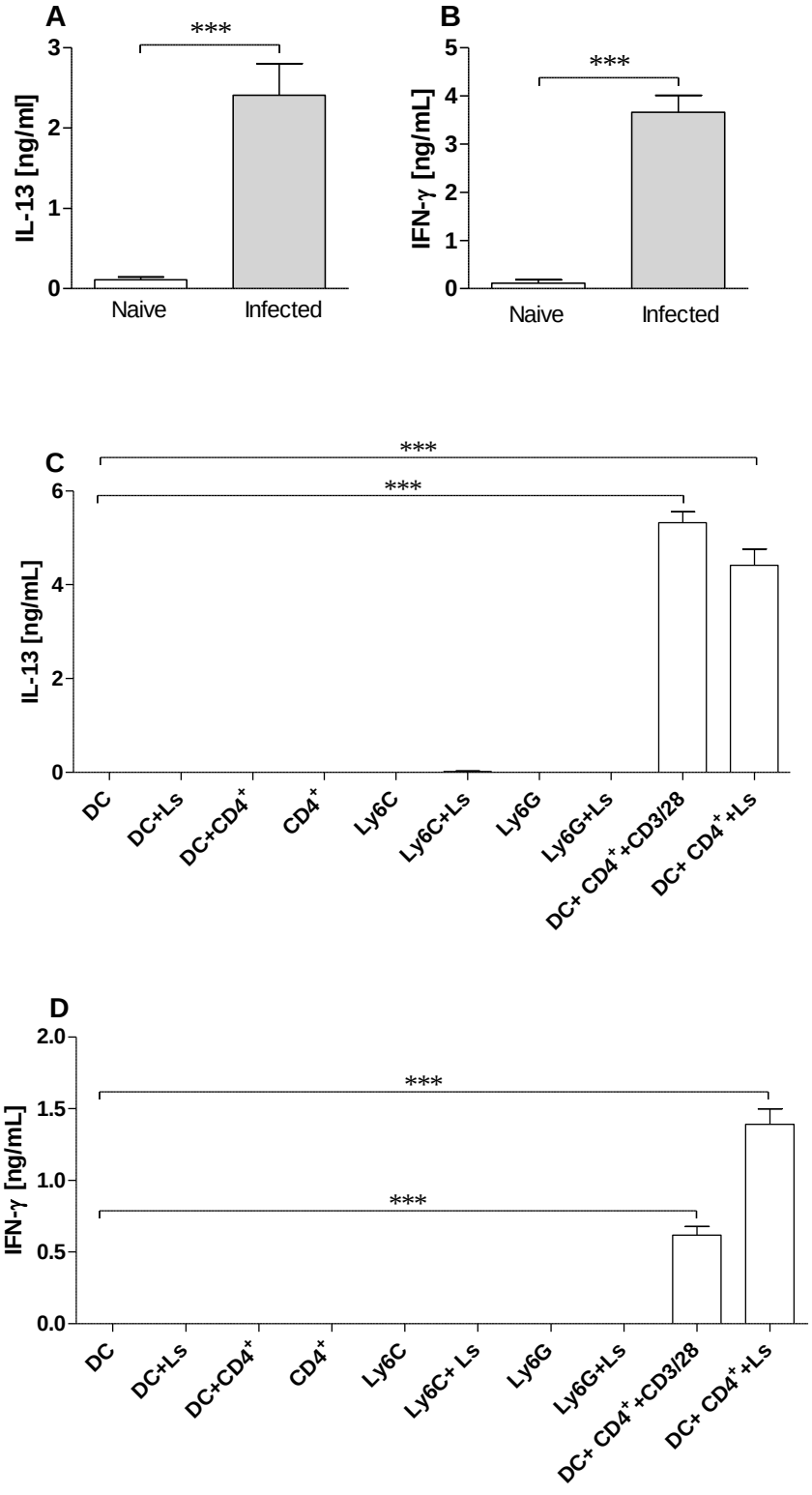

Figure 3.7: Hyporesponsiveness of naive CD4$^+$ T cells upon LsAg stimulation. CD4$^+$ T cells were isolated from Ls-infected or naive mice by flow cytometry. CD4$^+$ T cells (1x10^5) were cultured with GM-CSF-derived DC (5x10^4) and LsAg (50 µg/ml) for 72h. Supernatants were then screened for A) IL-13 and B) IFN-γ by ELISA. Graphs show mean ± SEM 1 of 2 co-culture assays using cells from 2-3 pooled mice from 1 infection study. On day 71 p.i., CD4$^+$ T cells and MDSCs subsets were isolated from Ls-infected mice by flow cytometry. CD4$^+$ T cells (1x10^5) or Ly6C$^+$/Ly6G$^+$ MDSCs (1x10^5) were cultured alone or

with GM-CSF-derived DC ($5x10^4$) and LsAg (50 µg/ml) or αCD3/28 (5 and 1,25 µg/ml) for 72h. Supernatants were then screened for C) IL-13 and D) IFN-γ by ELISA. Graphs show mean ± SEM of 1 of all co-culture assays performed in this thesis using cells from 4-10 pooled mice from independent infection studies. C) IL-2 and D) IL-5 Asterisks show significant differences (Mann-Whitney test) between the indicated groups (***p<0.001).

Figure 3.8 depicts data demonstrating that Mo-MDSCs (black bars) were able to significantly suppress the production of IL-13 ($p<0.05$ in Figure 3.8 A), IFN-γ ($p<0.01$ in Figure 3.8 B) and IL-2 ($p<0.05$ in Figure 3.8 C) but not IL-5 ($p=0.37$ in Figure 3.8 D) by filarial-specific $CD4^+$ T cells, comparatively to the negative control which contained no MDSCs (white bars). Surprisingly, PMN-MDSCs (grey bars) were not able to suppress the production of any of the above mentioned cytokines. The comparison of the cytokine levels between the Mo-MDSCs (black bars) and PMN-MDSCs (grey bars) showed no differences. The production of IL-10 was suppressed by neither Mo-MDSCs nor PMN-MDSCs and measuring the suppression of TNF-α and IL-5 was not a stable parameter. Thus to assess the effects of Mo-MDSCs on filarial-specific $CD4^+$ T cells in the rest of the study, only the suppression of IL-13 and IFN-γ (representing Th2 and Th1 responses, respectively) was measured since these cytokines were the most stable.

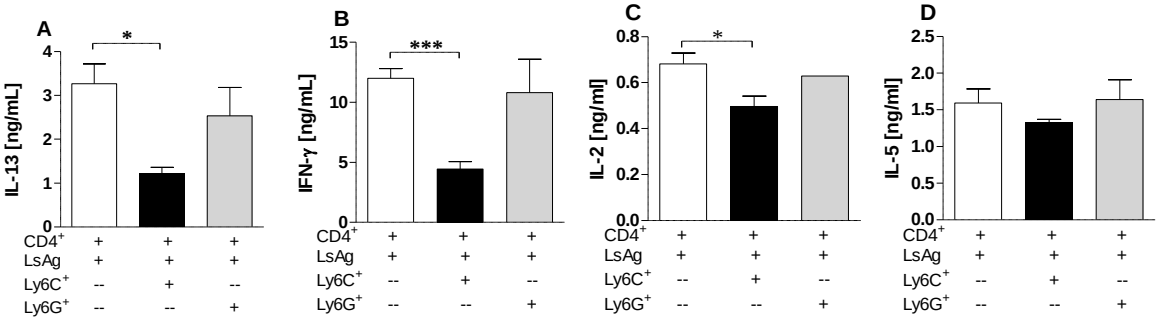

Figure 3.8: Suppression of filarial-specific $CD4^+$ T cells responses by Mo-MDSCs. On day 70-72 p.i., $CD4^+$ T cells and MDSCs subsets were isolated from Ls-infected mice by flow cytometry. $CD4^+$ T cells ($1x10^5$) were cultured with GM-CSF-derived DC ($5x10^4$) and LsAg (50 µg/ml) in the presence or absence of $Ly6C^+$ or $Ly6G^+$ MDSCs ($1x10^5$) for 72h. Supernatants were then screened for A) IL-13; B) IFN-γ; C) IL-2 and D) IL-5 by ELISA. Graphs show mean ± SEM 1 of 3 co-culture assays using cells from 4-6 pooled mice from 3 independent infections. Asterisks show significant differences (Mann-Whitney test) between the indicated groups (*p<0.05, ***p<0.001).

3.2.2 *Mo-MDSCs suppress cytokine production by Ls-specific CD4$^+$ T cell responses regardless of MF status*

In section 3.1.4, systemic MF counts were revealed to not have any correlation with MDSC levels. On this basis, it was tempting to speculate that the suppressive activity mediated by Mo-MDSCs (see Figure 3.8) was not associated with systemic MF status. To verify this, Mo-MDSCs and CD4$^+$ T cells were isolated from MF-producing (MF+) or non-MF-producing mice (MF-) on day 70-72 p.i. and co-cultured with GM-CSF-derived DC and LsAg for 72h. Thereafter, cytokine release was measured in the supernatant.

As expected, Figure 3.9 shows that Mo-MDSCs derived from either MF-producing (MF+) or non-MF-producing mice (MF-) were able to significantly suppress the production of IL-13 by Ls-specific CD4$^+$ T cells ($p<0.05$ and $p<0.05$ respectively; Figure 3.9 A). The production of IFN-γ was also suppressed (Figure 3.9 B) but suppression was only significant with Mo-MDSCs from MF- mice. These data confirmed the correlation showed in section 3.1.4.

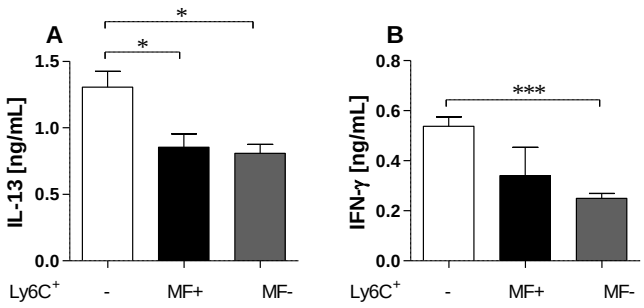

Figure 3.9: Suppression of filarial-specific CD4$^+$ T cells responses by Mo-MDSCs stemming from MF$^+$ and MF$^-$ mice Ls-infected mice. On day 70-72 p.i., CD4$^+$ T cells and MDSCs subsets were isolated from Mf-producing (Mf$^+$) or non Mf-producing (Mf$^-$) Ls-infected mice by flow cytometry. CD4$^+$ T cells ($1x10^5$) were cultured with GM-CSF-derived DC ($5x10^4$) and LsAg (50 µg/ml) in the presence or absence of Ly6C$^+$ or Ly6G$^+$ MDSCs ($1x10^5$) for 72h. Supernatants were then screened for A) IL-13; B) INF-γ by ELISA. Graphs show mean ± SEM of 2 co-culture assays using pooled cells from 4-16 mice from 2 independent infections. Asterisks show significant differences (Mann-Whitney test) between the indicated groups (*$p<0.05$, ***$p<0.001$).

3.2.3 *Mo-MDSCs derived from pre- and post-patent Ls-infected mice suppress CD4$^+$ T cell responses*

As mentioned in section 1.2.1, MF production in Ls-infected BALB/c mice begins around day 49-50 p.i. and peaks around day 72 p.i (Figure 3.3). However, immune responses to MF are indicated to be of considerable importance since ingestion of this life-stage (MF) by blood feeding vectors is paramount to their survival. It is known that immune responses are altered in patent and latent infections (Arndts et al., 2012; Rodrigo et al., 2016) and immune responses differ during infections in BALB/c mice (see Figure 3.10).

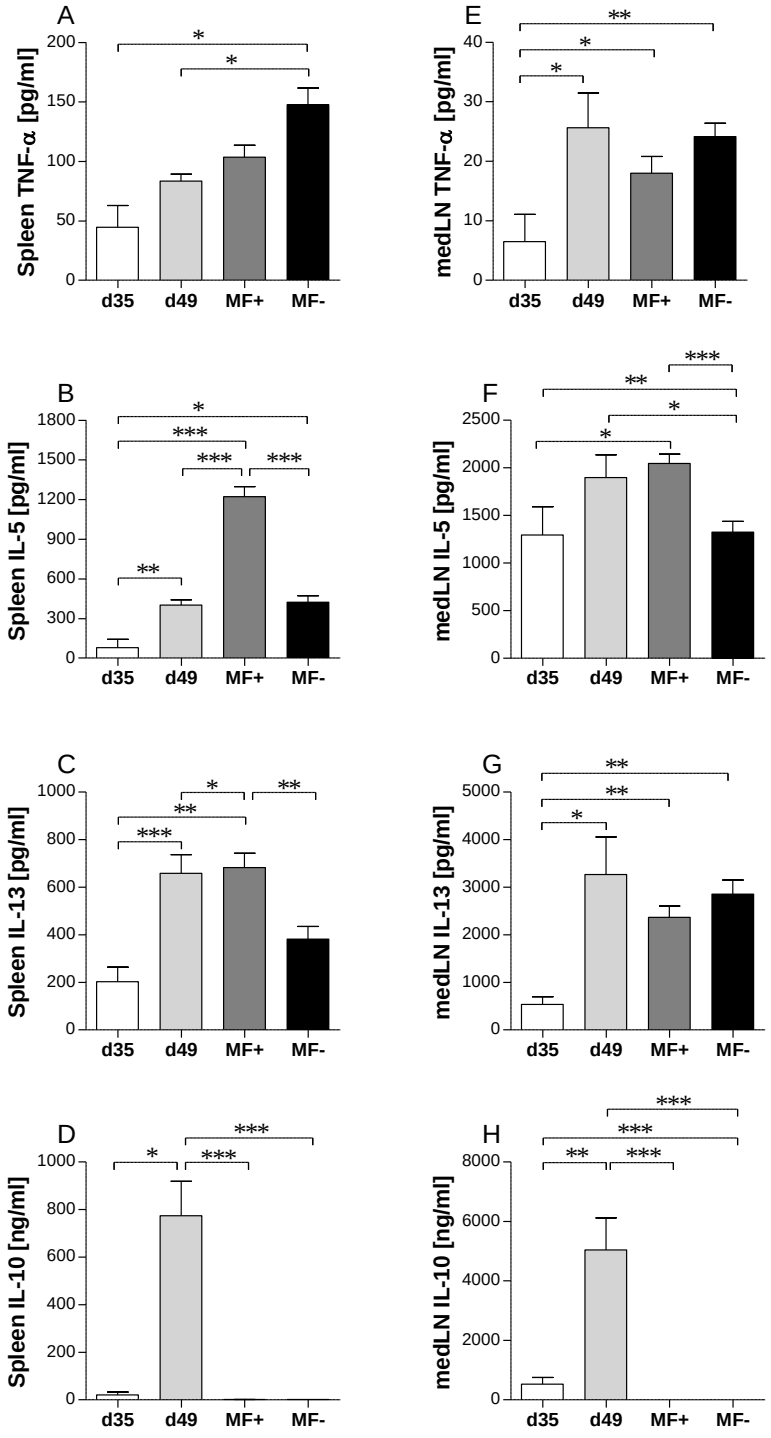

Figure 3.10: Immune responses in pre- and post-patent Ls-infected BALB/c mice. Wildtype BALB/c mice were naturally infected with *L. Sigmodontis* for 35, 49 and 72 days. On day 72, mice were screened for the presence of peripheral MF and lymphocytes were isolated from the spleen (A-D) or medLN (E-H). Cells were stimulated with 50µg/ml LsAg for 72 hours. Thereafter, levels of TNF-α (A,E), IL-5 (B,F), IL-13 (C,G) and IL-10 (D,H) were determined in the culture supernatant by ELISA. Graphs show mean ± SEM of individually assessed mice from 3 independent infection experiments (n=6 day 35, n=7 day 49, n=20 MF+ and n=11 MF- mice). Asterisks indicate significant differences (ANOVA or Student's t test) between the groups indicated by the brackets (*p<0.01, **p<0.05, ***p<0.001).

To test whether the suppression observed with Mo-MDSCs derived from day 72 p.i. infected mice was specific or not to that particular time point or to the post-patent stage, Mo-MDSCs and $CD4^+$ T cells were isolated from Ls-infected mice on day 45 (pre-patent) or 60 p.i. (post-patent) and were cultured with GM-CSF-derived DC and LsAg.

Figure 3.11 shows the levels of cytokines that were produced by Ls-specific $CD4^+$ T cells. Importantly, as with Mo-MDSCs isolated from Ls-infected BALB/c mice on day 72 p.i. (see Figure 3.8), Mo-MDSCs isolated on day 45 p.i. (Figure 3.11 A and B) or 60 p.i. (Figure 3.11 C and D) were able to suppress the production of IL-13 ($p<0.01$ and $p<0.01$; respectively) and IFN-γ ($p<0.01$ and $p<0.05$; respectively), by Ls-specific $CD4^+$ T cells. These data show that Mo-MDSCs isolated from both pre-patent and post-patent Ls-infected mice are equally capable of suppressing Ls-specific $CD4^+$ T cell responses.

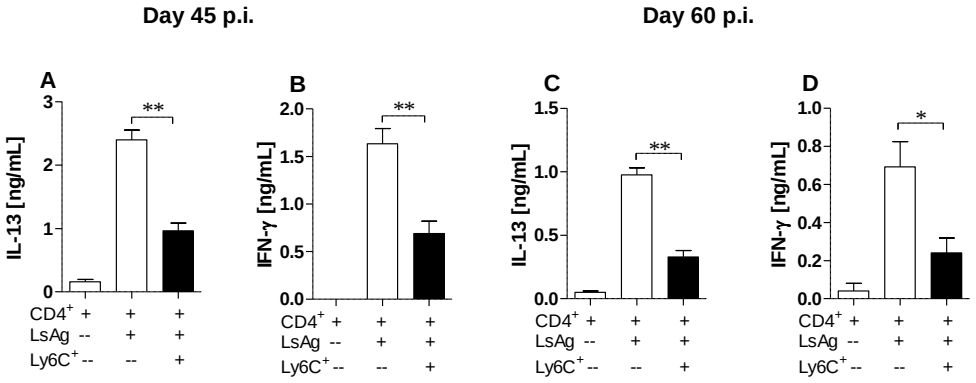

Figure 3.11: Suppression of filarial-specific $CD4^+$ T cells responses by pre-patent and post-patent Mo-MDSCs. On day 45 and 60 p.i., $CD4^+$ T cells and Mo-MDSCs ($Ly6C^+$) subsets were isolated from Ls-infected mice by flow cytometry. In brief, $CD4^+$ T cells ($1x10^5$) were cultured with GM-CSF-derived DC ($5x10^4$) and LsAg (50 µg/ml) in the presence or absence of $Ly6C^+$ MDSCs ($1x10^5$) for 72h. Supernatants were then screened for IL-13 (A,C) and IFN-γ (B,D) by ELISA. Graphs show mean ± SEM of 1 co-culture assay using pooled cells from 3-5 mice that were all infected at the same time point. Asterisks show significant differences (Mann-Whitney test) between the indicated groups (*$p<0.05$, **$p<0.01$).

3.2.4 *Ls-specific $CD4^+$ T cells produce IFN-γ and IL-13 upon LsAg stimulation*

To further demonstrate that the cytokines (IFN-γ and IL-13) that were shown to be suppressed by Mo-MDSCs were being specially released by T cells upon LsAg activation, $CD4^+$ T cells were isolated from Ls-infected mice on day 71 p.i., and stimulated with PMA (plus inhibitor) or LsAg

for 4h and then stained with CD4, IFN-γ and IL-13 antibodies to detect $CD4^+$ T cell-specific cytokine release.

Figure 3.12 shows that although Ls-specific $CD4^+$ T cells were able to produce IFN-γ and IL-13 without further stimulation (white bars), upon LsAg stimulation slightly higher levels of cytokines were observed (black bars). However, PMA was capable of inducing the highest levels of IFN-γ but the lowest levels of IL-13 (grey bars). These data indicate that Ls-specific $CD4^+$ T cells release Ls-specific IL-13 upon LsAg stimulation and IFN-γ release is not entirely dependent on LsAg stimulation.

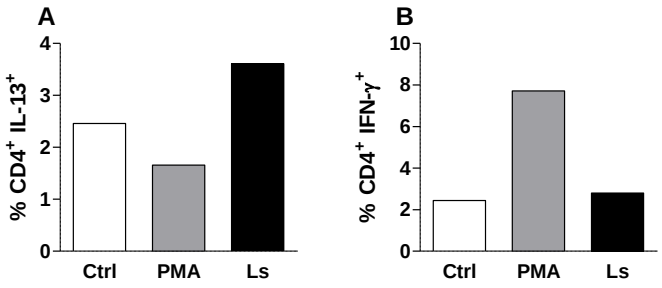

Figure 3.12: LsAg stimulation induces IFN-γ and IL-13 production by Ls-specific $CD4^+$ T cells. Wildtype BALB/c mice were naturally infected with Ls. On day 70-72 p.i., $CD4^+$ T cells were isolated from the spleen and left unstimulated or stimulated with LsAg or PMA for 4h and stained with a combination of CD4, IFN-γ and IL-13 antibodies to quantify levels of produced cytokines. Graphs show percentage of A) IL-13 and B) IFN-γ for LsAg (black bars), PMA (grey bars) and no further stimulated $CD4^+$ T cells (white bars).

3.3 IL-4R alpha and IL-5 deficiencies during Ls infection: role in MDSC-mediated suppression

Findings have indicated that IL-4 plays an important role in the immunity against murine Ls infection especially for the release of MF in BALB/c mice (Le Goff L et al., 2002; Volkmann et al., 2001). In addition, using adoptive transfer studies of viable MF, IL-5 –deficient BALB/c mice have been shown to have increased MF survival when compared to WT mice (Volkmann et al., 2003). These studies have explored the effects of IL-4R alpha (IL-4Rα) and IL-5 deficiencies separately but the outcome of infection and immune responses resulting from the lack of IL-13, IL-4 and IL-

5 activity in the same mice during Ls infection remains unclear. Furthermore, Mandruzzato and colleagues have suggested that the presence of the IL-4Rα is associated with the suppressive activity of Mo-MDSC in melanoma and colon carcinomas (Mandruzzato et al., 2009). Therefore, using IL-4Rα/IL-5 dKO BALB/c, the impact of such deficiencies during Ls infection and on MDSC function was investigated.

3.3.1 *MDSC-mediated filarial specific CD4$^+$ T-cell suppression occurs in an IL-4Rα-independent manner*

Studies have indicated that MDSCs suppress T cell responses through their IL-4Rα, a receptor that binds the Th2 related cytokines IL-4 and IL-13, which regulate IgE production by B cells. Indeed, cancer patients have been shown to have higher levels of IL-4Rα$^+$ MDSCs (Movahedi et al., 2008). Moreover, although researchers have provided evidence that receptor exists on both Mo-MDSC and PMN-MDSC subsets, further reports have shown that the suppression is only attributed to the Mo-MDSC subset (Mandruzzato et al., 2009). Thus, to investigate the role of IL-4/IL-5 signalling in regards to the suppressive ability of Mo-MDSCs during Ls infection, co-culture assays were performed as described in section 2.2.6 using cells from Ls-infected WT BALB/c or IL-4Rα/IL-5 dKO BALB/c mice.

Surprisingly, as shown in Figure 3.13, Mo-MDSCs derived from IL-4Rα/IL-5 dKO BALB/c mice as well as those derived from WT BALB/c, were able to suppress IL-13 (Figure 3.13 A, $p<0.01$) and IFN-γ (Figure 3.13 B, $p<0.01$) production by Ls-specific CD4$^+$ T cell responses indicating that neither the IL-4Rα nor IL-5 were involved in the observed suppression. Although Mo-MDSCs derived from IL-4Rα/IL-5 dKO BALB/c mice seemed to display a better suppressive ability compared to those from WT BALB/c mice, this trend was not statistically significant.

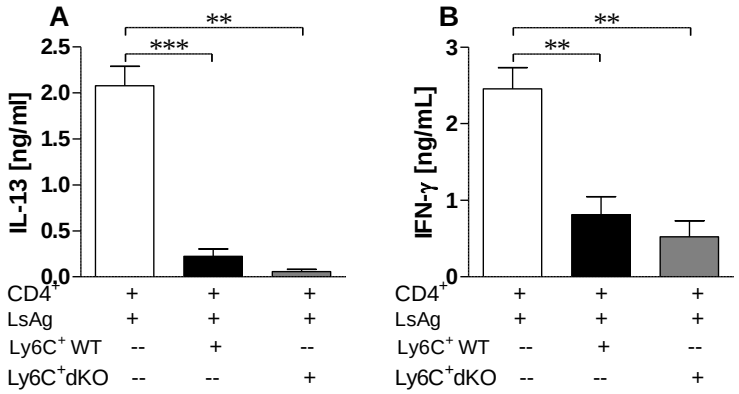

Figure 3.13: Mo-MDSCs suppression is IL-4Rα-independent. WT and IL-4Rα/IL-5 dKO BALB/c mice were naturally infected with Ls. On day 70-72 p.i., $CD4^+$ T cells and Mo-MDSCs subsets were isolated from Ls-infected mice by flow cytometry. WT $CD4^+$ T cells ($1x10^5$) were cultured with GM-CSF-derived DC ($5x10^4$) and LsAg (50 µg/ml) in the presence or absence of $Ly6C^+$ MDSCs ($1x10^5$) from WT (in black) or IL-4Rα/IL-5 dKO (in grey) for 72h. Supernatants were then screened for A) IL-13 and B) IFN-γ by ELISA. Graphs show mean ± SEM of 2/3 independent co-culture assays using pooled cells from 3-4 equally infected mice. Asterisks show significant differences (Mann-Whitney test) between the indicated groups (**p<0.01, ***p<0.001).

3.3.2 *High frequencies of Mo-MDSCs in the TC of Ls-infected IL-4Rα/IL-5 dKO BALB/c mice*

Since Mo-MDSCs derived from IL-4Rα/IL-5 dKO have shown differences in the suppressive ability compared to that from WT mice (although not statistically significant), the infiltration of MDSC populations within the TC was analyzed.

In the TC, levels of Mo-MDSC in either percentage or absolute cell number were higher in Ls-infected IL-4Rα/IL-5 dKO BALB/c when compared to WT mice (Figure 3.14 A and C, $p<0.01$ and 0.05, respectively) whereas populations of PMN-MDSC remained comparable (Figure 3.14 B and D). The baseline of MDSC frequencies was equal in naive WT and IL-4Rα/IL-5 dKO controls. This suggests that either the IL-4Rα or IL-5 or both had an impact on Mo-MDSC infiltration but not on that of PMN-MDSCs.

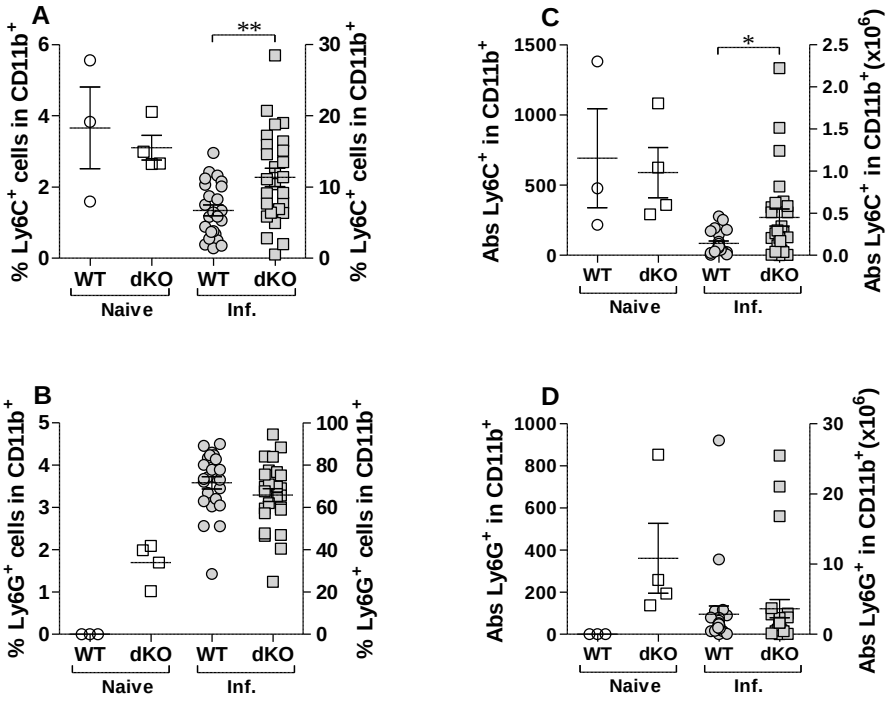

Figure 3.14: Increased frequencies and absolute cell numbers of Mo-MDSCs in Ls-infected IL-4Rα/IL-5 dKO BALB/c mice when compared to WT controls. WT and IL-4Rα/IL-5 dKO mice were left uninfected or naturally infected with Ls. On d70-72 p.i., cells were isolated from the thoracic cavity and stained with a combination of CD45, CD11b, Ly6C and Ly6G antibodies to differentiate monocytic ($CD11b^+Ly6C^+Ly6G^-$, Mo-MDSCs or $Ly6C^+$) and polymorphonuclear ($CD11b^+Ly6C^{int/lo}Ly6G^+$, PMN-MDSCs or $Ly6G^+$) MDSC populations. Comparison of percentage or absolute number of A) or C) Mo-MDSCs and B) or D) PMN-MDSCs within the $CD11b^+$ compartment. Symbols show values of n= 24 WT mice and n= 26 dKO mice in 3 independent infection studies. Asterisks indicate significant differences (Mann-Whitney test) between the groups indicated by the brackets (*p<0.05, **p<0.01).

3.3.3 *Ls-infected IL-4Rα/IL-5 dKO BALB/c mice harbor a higher worm burden and MF count when compared to WT BALB/c mice*

As mentioned above, MDSC populations positively correlated with worm burden but not systemic MF load (see section 3.1.4) and both the IL-4Rα and IL-5 were shown to impact parasite growth and MF clearance in Ls infection (Le Goff L et al., 2002; Volkmann et al., 2003; Volkmann et al., 2001). In accordance with this, parasitological parameters were analyzed in WT and IL-4Rα/IL-5 dKO BALB/c Ls-infected mice in the chronic phase. On day 72 p.i., worms were harvested from the thoracic cavity and screened for gender and length. MF counts were assessed in both blood and thoracic cavity fluid.

Importantly, worm burden was dramatically higher in IL-4Rα/IL-5 dKO when compared to WT BALB/c mice (Figure 3.15 A, p<0.001). In accordance, MF loads were also significantly elevated in IL-4Rα/IL-5 dKO when compared to WT BALB/c mice in blood (Figure 3.15 B, p<0.001) and at the site of infection, the TC (Figure 3.15 C, p<0.001) and also during the course of the infection (Figure 3.15 D). Furthermore, even though it has been reported that only a portion of Ls-infected BALB/c mice develop patency, all of the IL-4Rα/IL-5 dKO BALB/c mice became patent although wolbachia levels were higher in WT when compared to IL-4Rα/IL-5 dKO BALB/c mice (Figure 3.15 E, p<0.05) (Petit et al., 1992; Rodrigo et al., 2016). Collectively these data suggest that IL-4Rα and IL-5 deficiencies in BALB/c mice, increased worm burden and was associated with the induction of full patency and dramatic MF count during Ls infection (Ritter et al., 2017).

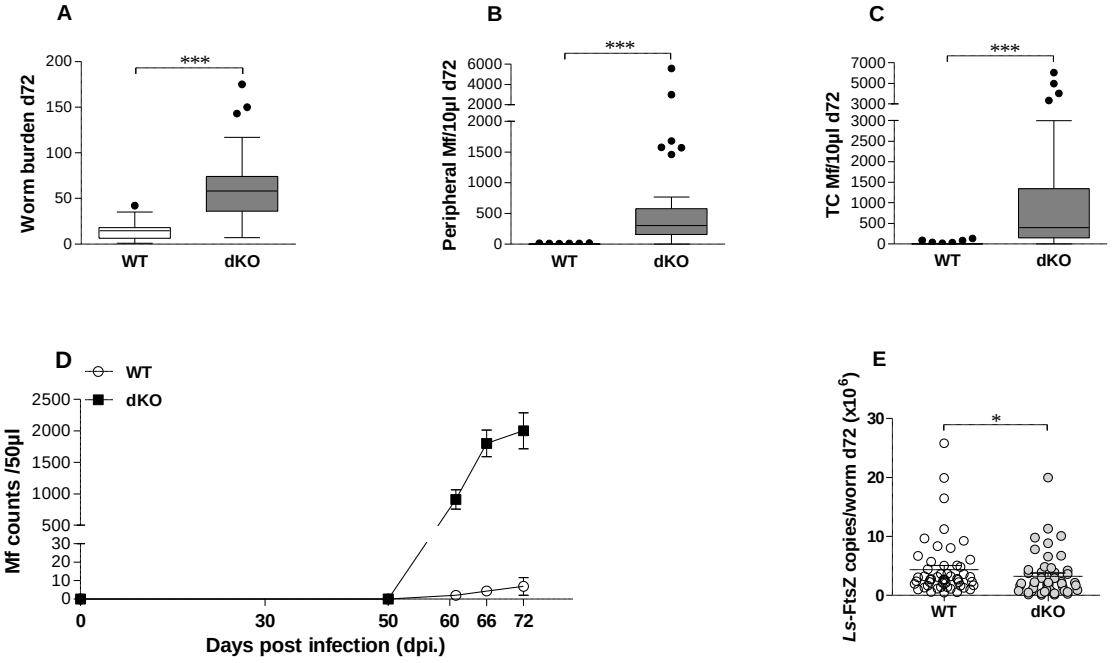

Figure 3.15: Elevated worm burden and MF count in IL-4Rα/IL-5 dKO versus WT BALB/c mice during Ls infection. WT BALB/c mice and IL-4Rα/IL-5 dKO mice were naturally infected with Ls. On day 71 p.i., worms were isolated from the thoracic cavity of individual mice and counted. A) displays worm burden on day 72 p.i. Mice were individually screened for the number of MF which was ascertained from 10 µl of B) blood or C) thoracic cavity fluid. D) shows MF counts during Ls infection. E) Levels of *Wolbachia* DNA were determined via a duplex PCR in individual adult female worms (n=51 WT and n=48 IL-4Rα/IL-5 dKO worms) on d72 p.i., data are from one of two independent infection studies (n=12 WT and n=15 IL-4Rα/IL-5 dKO mice) showing comparable results Graphs A), B) and C) show mean ± SEM of n= 36 WT mice and n= 43 dKO mice in 4 independent infection studies. Data in D) shows mean ± SEM from one of two independent infection studies (n=12 WT and n=15 IL-4Rα/IL-5 dKO mice) showing comparable results. Asterisks show significant differences (Mann-Whitney test) between the indicated groups (***p<0.001, *p<0.05).

Significantly higher worm burden and MF counts were observed in the thoracic cavity and periphery of Ls-infected IL-4Rα/IL-5 dKO when compared to WT BALB/c mice (see Figure 3.15). Subsequently, worms were counted according to their gender and the length was measured for each worm to analyze whether the two groups displayed any differences.

In line with the previous data, Ls-infected IL-4Rα/IL-5 dKO harbored significantly elevated numbers of male and female worms when compared to WT BALB/c mice in number (Figure 3.16 A, $p<0.001$) but not in percentage (Figure 3.16 B). Surprisingly, only male worms from the Ls-infected IL-4Rα/IL-5 dKO group were longer when compared to males from the WT BALB/c group (Figure 3.16 C, $p<0.001$). Female worms showed no significant differences between the two groups. Thus, these data demonstrated that Ls-infected IL-4Rα/IL-5 dKO not only harbor higher number of male and female worms when compared to WT BALB/c mice, but also offer a more suitable environment for the growth of male worms (Ritter et al., 2017).

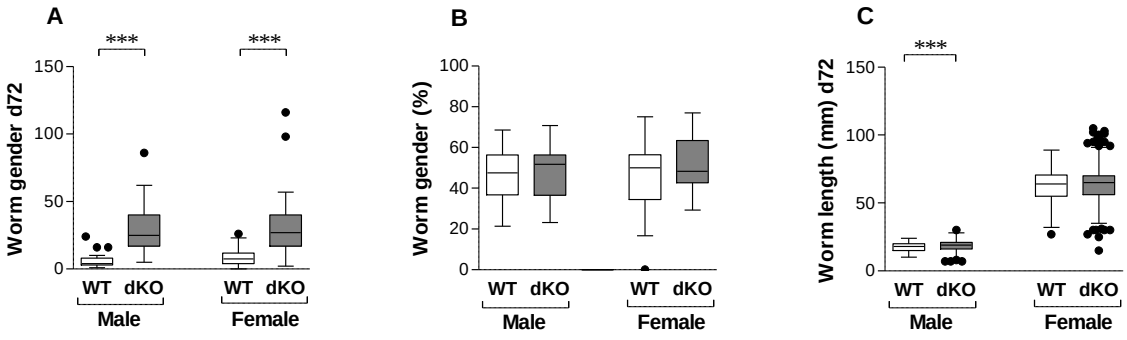

Figure 3.16: Male worms are longer in Ls-infected IL-4Rα/IL-5 dKO when compared to those from WT BALB/c mice. WT BALB/c mice and IL-4Rα/IL-5 dKO mice were naturally infected with Ls. On day 72 p.i., worms were isolated from the thoracic cavity of individual mice. They were counted, identified as male or female in A) number or percentage B) and C) the length of each worm was measured. Graphs show mean ± SEM of n= 36 WT mice and n= 43 dKO mice in 4 independent infection studies. Asterisks show significant differences (Mann-Whitney test) between the indicated groups (***$p<0.001$).

3.3.4 *IL-13 and IFN-γ production during Ls infection in IL-4Rα/IL-5 dKO BALB/c mice*

As mentioned above, no studies have demonstrated the implications of simultaneous IL-4Rα and IL-5 deficiencies in response to Ls infection. In the previous results sections, evidence was

provided that Mo-MDSCs could suppress IL-13 and IFN-γ production by Ls-specific $CD4^+$ T cells. Furthermore, IL-4Rα and IL-5 were not crucial for Mo-MDSC function. It is clear that Ls-infected IL-4Rα/IL-5 dKO BALB/c mice would have negligible levels of IL-13 but since it could be that Ls-infected IL-4Rα/IL-5 dKO and WT BALB/c mice display distinct ability for IFN-γ release, the possible differences in the production of IFN-γ in the two groups, have been evaluated in bulk cell and T cell assays. For confirmation of the dKO background, IL-13 release was also measured.

3.3.4.1 Ls-specific IFN-γ release is higher in co-cultures of cells from IL-4Rα/IL-5 dKO BALB/c mice

To compare the production of IFN-γ in IL-4Rα/IL-5 dKO BALB/c mice to that in Ls-infected WT BALB/c mice, single splenic and mediastinal lymph node (medLN) cells were cultured with or without LsAg.

As expected, regardless of the site (spleen or medLN) IL-13 production was higher in WT BALB/c mice when compared to IL-4Rα/IL-5 dKO BALB/c mice (Figure 3.17 A and C, $p<0.01$ and $p<0.001$, respectively) whereas IFN-γ production was interestingly higher in IL-4Rα/IL-5 dKO BALB/c mice when compared to WT BALB/c mice (Figure 3.17 B and D, $p<0.01$ and $p<0.001$, respectively), suggesting that IL-4Rα and IL-5 deficiencies significantly boost IFN-γ production (Ritter et al., 2017).

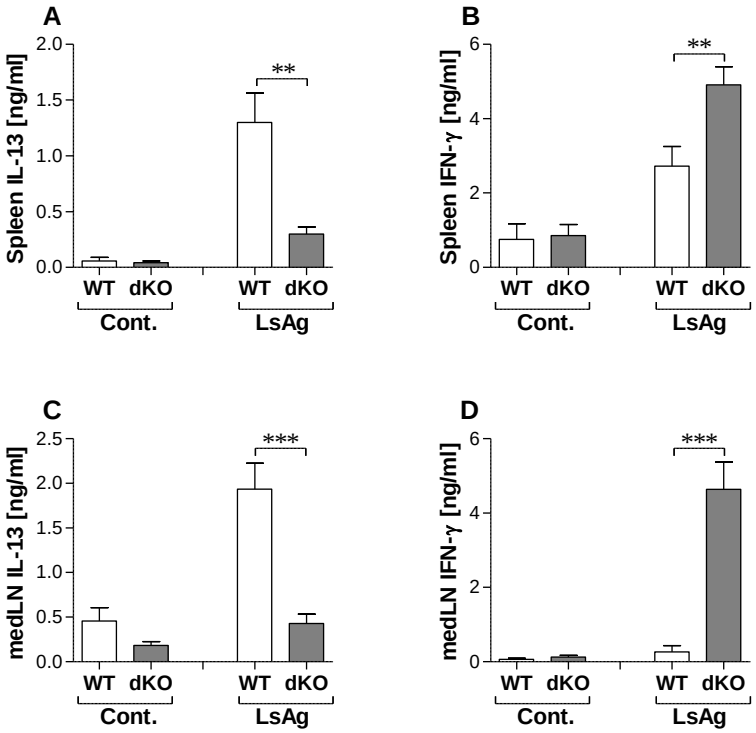

Figure 3.17: High levels of IFN-γ in cell co-cultures fromIL-4Rα/IL-5 dKO BALB/c mice. WT and IL-4Rα/IL-5 dKO BALB/c mice were naturally infected with Ls. On day 72 p.i., lymphocyte cultures were prepared from the spleen and medLN of individual mice and cultured with or without LsAg (50 µg/ml) for 96h. Supernatants were then screened for A) and C) IL-13 and B) and D) IFN-γ by ELISA. Graphs show mean ± SEM of (n= 20 WT mice and n= 24 dKO mice,for A) and B)) and (n= 24 WT mice and n= 25 dKO mice,for C) and D)) in 3 independent infection studies. Asterisks show significant differences (Mann-Whitney test) between the indicated groups (**p<0.01, ***p<0.001).

3.3.4.2 $CD4^+$ T cells derived from IL-4Rα/IL-5 dKO BALB/c mice secrete elevated levels of IFN-γ production upon re-stimulation with LsAg

In the above section it was shown that *in vitro* cultures of cells from the spleen or medLN of Ls-infected IL-4Rα/IL-5 dKO BALB/c mice produced strong IFN-γ responses. To assess the source of IFN-γ, $CD4^+$ T cell responses were measured in response to filarial-specific (LsAg) and filarial non-specific stimulation (αCD3/28).

Of interest, IFN-γ production was higher in IL-4Rα/IL-5 dKO upon both specific (LsAg) or non-specific stimulation (αCD3/28) when compared to WT BALB/c mice (Figure 3.18 B and E, $p<0.05$ and $p<0.01$, respectively), indicating that $CD4^+$ T cells might be the inducers of IFN-γ elevation in IL-4Rα/IL-5 dKO BALB/c mice. IL-13 data were similar to the results in the section above (Figure

3.16 A and D, p<0.001 and p<0.001, respectively). Since findings have described high Th17 responses along with increased Th2 responses in patients with severe dermal pathologies during onchocerciasis (Katawa et al., 2015), IL-17A levels have been assessed in T cell cultures. Importantly, results revealed that $CD4^+$ T cells from IL-4Rα/IL-5 dKO BALB/c mice, when in presence of GM-CSF-derived DC, were able to produce elevated amounts of IL-17A without stimulation or stimulated with non-specific Ag (αCD3/28) (Figure 3.18 C and F, p<0.05 and p<0.05, respectively) although $CD4^+$ T cells from WT BALB/c mice induced higher levels of the cytokine under LsAg stimulation (Ritter et al., 2017).

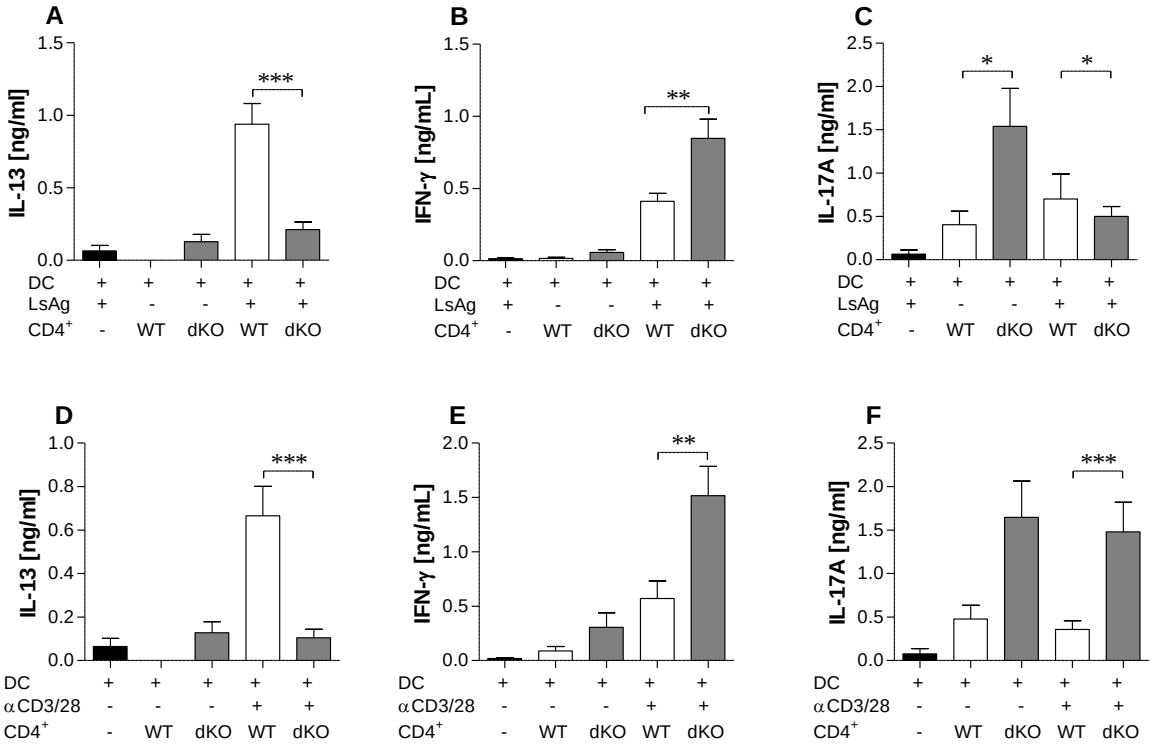

Figure 3.18: $CD4^+$ T cells as producers of IFN-γ in Ls-infected IL-4Rα/IL-5 dKO BALB/c mice. WT BALB/c mice and IL-4Rα/IL-5 dKO mice were naturally infected with Ls. On day 72 p.i., $CD4^+$ T cells were isolated from Ls-infected mice by flow cytometry. $CD4^+$ T cells ($1x10^5$) were cultured with GM-CSF-derived DC ($5x10^4$) with or without LsAg (50 µg/ml) or αCD3/28 (5 and 1,25 µg/ml) for 72h. Supernatants were then screened for A) and D) IL-13, B) and E) IFN-γ and C) and F) IL-17A by ELISA. Graphs show mean ± SEM of 4 culture assays using cells from 5-8 pooled mice from 2 independent infections. Asterisks show significant differences (Mann-Whitney test) between the indicated groups (*p<0.05, **p<0.01, ***p<0.001).

Apart from the full patency, elevated worm burden and longer male worms and higher MF count in Ls-infected in IL-4Rα/IL-5 dKO when compared to WT BALB/c mice, these mice show a more

pronounced inflammation in the pleural lung and diaphragm when compared to WT controls. This occurs at the final moult when worms become adults. With regards to the systemic responses, several chemokines like IP-10, MIP-1α, MIP-1β MIP-2 and RANTES were significantly increased in infected IL-4Rα/IL-5 dKO mice which have been shown to be crucial for immune cells recruitment. In addition, it could be that such milieu with increased chemokine gradients supports filarial development (Ritter et al., 2017).

3.4 Screening of mechanisms that may underline MDSC-mediated suppression during Ls infection

In the above sections, Mo-MDSCs were shown to have suppressive activity against Ls–specific $CD4^+$ T cell responses *in vitro* including IL-13 and IFN-γ production (see section 3.2). The suppression was demonstrated not to be dependent on whether the developed a patent state, that is, MF release into the periphery (section 3.2.2) and the suppressive nature of Mo-MDSCs was seen in both pre-patent (day 45) and patent (days 60 and 70-72) phases of infection (section 3.2.3 and 3.2.1). In addition, lack of IL-4/IL-5 signalling had no significant effect on the suppression (see section 3.3). Consequently, in this section the mechanisms involved in Mo-MDSC activity were more deeply investigated. As mentioned above, evidence has been provided that MDSCs function through either soluble factors (Hu et al., 2014; Sauer et al., 2001) or receptors (Lesokhin et al., 2012; Polz et al., 2014). This section explored different pathways that had the potential to be the underlying relevant mechanism(s) involved in Mo-MDSC-mediated suppression.

3.4.1 *CCR2 blockade does not impact Mo-MDSC function*

CCR2 is a receptor present on the surface of Mo-MDSCs but not PMN-MDSCs (Huang et al., 2007). Furthermore, some findings have suggested that this receptor influences the suppressive activity of Mo-MDSCs as seen models of cancers including skin cancer and in patient with melanoma (Gehad et al., 2012; Lesokhin et al., 2012). Accordingly, the implication of CCR2 in the Mo-MDSC-mediated suppression of filarial-specific $CD4^+$ T cell responses was analysed using anti-CCR2 neutralizing antibody (see section 2.2.6).

Figure 3.17 depicts the levels of cytokines that were produced by Ls-specific $CD4^+$ T cells following *in vitro* culture with Mo-MDSC and anti-CCR2. Interestingly, Mo-MDSCs were capable of suppressing IL-13 (Figure 3.19 A, $p<0.01$) and IFN-γ production (Figure 3.19 B, $p<0.01$) by Ls-specific $CD4^+$ T cells, even in the presence of anti-CCR2 neutralizing antibody: suggesting that they function independently of CCR2. However, the production of IFN-γ by Ls-specific $CD4^+$ T cells went significantly down in the presence of anti-CCR2 neutralizing antibody (Figure 3.19 B, $p<0.05$) which indicates that the absence of CCR2 receptor signalling hinders the production of IFN-γ following specific recall. Of note, mouse IgG1B, which is an isotype control for anti-CCR2 antibody showed no significant changes Collectively, these data demonstrated that blockade of CCR2 receptor did not remove the inhibition of Ls-specific $CD4^+$ T cell responses exerted by Mo-MDSCs.

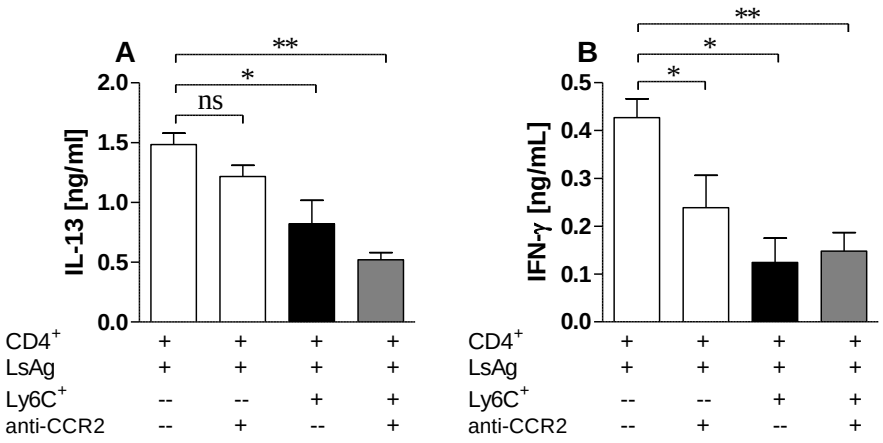

Figure 3.19: Mo-MDSC suppression of filarial-specific $CD4^+$ T cell responses is CCR2-independent. WT BALB/c mice were

naturally infected with Ls. On day 71 p.i., $CD4^+$ T cells and Mo-MDSCs were isolated from Ls-infected mice by flow cytometry. $CD4^+$ T cells ($1x10^5$) were cultured with GM-CSF-derived DC ($5x10^4$) and LsAg (50 µg/ml) in the presence or absence of $Ly6C^+$ MDSCs ($1x10^5$) and with or without anti-CCR2 (20 µg/ml) for 72h. Supernatants were then screened for A) IL-13 and B) IFN-γ by ELISA. Graphs show mean ± SEM of 1 of 3 co-culture assays using pooled cells from 5-10 mice from 3 independent infection studies showing comparable results. Asterisks show significant differences (Mann-Whitney test) between the indicated groups (*p<0.05, **p<0.01).

3.4.2 *Mo-MDSCs suppressive activity on filarial-specific $CD4^+$ T cells is not cell-cell contact dependant*

Recently, a study indicated that the suppressive activity of MDSCs occurred when these cells came into contact with T cells (Crook et al., 2015). To determine whether the suppressive activity of Mo-MDSC function on filarial-specific $CD4^+$ T cells required cell-cell contact, co-culture assays were performed using transwell inserts. In short, isolated Mo-MDSCs and $CD4^+$ T cells from infected WT BALB/c mice, day 70-72 p.i., were cultured with GM-CSF-derived DC and LsAg for 72h. In some cultures, the Mo-MDSCs were placed in the transwell insert, which is permeable to soluble factors but does not allow physical cell-cell contact.

Figure 3.20 reveals that in the absence of cell-cell contact, the ability of Mo-MDSCs to suppress IL-13 (Figure 3.20 A, $p<0.01$) and IFN-γ production (Figure 3.20 B, $p<0.01$) by filarial-specific $CD4^+$ T cells was maintained. This indicated that the suppression mediated by Mo-MDSCs on $CD4^+$ T cells was not cell-cell contact dependent and suggested that a soluble factor might be responsible for that function. These data tallied with the findings that neither the IL4R-α nor the CCR2 receptor was required for the suppression (see sections 3.3.1 and 3.4.1, respectively). Unexpectedly, in contrast to IFN-γ, the production of IL-13 by filarial-specific $CD4^+$ T cells was further suppressed in the absence of cell-cell contact (Figure 3.20 A, $p<0.05$), pointing out that cell-cell contact could interfere in Mo-MDSC-mediated suppression of IL-13. Of note, suppression of neither IL-13 nor IFN-γ, was abrogated in the absence of cell-cell contact. This indicated that although cell-cell contact could strengthen the suppression of IL-13 production by filarial-specific $CD4^+$ T cells, soluble mediators might be crucial for Mo-MDSC function.

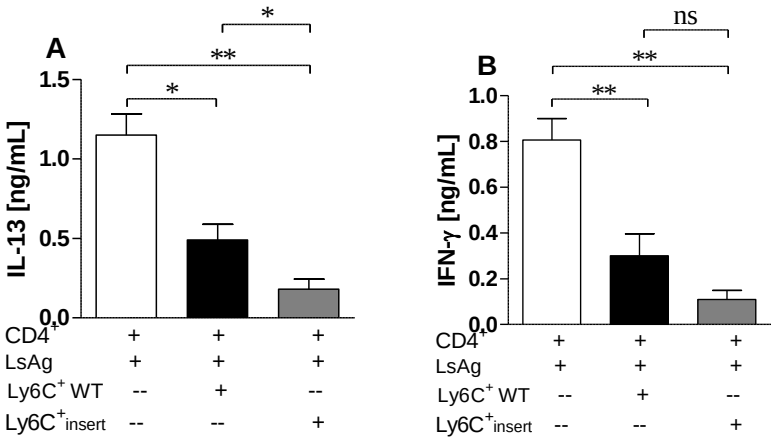

Figure 3.20: Suppression of filarial-specific CD4$^+$ T cell responses by Mo-MDSCs is not cell-cell contact dependent. WT BALB/c mice were naturally infected with Ls. On day 71 p.i., CD4$^+$ T cells and MDSCs subsets were isolated from Ls-infected mice by flow cytometry. CD4$^+$ T cells (1x10^5) were cultured with GM-CSF-derived DC (5x10^4), LsAg (50 µg/ml) and Ly6C$^+$ MDSCs (1x10^5) for 72h. For cell-cell contact analysis, Ly6C$^+$ MDSCs were placed in an insert. Supernatants were then screened for A) IL-13 and B) IFN-γ by ELISA. Graphs show mean ± SEM of 2 co-culture assays using pooled cells from 5 infected mice. Asterisks show significant differences (Mann-Whitney test) between the indicated groups (*p<0.05, **p<0.01).

3.4.3 *Neutralizing IL-10, IL-6 or TNF-α does not rescue IL-13 and IFN-γ production*

It has been reported that increases in IL-10 and IL-6 levels correlated with augmentation of Mo-MDSC levels in patients with cancer (Arihara et al., 2013; Mao et al., 2013). Using a murine model of airway allergic inflammation, Zhang and colleagues also showed that levels of total MDSCs correlated with high amounts of IL-10 and low levels of IL-12 in bronchoalveolar fluid (Zhang et al., 2013). Moreover, studies have suggested that the induction of Mo-MDSC subset can also occur upon TLR2/6 activation and infections with cutaneous bacteria led to elevated IL-6 production via TLR2/6 which favoured MDSC accumulation in the skin; in turn those MDSCs suppressed both CD4$^+$ and CD8$^+$ T cell responses (Skabytska et al., 2014). Recently MDSCs were shown to phagocytose *Mycobacterium tuberculosis* in a murine model of tuberculosis (TB) and consequently release IL-10, IL-6 and IL-1α (Knaul et al., 2014). In addition, Hu and colleagues have provided evidence for the requirement of the tumor necrosis factor receptor 2 (TNFR2) for MDSCs suppressive activity (Hu et al., 2014). However, Polz *et al.,* did demonstrate that TNFR2 expression is required for the generation and function of Mo-MDSCs *in vitro* (Polz et al., 2014).

On the basis of these findings, the influence of IL-10 and IL-6 on Mo-MDSC suppressive activity was explored using anti-IL-10 and anti-IL-6 neutralizing antibodies (see section 2.2.6). Since TNFR2 has been suggested as a potential mechanism for MDSC suppression as well, this parameter was studied too using anti-TNF-α neutralizing antibody (see section 2.2.6).

Figure 3.21 shows that neutralizing IL-10, IL-6 or TNF-α did not rescue IL-13 production by Ls-specific $CD4^+$ T cells, indicating that these cytokines were not relevant for Mo-MDSC suppressive activity (Figure 3.21 A, B and C, $p<0.05$, $p<0.01$ and $p<0.001$, respectively). Similarly, IFN-γ production was not impaired in the presence of anti-IL-10, anti-IL-6 or anti-TNF-α neutralizing antibodies (Figure 3.21 D, E and F, $p<0.05$, $p<0.01$ and $p<0.01$, respectively). In addition, mouse IgG1, which is an isotype control for anti-IL-10, anti-IL-6 or TNF-α antibodies showed no significant changes.

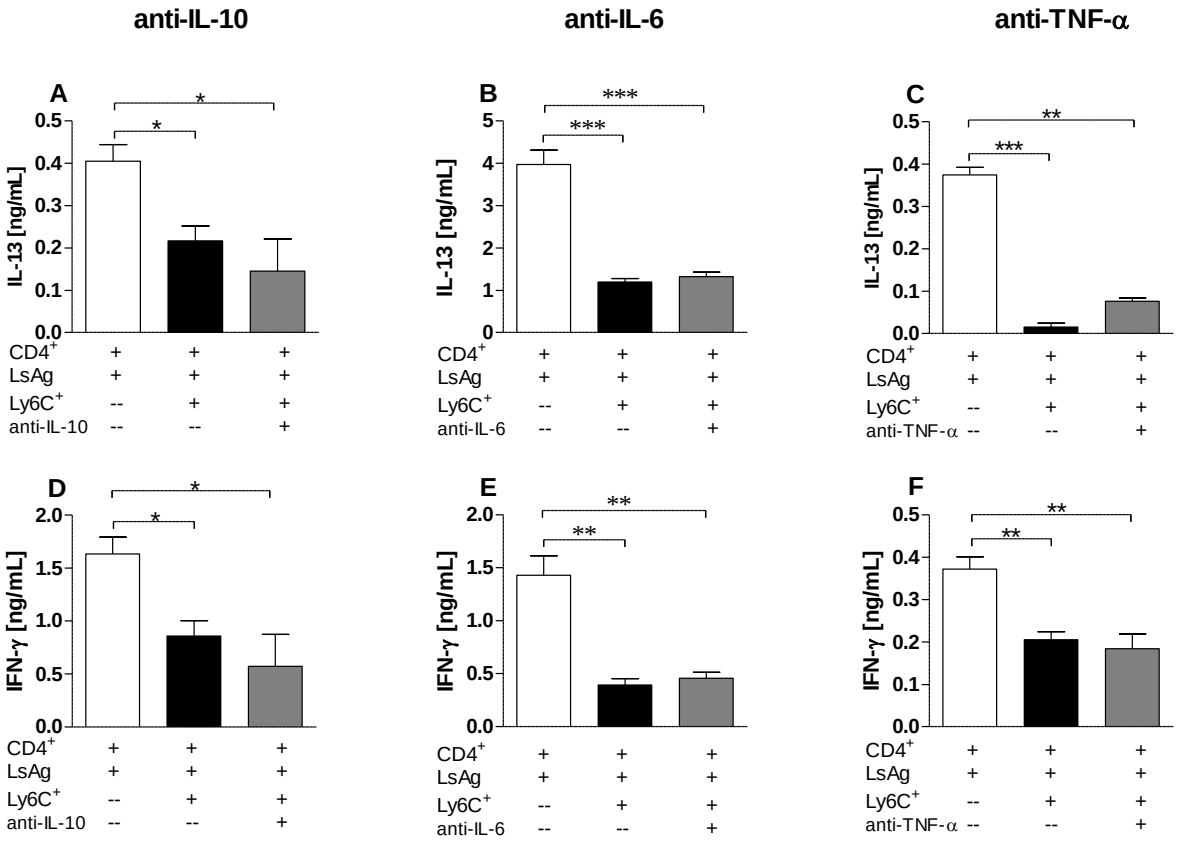

Figure 3.21: Mo-MDSCs suppression of filarial-specific $CD4^+$ T cell responses does not require IL-10, IL-6 or TNF-α. WT

BALB/c mice were naturally infected with Ls. On day 71 p.i., $CD4^+$ T cells and Mo-MDSCs were isolated from Ls-infected mice by flow cytometry. $CD4^+$ T cells ($1x10^5$) were cultured with GM-CSF-derived DC ($5x10^4$) and LsAg (50 µg/ml) in the presence or absence of $Ly6C^+$ MDSCs ($1x10^5$) and with or without anti-IL-10 (2 µg/ml), IL-6 (10 µg/ml) or TNF-α (0.5 µg/ml) for 72h. Supernatants were then screened for A, B and C) IL-13 and D, E and F) IFN-γ by ELISA. Each graph shows mean ± SEM of 3 of 7 co-culture assays using cells from 5-10 infected mice from 7 independent infection studies. Asterisks show significant differences (Mann-Whitney test) between the indicated groups (*p<0.05, **p<0.01, ***p<0.001).

3.4.4 *TGF-β blockade removes the suppression of IFN-γ production*

A study has indicated that there is a release of TGF-β, NO, ROS and IL-10 by MDSCs, which have been found to be suppressive, upon transmembrane and secreted tumor necrosis factor (tm-TNF and s-TNF) activation (Hu et al., 2014). On this basis, the involvement of the TGF-β/pathway in Mo-MDSC function was investigated using anti-TGF-β neutralizing antibody (see section 2.2.6).

Figure 3.22 demonstrates that the presence of anti-TGF-β neutralizing antibody in the culture did not impair the ability of Mo-MDSCs to suppress IL-13 (Figure 3.22 A, $p<0.01$) but the suppression on IFN-γ production by filarial-specific $CD4^+$ T cells, was significantly abrogated (Figure 3.22 B, $p<0.01$), inferring that this cytokine might play a partial role in Mo-MDSC suppression. Interestingly, the production of both IFN-γ and IL-13 was boosted in the presence of the neutralizing antibody in control wells (Figure 3.22, white bars) but the abrogation of IFN-γ production occurred only in the presence of Mo-MDSCs (Figure 3.22 B, $p<0.01$). Of note, MOPC-21, which is an isotype control for anti-TGF-β antibody showed no significant changes. This emphasized that TGF-β was involved in Mo-MDSC-mediated suppression of IFN-γ production.

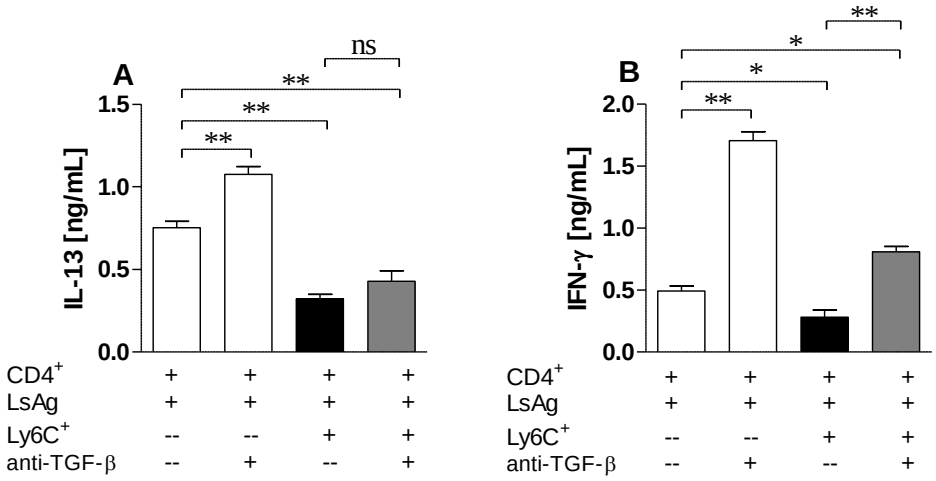

Figure 3.22: Mo-MDSCs suppression of IFN-γ by Ls-specific CD4$^+$ T cell is TGF-β dependent. WT BALB/c mice were naturally infected with Ls. On day 71 p.i., CD4$^+$ T cells and Mo-MDSCs were isolated from Ls-infected mice by flow cytometry. CD4$^+$ T cells (1x10^5) were cultured with GM-CSF-derived DC (5x10^4) and LsAg (50 µg/ml) in the presence or absence of Ly6C$^+$ MDSCs (1x10^5) and in the presence or absence of anti-TGF-β (10 µg/ml) for 72h. Supernatants were then screened for A) IL-13 and B) IFN-γ by ELISA. Graphs show mean ± SEM of 1 of 3 co-culture assays using cells from 5-10 infected mice from 3 independent infection studies. Asterisks show significant differences (Mann-Whitney test) between the indicated groups (**p<0.01).

3.4.5 *Nitric oxide is involved in Mo-MDSC mediated suppression of IL-13 production*

In a collagen-induced arthritis model, Crook *et al.* have demonstrated that Mo-MDSCs limited autologous B cell proliferation and antibody production in an NO and PGE_2-dependent manner (Crook et al., 2015). Thus, in the following experiment the requirement of NO in Mo-MDSC mediated suppressive activity on Ls-specific CD4$^+$ T cell responses, was tested. Again, Mo-MDSCs and CD4$^+$ T cells were isolated from infected WT BALB/c mice and cultured with GM-CSF derived DC and LsAg in the presence or absence of L-NMMA (Abcam, Cambridge, UK), which is an inhibitor of NOS (NOS being an enzyme which catalyzes NO production) (see section 2.2.6).

Surprisingly, inhibiting NOS in the culture milieu, rescued the production of IL-13 (Figure 3.23 A) by Ls-specific CD4$^+$ T cells whereas the production of IFN-γ remained suppressed (Figure 3.23 B, p<0.01) and NO levels were higher in the wells with positive control when compared to those with Mo-MDSCs (Figure 3.23 C, p<0.01). Of note, sterile PBS was used as isotype control for the NOS inhibitor and showed no significant changes. These data suggested that NO is a mediator of

Mo-MDSC-mediated suppression on IL-13 production and shows that there are two potential pathways in which MDSCs suppress filarial specific responses.

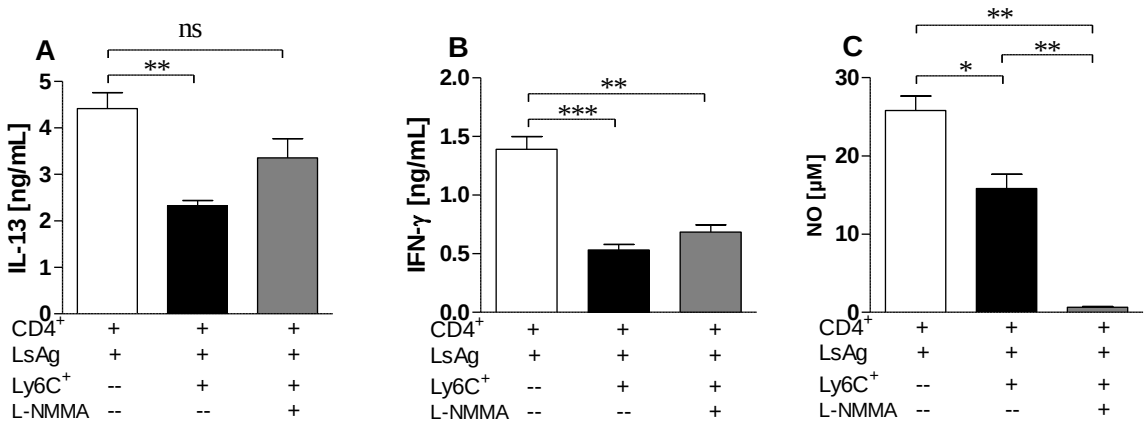

Figure 3.23: Differential role of nitric oxide (NO) in Mo-MDSCs mediated suppression. WT BALB/c mice were naturally infected with Ls. On day 71 p.i., $CD4^+$ T cells and Mo-MDSCs were isolated from Ls-infected mice by flow cytometry. $CD4^+$ T cells ($1x10^5$) were cultured with GM-CSF-derived DC ($5x10^4$) and LsAg (50 µg/ml) in the presence or absence of $Ly6C^+$ MDSCs ($1x10^5$) and with or whithout L-NMMA (5 mM) for 72h. Supernatants were then screened for A) IL-13 and B) IFN-γ by ELISA or C) nitrite oxide by Griess reaction. Graphs show mean ± SEM of 1 of 3 co-culture assays using cells from 5-10 infected mice from 3 independent infection studies. Asterisks show significant differences (Mann-Whitney test) between the indicated groups (*p<0.05, **p<0.01, ***p<0.001).

3.5 Gene profilling of MDSC subsets arising during Ls infection: innate and adaptive immune responses

In order to perform an in-depth analysis of MDSC subsets, Mo-MDSCs and PMN-MDSCs were isolated and sorted from the TC of infected WT BALB/c mice on day 71 p.i. and naive mice (standing for controls). Their extracted RNAs served to assess the profile of innate and adaptive genes using the RT2 profiler PCR array mouse Innate & Adaptive Immune Responses kit (Qiagen, Gielgen).

An overview of the genes that were down- or up-regulated in Mo-MDSCs and PMN-MDSCs isolated from Ls-infected WT BALB/c mice when compared to those from naive mice, is depicted in Tables 3.1, 3.2, 3.3 and 3.4, respectively. Surprisingly, data from the PCR array showed that both Mo-MDSCs and PMN-MDSCs isolated from infected mice displayed an up-regulation of

FOXP3 (Forkhead box P3), a transcription factor for regulatory T cells (Tregs) that is actively involved in their regulatory pathway (Tables 3.3 and 3.4). However, a down-regulation of genes including C3 (Complement component 3), CCR6 (Chemokine (C-C motif) receptor 6) and IL-18 (Interleukin 18) was observed in the two subsets (Tables 3.1 and 3.2). The three latter genes play a major role in complement activation, migration and recruitment of effector cells and cell-mediated immunity, respectively; during inflammatory responses. In addition, the array demonstrated that the two subsets from infected mice up-regulated the gene NFKB1 (Nuclear factor of kappa light polypeptide gene enhancer in B-cells 1, p105), of which the product NF-kB, stimulates the expression of a range of genes involved in biological functions. This globally indicated that the two subsets seem to share high regulatory and rather low inflammatory properties.

When considering the Mo-MDSC population, the array further showed that MYD88, the central adaptor protein used by most TLRs (Toll-like receptors) to activate NF-kB was highly expressed in Mo-MDSCs isolated from infected mice when compared to the naive control (p=0.005016) (see Table 3.3). Substantiating this, was the positive fold-change observed in TLR8 (p=0.015218) and together with the up-regulation of NFKB1, indicated that NF-kB might play a role in Mo-MDSC suppressive activity. Interestingly, the genes for the cytokines IFN-γ and IL-13 were also up-regulated in Mo-MDSCs isolated from Ls-infected WT BALB/c mice when compared to those from naive controls (p=0.002364 and 0.027058, respectively) (Table 3.3), suggesting the ability of the cells to release such cytokines. Other genes that were up-regulated in Mo-MDSCs included FasL (Fas ligand, p= 0.000814), LY96 (Lymphocyte antigen 96, also known as MD2, a protein which is associated with TLR4 and induces responsiveness to LPS, p= 0.03942), Mpo (Myeloperoxidase, p= 0.017737) and TBX21 (T box 21, p= 0.012174) (Table 3.3). Such genes are primarily involved in innate responses against cancer, bacteria and other microorganisms and

their up-regulation illustrates that Mo-MDSCs, in this setting, could qualify for an innate immune group of cells. On the other hand these data were unexpected since it is well established that MDSC subsets inhibit anti-cancer immunity.

In contrast, IRF3 and 7 (Interferon regulatory factor 3 and 7), genes involved in immunity against viral infection were down-regulated (p=0.000229 and 0.004402, respectively), implying that there may be an impaired ability of these infection-derived Mo-MDSCs to counteract viruses. Data from the PCR array further indicated that Mo-MDSCs possessed no capacity for antigen presentation to $T_{\chi\delta}$ cells, as shown by the negative fold-change of H2-T23 gene (Histocompatibility 2, T region locus 23, p=0.000019). In line with the down-regulation of IL-18 in both MDSC subsets, Mo-MDSCs showed additionally a negative fold-change in the expression of IL-1α, a cytokine that can be released upon inflammasome activation (p=0.014621). NOD1 (Nucleotide-binding oligomerization domain containing 1, a receptor involved in the secretion of IL-1β, a major pro-inflammatory cytokine following inflammasome activation) was also down-regulated as revealed by the array (p=0.045602), ruling out the implication of the inflammasomes in Mo-MDSC suppressive activity. In fact, frequencies of MDSC populations in the TC of Ls-infected ASC-deficient mice (a central adaptor molecule in the inflammasome pathway) and WT BALB/c mice on days 10 and 72 p.i. indicated that the lack of ASC did not impair the two MDSC subsets although PMN-MDSC levels were found to be increased in ASC-deficient mice on day 10 (Figure 3.24). Surprisingly, MAPK1 (Mitogen-activated protein kinase 1) was also down-regulated (p=0.000283), although CXCR3 (Chemokine (C-X-C motif) receptor 3) which when bound by its ligands activates MAPK1, was up-regulated (p=0.005499). More intriguing was the opposite regulation observed in IFNGR1 (Interferon gamma receptor 1) (down-regulated, p=0.002929) and IFN-γ (up-regulated, p=0.002364), contrasting with the results of *in vitro* assays (see Figure 3.7). Further down-regulated genes included ITGAM (Integrin

alpha M, p=0.000007), CCR5 (Chemokine (C-C motif) receptor 5, p=0.015038), TRAF6 (Tnf receptor-associated factor 6, p=0.000131) and RORC (RAR-related orphan receptor gamma, p=0.00539) (Table 3.1).

With regards to the genes regulated in the PMN-MDSC subset alone, the PCR array data showed a down-regulation of NFKBIA (polypeptide gene enhancer in B-cells inhibitor, alpha; p=0) which supports the up-regulation of NFKB1 (p=0.01314) and the gene responsible for NLRP3 (NOD-like receptor family, pyrin domain containing 3) inflammasome was also down-regulated (p= 0.006923) (Table 3.2). The up-regulated genes comprised of CD86 (p=0.014497), CXCL10 (p=0.024228), IFNAR1 (p=0.040521), NOD2 (p=0.01544) and STAT3 (p=0.009197) (Table 3.4).

Table 3.1: Down-regulated genes in Mo-MDSCs

Gene	**Description**	**p-value**
C3	Complement component 3	0
CCR5	Chemokine (C-C motif) receptor 5	0.015038
CCR6	Chemokine (C-C motif) receptor 6	0.00881
H2-T23	Histocompatibility 2, T region locus 23	0.000019
IFNGR1	Interferon gamma receptor 1	0.002929
IL18	Interleukin 18	0.041412
IL-1α	Interleukin 1 alpha	0.014621
IRF3	Interferon regulatory factor 3	0.000229
IRF7	Interferon regulatory factor 7	0.004402
ITGAM	Integrin alpha M	0.000007
MAPK1	Mitogen-activated protein kinase 1	0.000283
NOD1	Nucleotide-binding oligomerization domain containing 1	0.045602
RORC	RAR-related orphan receptor gamma	0.00539
TRAF6	TNF receptor-associated factor 6	0.000131

Table 3.2: Down-regulated genes in PMN-MDSCs

Gene	Description	p-value
C3	Complement component 3	0
CCR6	Chemokine (C-C motif) receptor 6	0.022937
IL-18	Interleukin 18	0.020914
NFKBIA	polypeptide gene enhancer in B-cells inhibitor, alpha	0
NLRP3	NLR family, pyrin domain containing 3	0.006923

Table 3.3: Up-regulated genes in Mo-MDSCs

Gene	Description	p-value
CXCR3	Chemokine (C-X-C motif) receptor 3	0.005499
FasL	Fas ligand (TNF superfamily, member 6)	0.000814
FOXP3	Forkhead box P3	0.00323
IFN-γ	Interferon gamma	0.002364
IL-13	Interleukin 13	0.027058
LY96	Lymphocyte antigen 96	0.03942
MPO	Myeloperoxidase	0.017737
MYD88	Myeloid differentiation primary response gene 88	0.005016
NFKB1	Nuclear factor of kappa light polypeptide gene enhancer in B-cells 1, p105	0.045602
TBX21	T-box 21	0.012174
TLR8	Toll-like receptor 8	0.015218

Table 3.4: Up-regulated genes in PMN-MDSCs

Gene	Description	p-value
CD86	CD86 antigen	0.014497
CXCL10	Chemokine (C-X-C motif) ligand 10	0.024228
FOXP3	Forkhead box P3	0.003258
IFNAR1	Interferon (alpha and beta) receptor 1	0.040521
NFKB1	Nuclear factor of kappa light polypeptide gene enhancer in B-cells 1, p105	0.01314
NOD2	Oligomerization domain containing 2	0.01544
STAT3	Signal transducer and activator of transcription 3	0.009197

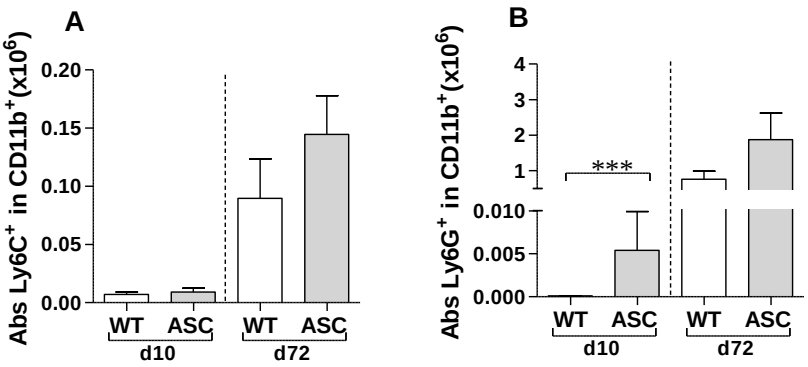

Figure 3.24: Higher frequencies of PMN-MDSCs in Ls-infected ASC-deficient mice at an early time point. WT and $ASC^{-/-}$ BALB/c mice were naturally infected with Ls for 10 and 72 days. Thereafter, cells were isolated from the thoracic cavity and stained with a combination of CD45, CD11b, Ly6C and Ly6G antibodies to differentiate monocytic ($CD11b^{+}Ly6C^{+}Ly6G^{-}$, Mo-MDSCs or Ly6C) and polymornuclear ($CD11b^{+}Ly6C^{int/lo}Ly6G^{+}$, PMN-MDSCs or Ly6G) MDSC populations. A) Mo-MDSC and B) PMN-MDSC subsets within the $CD11b^{+}$ cell compartment of infected mice. Day 10 WT n= 10 and $ASC^{-/-}$ n=14; day 72 WT n=6 and $ASC^{-/-}$ n=5. Graphs show mean ± SEM from one infection study per time point. Asterisks indicate significant differences (Mann-Whitney test) between the groups indicated by the brackets (***$p<0.001$).

4. DISCUSSION

67.88 million people are infected with LF in countries including sub-saharan african, south-east asian and south american countries (Ramaiah and Ottesen, 2014). Three species of filarial nematode parasites known as *W. bancrofti*, *B. malayi* and *B. timori* cause the disease with *W. bancrofti* being responsible for 90% of cases (WHO, 2015). In endemic areas for LF, populations are classified as endemic normal, asymptomatic which are either patent (MF+) or latent (MF-) and symptomatic individuals which present swelling of the limbs or hydrocele. Since MF+ subjects pose the higher risk of transmitting the infection, they should be given special attention in order to control the spread of the disease (Arndts et al., 2012). In infected patients, only 50% will become patent and this is well represented in the laboratory BALB/c mouse strain when naturally infected with Ls; which is then used as a murine model to study filarial infections (Graham et al., 2005; Hoffmann et al., 2001; Le Goff L et al., 2002; Petit et al., 1992; Rodrigo et al., 2016). Ls infection has been shown to induce regulatory cell populations including Tregs, IL-10 producing cells and AAMs (Ajendra et al., 2014) (see section 1.2). Recently, another regulatory cell population termed MDSCs have been described. MDSCs are immature myeloid cells and are precursors of dentritic cells (DC), macrophages and/or granulocytes and it is now well accepted that they encompass two subsets: monocytic MDSCs (Mo-MDSCs) and granulocytic or polymorphonuclear MDSCs (PMN-MDSCs). These subsets function through different mechanisms: whilst Mo-MDSCs function via nitric oxide (NO), PNM-MDSCs react through ROS (reactive oxygen species) and Arg-1. In human or murine models of disease, MDSCs have been shown to have a role in cancer, bacterial and parasitic infections, acute and chronic inflammation and other pathological conditions including AIDS as reviewed in Tamadaho et al (Tamadaho et al., 2018) (see section 1.3). Data described here show that MDSCs are induced and expand at the site of infection during Ls infection and displayed distinct functional activities

according to their subsets. Interestingly, in contrast to PMN-MDSCs, Mo-MDSCs had the ability to suppress IFN-γ and IL-13 production by Ls-specific $CD4^+$T cells through the release of TGF-β and NO, as the blockade of these two components prevented IFN-γ and IL-13 respectively. However, both subsets significantly up-regulated regulatory genes while the expression of pro-inflammatory genes was at very low levels.

4.1 Identification of MDSC subsets during Ls infection

MDSCs present phenotypic and functional features that discriminate them from mature innate cells including DC, macrophages and granulocytes as reviewed by Bronte *et al* (Bronte et al., 1999). They can be distinguish as $CD11b^+Ly6C^{hi}Ly6G^-$ for Mo-MDSCs and $CD11b^+Ly6C^{lo}$/int$Ly6G^+$ for PMN-MDSCs. Studies have reported the role of MDSCs in malignancies, infectious and other pathological conditions (Knaul et al., 2014; Pan et al., 2013; Voisin et al., 2004) but their role in helminth infections remains unclear. Thus, using the laboratory BALB/c mouse strain, which allows the complete Ls life-cycle, MDSC subsets at the site of infection were investigated during Ls infection by flow cytometry. Data revealed that in the absence of infection, very few MDSCs were within the TC fluid whereas large numbers of the cells were identified after infection. Furthermore, there was a significantly high number of PMN-MDSCs when compared to Mo-MDSCs in the period of time where MF release reached its peak: days 70-72 p.i. These data confirmed results from Youn *et al.*, which have demonstrated that in contrast to Mo-MDSCs which accumulated at lower levels, PMN-MDSCs have been seen to exponentially accumulate in tumor models (Youn et al., 2008). However, other studies from the same authors have claimed for a possible switch of Mo-MDSCs into PMN-MDSCs through Rb1 (Youn et al., 2013). It is unlikely that this same scenario applies in this study as tracking MDSC populations throughout the course the infection showed no indication of significant increases in Mo-MDSCs whereas

PMN-MDSC levels dramatically increased after moulting into adult worms, at approximately day 30.

In cancer, MDSC frequencies have been associated with both the state and progression of pathology (Almand et al., 2000; Arihara et al., 2013) and the presence of these cells has become a sign for mortality (Gabitass et al., 2011). Here, MDSC infiltration positively correlated with worm burden (strongly) as well as with MF counts in the TC fluid (at least weakly) but not at a systemic level. On the one hand, these data suggest that the worms offer a favourable ground for MDSC infiltration or vice versa, promoting chronic infection. This is in line with recent findings which demonstrated that after adoptive transfer of MDSCs, there was a persistent chronic phase of infection with the nematode *Heligmosomoides polygyrus bakeri*, (Valanparambil et al., 2017). On the other hand, since the release of MF has been reported to be indispensible for transmission (Arndts et al., 2012), the irrelevance of systemic MF for MDSC infiltration might indicate that these cells only act during ongoing infections and do not guarantee further infection. However more in depth analysis are need to support this hypothesis.

4.2 Mo-MDSCs suppress filarial-specific $CD4^+$ T cell responses

The hallmark of MDSCs is their suppressive ability on T cell responses and within the context of this thesis, a co-culture assay was designed in order to evaluate MDSC function on $CD4^+$ T cell responses during Ls infection; as studies have provided evidence that those cells play a critical role during the inflammation (Al-Qaoud et al., 1997). Here, data revealed for the first time that upon re-stimulation of $CD4^+$ T cells from infected mice with LsAg, the presence of Mo-MDSCs but not PMN-MDSCs from infected mice was sufficient to impair the release of IL-2, IFN-γ, and IL-13 but not IL-5 and suppression was not dependent on patency. In line with this, Cui *et al.,* using

flow cytometry, demonstrated the suppression of IL-2 and IFN-γ production by $CD4^+$ T cells and also that of granzyme B production by $CD8^+$ T cells in ovarian cancer patients (Cui et al., 2013). In addition, Ren and colleagues described an increase of IFN-γ production by $CD4^+$ T cells after MDSC depletion from PBMCs of HCV patients, suggesting a suppressive function of MDSCs although the effect of Mo-MDSCs was not specifically ascertained (Ren et al., 2016). In contrast, data from primary glioblastoma patients have found that Mo-MDSCs were not able to suppress T cell responses, confining the suppressive function in that scenario to neutrophilic MDSCs. Indeed, these authors have observed diverse MDSC subsets including monocytic, granulocytic, neutrophilic, eosinophilic and immature MDSCs and have reported a slight inhibition of T cell responses by eosinophilic MDSCs (Dubinski et al., 2016).

In regards to murine settings, Zhu and colleagues have found that in a murine model of hepatitis, $SSC^{high}CD11b^{high}Ly\text{-}6C^{high}Ly\text{-}6G^{low}$MDSCs, corresponding to Mo-MDSCs, were the only subsets capable of suppressing $CD4^+$ T cell responses (and weakly $CD8^+$ T cells), while the other MDSC-like (likely PMN-MDSCs) compartment was not capable of doing so (Zhu et al., 2014). Recently, isolated $CD11c^-CD11b^+Gr1^+$ cells from mice infected with *Heligmosomoides polygyrus bakeri* infection suppressed OVA-specific $CD4^+$ T cell proliferation (Valanparambil et al., 2017). Although these findings were partially in accordance with the suppression observed in this study, they did not differentiate between Mo-MDSCs and PMN-MDSCs and did not inform on the role of MDSCs on helminth-specific responses. Elsewhere, studies in C57BL/6 mice have noted the inhibition of not only T cell responses but also that of B cell responses by Mo-MDSCs in murine LP-BM5 retroviral infection (Green et al., 2013; Rastad and Green, 2016). However, such investigations do not explain the non-suppressive ability of PMN-MDSCs observed here. This study revealed that the MDSC-mediated suppressive function was not associated with cell accumulation, as PMN-MDSC numbers in the TC were higher when compared to Mo-MDSCs. Considering the fact

that, these results were observed in an *in vitro* co-culture, in those scenarios, a compenent (cytokine/chemokine/cell type) may be missing that aids the suppression of $CD4^+$ T cell responses by PMN-MDSCs. Also, it is possible that the parameter being suppressed by these cells were not measured. Future investigations could look at the effect of the lack of PMN-MDSCs on patency or filarial development or whether there are able to suppress other cells such as $CD8^+$ T cells or B cells during infection. Previously, the suppressive activity of both PMN and Mo-MDSCs was claimed to be comparable in various models of tumor-bearing mice (Youn et al., 2008). In contrast, Raber and colleagues indicated that PMN-MDSCs were better at impairing proliferation and expression of effector molecules in activated T cells when compared to Mo-MDSCs at the tumor site of several tumor models including lung carcinoma and melanoma (Raber et al., 2014). It could be that a different scenario occurs at systemic level. In this study, only Mo-MDSCs were isolated from the site of infection whereas $CD4^+$ T cells were from the spleen of infected mice. Further studies could investigate the impact Mo-MDSCs on $CD4^+$ T cells, coming both from the same site; either from the TC, blood or other tissues.

4.3 Impact of Ls infection on IL-4Rα/IL-5 dKO BALB/c mice

Firstly, highly increased numbers of MF and adult worms and 100% patency were observed in Ls-infected IL-4Rα/IL-5 dKO BALB/c mice on days 70-72 p.i., when compared to wildtype controls. This confirms data of previous studies that provided evidence for elevated MF release in the absence of IL-4 and IL-5 secretion in murine filariasis (Le Goff L et al., 2002; Volkmann et al., 2003; Volkmann et al., 2001). In addition, IL-4 has been reported to retain MF development in *Brugia pahangi* infected mice (Devaney et al., 2002). Interestingly, these findings suggested no conflicting role of IL-13 on parasite development as the authors found that both WT and the IL-4-deficent mice groups had comparable levels of IL-13. Data described here showed that, while an

increase was observed in the numbers of both male and female worms in Ls-infected IL-4Rα/IL-5 dKO BALB/c mice, an increase in length was observed only in male worms, arguing for a possible relevance of Th2 cytokines on worm gender. Interestingly, while no immune-competent laboratory mouse strain has been found to be permissive for human *Loa loa* infection, Tendongfor and colleagues have noted higher survival of *Loa loa* worms in IL-4R/IL-5 dKO BALB/c mice (Tendongfor et al., 2012), suggesting that IL-4/IL-5 signalling is also critical for controlling the development other filarial parasites.

Secondly, co-culture experiments revealed that spleen and mLN from Ls-infected IL-4Rα/IL-5 dKO BALB/c mice produced elevated levels of IFN-γ following re-stimulation with LsAg. Correspondingly, higher levels of this cytokine were measured in cell-culture supernatants of Ls-specific $CD4^+$ T cells from these mice when compared to WT clearly suggesting that those cells are a source of IFN-γ. As expected, IL-13 levels were lower in Ls-infected IL-4Rα/IL-5 dKO BALB/c mice when compared to that of WT mice. This implied a dramatic polarization towards Th1 responses in these deficient mice. In 2012, findings from Ziewer and colleagues described the induction of IFN-γ in BALB/c mice after immunization with Alum-MF which led to decreased microfilaraemia (Ziewer et al., 2012). It will be interesting to investigate the effects of such immunization in IL-4Rα/IL-5 dKO BALB/c mice. Of note, IFN-γ induction in Ls-infected IL-4Rα/IL-5 dKO BALB/c mice was accompanied by elevated IL-17A levels and accentuated pathology at the site of infection (Ritter et al., 2017). In a recent study on onchocerciasis it was reported that patients with severe dermal pathologies presented elevated Th2 (IL-4) and Th17 responses (Katawa et al., 2015).

Thirdly, increased numbers of Mo-MDSCs were found in Ls-infected IL-4Rα/IL-5 dKO BALB/c mice when compared to WT controls whereas the proportion of PMN remained unchanged within the two groups. As mentioned above, the Mo-MDSCs, that were shown to be suppressive, remained

at a constant steady state throughout infection whereas numbers of PMN-MDSCs continued to increase in Ls-infected WT BALB/c mice (see section 3.1.3). The data here clearly shows that the lack of IL-4/IL-5 signalling seems to facilitate Mo-MDSCs in Ls-infected IL-4Rα/IL-5 dKO BALB/c mice on days 70-72 p.i. However, the kinetics of the two MDSCs subsets was not traced during the course of infection in those mice and therefore future research could compare the influence of the simultaneous lack of IL-4Rα and IL-5 on MDSC expansion during infection. Furthermore, the suppressive function of Mo-MDSCs was not impaired in IL-4Rα/IL-5 dKO BALB/c mice contrasting with studies from Mandruzzato and colleagues who have suggested that the presence of IL-4Rα is only associated with the suppressive activity of Mo-MDSCs in melanoma and colon carcinomas (Mandruzzato et al., 2009). In line with the findings of this study, are data which used IL-4Rα KO mice and indicated that IL-4Rα is not indispensible for MDSC function (Sinha et al., 2012) and in this study, Mo-MDSCs did not suppress IL-5 production by Ls-specific $CD4^+$ T cells from WT mice. Further investigations using single IL-5 KO and IL-4Rα could help to rule out clearly the relevance of such pathways in the observed Mo-MDSC suppressive activity.

4.4 Mo-MDSCs function through receptor-independent pathway

In the recent years, authors have provided evidence for diverse mechanisms used by MDSCs for their suppressive activities. These include receptor- (CCR2, TNFR2, IL-4Rα), or soluble factor-based pathways (mostly NO and ROS) as reviewed by Nagaraj *et al.* (Nagaraj et al., 2013). Previously, patients with cancer have been reported to exhibit high levels of IL-$4R\alpha^+$ MDSCs with suppressive abilities (Movahedi et al., 2008). Here, as already discussed in the precedent section, the lack of this receptor induced an environment that allowed a higher number of Mo-MDSCs at the site of infection (see section 3.3.2). In fact, co-cultures of Mo-MDSCs isolated from Ls-infected IL-4Rα/IL-5 dKO BALB/c mice could suppress IL-13 and IFN-γ production by Ls-specific

$CD4^+$ T cells even further (although not significantly). This confirmed data from Sinha and colleagues who described a maintained suppressive function of MDSCs after using MDSCs derived from IL-4Rα KO mice in several model of tumors. The impact of PMN-MDSCs could be excluded since the authors have performed assays using separately Mo-MDSCs and PMN-MDSCs similar to the isolation procedure performed in these studies.

Recently, studies in obese mice with renal tumors have highlighted the implication of the CCL2/CCR2 pathway in the development of an immunosuppressive environment through MDSCs (Hale et al., 2015). CCR2 played a role in specifically facilitating the recruitment of mature monocyte/macrophages as well as MDSCs to areas of inflammation and injury (Charo and Ransohoff, 2006; Gehad et al., 2012; Lesokhin et al., 2012). In an attempt to evaluate the role of CCR2in MDSC function during Ls-infection, anti-CCR2 neutralizing Ab was used in the aforementioned co-culture assays (see section 3.4.1) and showed that Mo-MDSCs kept their suppressive ability even during CCR2 blockade: conferring no significance to the chemokine receptor in the setting of this thesis. In contrast to that and using MDSCs generated from $CCR2^{-/-}$ C57BL/6 mice, Qin and colleagues showed that these cells failed to migrate to islet allografts and to suppress $CD8^+$ T cells under *in vivo* conditions which resulted in enhanced Tregs activity. However, they were able to exert *in vitro* inhibition (Qin et al., 2016). Since CCR2 is mainly involved in the migration of cells, which occurs during the course of infection, it is possible that the anti-CCR2 neutralizing Ab as used in this study, was not able to block the activity of the receptor *in vitro* and perhaps that Mo-MDSCs require CCR2 to influence only $CD8^+$ T cell but not $CD4^+$ T cell responses. These reasons could explain the conflicting results observed here and also the fact that these authors used generated MDSCs. In addition, data from Schmid *et al*, indicated that the CCR2 receptor was impaired in Mo-MDSCs derived from *Leishmania major* infected BALB/c when compared to those from C57BL/6 mice (Schmid et al., 2014), suggesting that the

presence and thus the activity of this receptor in mice may be strain-dependent. Therefore to clarify the role that CCR2 plays in MDSC function during Ls infection, more experiments are needed using $CCR2^{-/-}$ BALB/c mice and especially, using MDSCs that lack the receptor. In addition, it will be interesting to investigate whether MDSC act synergistically with Tregs to control Ls-stemmed inflammation since research related to this thesis reported an expansion of Tregs throughout Ls-infection in BALB/c mice (Rodrigo et al., 2016).

In 2016, studies demonstrated that MDSCs promoted the expansion of IgA-producing B cells in a contact-dependent manner and MDSC function was abrogated in TNFR2 KO mice (Xu et al., 2016). These findings are in line with other researches that have demonstrated the role of TNFR2 in MDSC generation and suppressive activities (Hu et al., 2014; Polz et al., 2014). Results generated here, using anti-TNF-α neutralizing Ab due to the lack of acces to genetically deficient TNFR2 BALB/c KO mice, informed on the non-relevance of such cytokine for Mo-MDSC function. This contrasts with the recent observations reported by Atretkhany and colleagues who used TNF humanized (hTNF KI) mice, to show that blockade of TNF activity ameliorated fibroblastic sarcoma growth and led to a decreased MDSC accumulation (Atretkhany et al., 2016). However, more in depth analysis are required before such findings can be generalized to the Ls infection system. Nonetheless, cell-contact pathways could be clearly excluded as the main functional mechanism for Mo-MDSC suppressive activity since Mo-MDSCs were able to suppress IL-13 (here even better) and IFN-γ production by Ls-specific $CD4^+$ T cells in transwell assays (section 3.4.2). This contradicts earlier data which explained that Mo-MDSCs inhibit $CD4^+$ T and B cell proliferation and antibody production by B cells in a cell-contact dependent manner in the CIA model of autoimmune disease (Crook et al., 2015) suggesting that these cells may employ a different mechanism in non-pathogenic scenarios.

4.5 Soluble factors control Mo-MDSC function during Ls infection

Under pathological conditions, studies have suggested an association between MDSC accumulation and IL-6 in both mouse and human settings (Knaul et al., 2014; Mao et al., 2013; Skabytska et al., 2014). Recently, Peng and colleagues proposed a cross-talk between the release of IL-6 from MDSCs. This release phophorylates STAT3 and activates Notch in an NO-dependent manner to prolong STAT3 activation (Peng et al., 2016). However, their suggested pathway was deciphered using total MDSCs and evidence has been provided that Mo-MDSCs and PMN-MDSCs require STAT1 and STAT3, respectively (Albeituni et al., 2013). Their argument, might on the one hand, be partially supported by the fact that the suppressive function of Mo-MDSCs can be abrogated in the presence of a NOS inhibitor. On the other hand; it contrasts data presented in the current setting since here, there was no requirement of IL-6 for Mo-MDSC function during Ls infection. Paradoxically, others have illustrated that in the presence of mesemchymal stem cells (MSCs) from chronic myeloid leukemia (CML), the generation of G-MDSCs (likely PMN-MDSCs) has been induced which was associated with a high expression of TGF-β, IL-6 and IL-10. Moreover, they recorded higher expression levels of TNF-α, IL-1β, COX2 and IL-6 in these CML-MSCs derived G-MDSCs when compared to those stemming from healthy donors (HD)-MSCs (Giallongo et al., 2016). Although this did not match the setting used in the described Ls infection studies, due to differences in the subset of MDSCs: here, the function of Mo-MDSCs but not PMN-MDSCs was assessed, it nevertheless indicated probable factors implicated in MDSC function.

Co-culture experiments with anti-IL-10 neutralizing Ab also revealed that Mo-MDSCs did not require this cytokine for their functional activity, neither for the suppression of IFN-γ production nor that of IL-13. These observations differ from those noted in a murine model of airway allergic inflammation or individuals with hepatocellular carcinoma (Arihara et al., 2013; Zhang et

al., 2013). Likewise, evidence has been provided that MDSCs synthesize IL-10 in response to biofilm-associated *S. aureus* where they lead to the persistence of the bacterial infection (Heim et al., 2015). Findings in Ls infection with C57BL/6 mice have shown that the suppression of the onset of Ag-specific cellular responses requires T cell-derived IL-10 (Haben et al., 2013) but other reports have pointed out a hyporesponsiveness of $CD4^+$ T cells occurring in Ls infection with BALB/c mice in an IL-10 independent manner (Taylor et al., 2006; Taylor et al., 2005). However the role of IL-10 for Ls infection-derived Mo-MDSCs remains unclear.

Another immunomodulatory molecule relevant in filarial infections is TGF-β and studies using cells from LF infected patients have demonstrated the rescue of IFN-γ production in the presence of anti-TGF-β blocking Ab *in vitro*. In addition, elevated levels of TGF-β producing $CD4^+$ T cells have been shown in Ls-infected mice upon induction of airway disease in a murine model of asthma, which participated in the amelioration of airway reactivity and dramatically decreased after administration of anti-TGF-β blocking Ab (Babu et al., 2006). Here, results revealed a role of TGF-β in the suppression of IFN-γ production by Ls-specific $CD4^+$ T cells by infection-derived Mo-MDSCs. These results build on findings in a murine model of AIDS that have illustrated a crucial role for iNOS, ROS or cysteine in Mo-MDSC suppressive activity and more importantly, have shown TGF-β to enable the induction of such function in these cells against B cell responses (Rastad and Green, 2016). Conversely, a new report has demonstrated a direct relationship between Tregs and MDSC differentiation and function in a murine model of colitis (Lee et al., 2016). Indeed, these investigations have shown that TGF-β, induced by Tregs, polarizes MDSCs towards Mo-MDSC differentiation with strong inhibitory effects. Based on the results of this thesis, it might seem obvious that Mo-MDSCs employed TGF-β to suppress IFN-γ production by Ls-specific $CD4^+$ T cells.

In the presence of L-NMMA, which is an inhibitor of NOS, Mo-MDSCs failed to suppress IL-13 production by Ls-specific $CD4^+$ T cells whereas IFN-γ suppression remained intact. In support of this, investigations using a murine model of hepatitis described the involvement of NO in the suppressive function of Mo-MDSCs. However, in contrast to the studies described here it was shown to be a cell-contact dependent mechanism and there were elevated expression levels of CCR2 on the cells (Zhu et al., 2014). In addition, isolated $CD11c^-CD11b^+Gr1^+$ cells have been found to suppress OVA-specific $CD4^+$ T cell proliferation in infection caused by *Heligmosomoides polygyrus bakeri*. This suppression occurred in an NO-dependent manner and nematode specific IL-4 production *in vitro* (Valanparambil et al., 2017). With regards to filariasis, previous studies have demonstrated an IFN-γ-dependent induction of NO which impaired the *in vitro* proliferation of Ag-specific splenocytes and $CD4^+$ T cells in a *Brugia pahangi* model upon MF infection. These findings suggested parasite stage-based responses as infection with L3-stage larvae led to different responses (O'Connor and Devaney, 2002; O'Connor et al., 2000). This suggests the requirement of IFN-γ for Mo-MDSC suppression of IL-13 and might explain the failure of the suppression of IFN-γ production by Ls-specific $CD4^+$ T cells in the presence of NOS inhibitor. Therefore, in further co-culture experiments, it will be interesting to examine the scenario during *in vitro* IFN-γ blockade. Furthermore, *in vivo* MF clearance in an Ls model, which is a completely different scenario than a chronic setting, has been shown to use a NO-independent mechanism (Hoffmann et al., 2001; Pfaff et al., 2000). Similar results have been found using *in vivo* assays with *B. malayi* infection (Gray and Lawrence, 2002), setting out seemingly possible conflicting data for in vivo function of Mo-MDSCs during Ls infection.

4.6 Profile of gene regulation in MDSC subsets during Ls infection

This section discusses, the observations related to the gene expression profiles observed in MDSC populations during Ls infection. Interestingly, when compared to Mo-MDSCs isolated from naive mice, Mo-MDSCs from Ls-infected mice showed significantly, a) up-regulation of the genes: CXCR3, FasL, FOXP3, IFN-γ, IL13, LY96, MPO, MYD88, NFKB1, TBX21 and TLR8 and b) down-regulation of: C3, CCR5, CCR6, H2-T23, IFNGR1, IL-1α, IL-18, IRF3, IRF7, ITGAM, MAPK1, NOD1, RORC and TRAF6. With regards to PMN-MDSCs, comparison between cells isolated from naive versus Ls-infected showed a) up-regulation of the genes: CD86, CXCL10, FOXP3, IFNAR1, NFKB1, NOD2 and STAT3 and b) the down-regulation of genes including: C3, CCR6, IL18, NFKBIA and NLPR3.

4.6.1 The regulation of genes responsible for soluble factors in Mo-MDSC function

The pro-inflammatory activity of inflammasomes induces IL-1β and IL-1α secretion and the release of IL-1α is both NLRP3-dependent and NLRP3-independent (Gross et al., 2012; Ritter et al., 2010; Yazdi and Drexler, 2013). For instance, the NLRP3-dependent release of IL-1α has been shown to be activated upon exposure to nanoparticles (Yazdi et al., 2010). Using deficient-mice, IL-1α has been found to participate in the control of *Candida albicans* infection (Vonk et al., 2006) and also to be relevant in diabetes (Kamari et al., 2011). Here, results provided evidence that the gene responsible for IL-1α expression is shut down in Mo-MDSCs during Ls infection and the presence of Mo-MDSCs in co-culture assays did not affect IL-1β production (data not shown), suggesting that Mo-MDSC function might not be influenced by IL-1 cytokines. In agreement with these findings, studies in patients with Cryopyrin-associated periodic syndromes under anti-IL-1 therapy have noted elevated MDSC numbers that displayed suppressive activity (Ballbach et al., 2016). This indicated the non-requirement of IL-1 for MDSC function in such settings. In contrast, MDSCs that stemmed from adipocyte-tissues have been reported to impair B lymphopoiesis in

an IL-1 (both IL-1α and IL-1β) dependent manner (Kennedy and Knight, 2015), suggesting a differential role for IL-1 molecules in MDSC function according to the pathology, cell type and location. Furthermore, MDSCs have been shown to phagocytose *Mycobacterium tuberculosis* and produce high levels of IL-1α (Knaul et al., 2014). Additionally, IL-18, another component released upon activation of the inflammasomes, was found to be down-regulated in both Mo-MDSCs and PMN-MDSCs subsets isolated from Ls-infected mice when compared to those of naive mice. Considering the fact that in this study, at day 72 p.i., FACS data revealed no differences in the infiltration of either Mo-MDSCs or PNM-MDSCs in WT when compared to ASC-deficient (apoptosis-associated speck-like protein containing CARD) mice (Figure 3.24); and since the Nlrp3 gene was also found to be down-regulated in PMN-MDSCs from infected mice, the involvement of the expression of inflammasome molecules for MDSC expansion could be excluded, although it could be that the inflammasomes support Mo-MDSC function in other ways. For instance, studies have reported that IL-18-induction promote the differentiation and suppressive activities of generated Mo-MDSCs in C57BL/6 mice (Lim et al., 2014). Further studies should investigate whether inflammasome pathways play a role in Mo-MDSC suppressive activities in BALB/c during Ls infection.

PCR array data revealed a high expression of IL-13 in Mo-MDSCs isolated from Ls infected mice, which is interesting since these cells were able to suppress the release of IL-13 by $CD4^+$ T cells upon re-stimulation with Ls antigen and *in vitro* levels of IL-13 from infection-derived Mo-MDSCs were megligible. Building on these observations were findings from Gabitass and colleagues who have measured increased levels of IL-13 in PBMCs from patients with pancreatic, esophageal and gastric cancers. Interestingly, IL-13 levels also correlated with MDSCs numbers (Gabitass et al., 2011). Elsewhere, $CD11b^+$IL-4Rα^+ MDSCs have been reported to produce IL-13 and IFN-γ which led to the suppression of $CD8^+$ T cells (Gallina et al., 2006). Previously, studies have shown the

generation of MDSCs within four days from BM using G-CSF and GM-CSF and the addition of IL-13. These IL-13-induced MDSCs exhibited high *in vitro* and *in vivo* suppressive abilities during graft-versus-host disease and have been revealed to correspond to Mo-MDSCs (Highfill et al., 2010). Also patients with hepatocellular carcinoma have displayed elevated concentrations of IL-10, IL-13 and VEGF concentrations which correlated with levels of $CD14^{+}HLA\text{-}DR^{-/lo}$ MDSCs (Mo-MDSCs) (Arihara et al., 2013). An association has been observed between IL-13 and MDSCs and M2 macrophages in esophageal cancer (Gao et al., 2014). However, data from these results showed an opposite trend for IFN-γ, contrasting with the PCR results found here as both IL-13 and IFN-γ were highly expressed in Mo-MDSCs. Nevertheless, studies by Gabitass *et al.*, have shown the production of IL-13 and IFN-γ by MDSCs (Gabitass et al., 2011), supporting the PCR data but contrasting with the *in vitro* measurements of these cytokines in Mo-MDSCs. To respond to IFN-γ, cells require the surface expression of a heterodimeric receptor, IFNGR, which consists of the IFNGR1 and IFNGR2 subunits (Rayamajhi et al., 2010). Unexpectedly, PCR data revealed down-regulation of IFNGR1 in Mo-MDSCs isolated from Ls infected mice, ruling out any autocrine effect of IFN-γ on Mo-MDSCs. In accordance with these results are findings that have reported an association between the reduced activation of macrophages by IFN-γ and an increased reduction of *ifngr1* (but not *ifngr2*) transcripts in *L. monocytogenes* infection (Rayamajhi et al., 2010). Furthermore, the present data showed a down-regulation of interferon regulatory factors (IRF-3 and IRF-7) in support to the down-regulation of IFNGR1. However, regulation of IRF7 has been documented only for PMN-MDSCs but not Mo-MDSCs in various cancer patients (Yang Q et al., 2017), indicating that these investigations conflicted data of this study. Interestingly, results from the PCR array showed that the genes responsible for IFNAR1 (Interferon (alpha and beta) receptor 1) was up-regulated in the PMN subset, corroborating with

recent findings which have suggested that the activation of MDSCs through IFNAR pathway in a model of cancer (Shime et al., 2014).

The gene controlling the production of the chemokine CXCL10, an attractant for $CD8^+$ T cells (CTLs), was up-regulated in PMN-MDSCs from Ls-infected mice. In contrast, a study has shown the inverse association of this chemokine with MDSC development in human prostate cancer (Muthuswamy et al., 2016). When considering PMN-MDSCs specifically, a report has previously indicated that an increase in CXCL10 and CTLs levels has been attributed to a reduction of PMN-MDSC numbers in the tumor microenvironment and has been accompanied by a delay of pathogenesis in a model of glioma (Fujita et al., 2011). Here although PMN-MDSCs were elevated in the TC, an up-regulation of CXCL10 was observed implying that CXCL10 supported PMN-MDSC accumulation. It was also probable that this chemokine negatively regulated PMN-MDSC suppressive activity but further experiments are needed to confirm such hypothesis.

Myeloperoxidase (MPO) is a major component of the primary (azurophilic) granules especially in young neutrophils and is also present in much lower concentrations in monocytes and macrophages (Prata et al., 2016). It has been suggested as a characteristic for chronic inflammation, as reviewed elsewhere (Prokopowicz et al., 2012). Here, high expression of the MPO gene was found in Mo-MDSCs isolated from Ls-infected mice when compared to those of naive mice, suggesting that Ls infection induced elevated MPO expression in Mo-MDSCs. Previously, MPO has been demonstrated to have the potential of controlling disease activity and treatment outcomes in patients with ulcerative colitis (Wagner et al., 2008). However, recent studies have shown decreased MPO activity after the transplantation of bone marrow-derived G-MDSCs from normal mice to colitis models resulting in increased survival rate (Su et al., 2013). Different results have been generated in the context of this thesis, as the up-regulation of the MPO gene observed here was related to the Mo-MDSC subset.

PCR data further demonstrated down-regulation of the Complement component C3 in both Mo-MDSCs and PMN-MDSCs. Consistent with these results, a report has indicated that complement component C3 deficiency is associated with a favorable condition for MDSC induction with beneficial effects, in a model of diabetes (Gao et al., 2014). Inversely, hepatic stellate cells derived from mice lacking Complement component C3, have been shown to display an impaired MDSC induction and in doing so exhibited no protection on co-transplanted islet allografts (Hsieh et al., 2013), suggesting a pathology-related regulation by the complement component C3.

4.6.2 The regulation of receptor and transcription factor genes and other genes in MDSC populations

NOD1 mediates the sensing of a motif of peptidoglycan that is produced by most Gram-negative and specific Gram-positive bacteria such as *Listeria monocytogenes* (Chamaillard et al., 2003; Girardin et al., 2003). In addition, NOD1 has been shown to trigger the recruitment of immune cells (Masumoto et al., 2006). Results generated during this thesis indicated the down-regulation of this molecule in Mo-MDSCs, suggesting that Mo-MDSCs might not be recruited through recognition of NOD1. In contrast, findings in *B. malayi* subjects have shown elevated expression of NOD1 and NOD2 in lymphedema patients compared to asymptomatic individuals (Babu et al., 2009). Recently, studies have reported that NOD1 activation can occur in a *Wolbachia*-dependent manner (Ajendra et al., 2016). Here, Mo-MDSC suppression function was ascertained upon re-stimulation with LsAg which contains *Wolbachia* and therefore it would be interesting to assess the behavior of Mo-MDSCs upon stimulation with *Wolbachia*-depleted LsAg. Importantly the aforementioned study has deciphered a NOD2-dependent mechanism for neutrophil recruitment at early stage of Ls infection (Ajendra et al., 2016), suggesting elevated numbers of neutrophils at this phase. However, in this thesis PMN-MDSCs, which are a granulocytic

(neutrophilic) subset, that were isolated from Ls-infected mice at later time point (on day 71 p.i.), elicited an up-regulation of NOD2, pointing out their requirement of such a receptor to accumulate in the TC even at late stage of infection.

CCR6, a chemokine receptor associated with DC and T cell housing, was found down-regulated in both subsets of MDSCs during Ls infection. Furthermore, data from Mo-MDSCs especially indicated the down-regulated expression of CCR5. In support with this are data that have been recently provided in a collagen-induced arthritis (CIA) mouse model in which, Mo-MDSCs have been associated with lower expression levels of IL-10, TGF-β1, CCR5, and CXCR2 mRNA (Wang et al., 2015). In contrary, other studies have demonstrated the up-regulation of CCR5 ligands in Mo-MDSCs and have conferred an up-regulation of CCR5 itself on Tregs. In fact, the authors have claimed that MDSCs have been capable of attracting Tregs based on their increased expression of CCR5 (Schlecker et al., 2012).

Surprisingly, here, data from the PCR array demonstrated the up-regulation of the FOXP3 gene in Mo-MDSCs and PMN-MDSCs during Ls infection, indicating that both subsets might share the expression of the surface marker Foxp3 together with Tregs that could support their role as regulator of immune responses and this also indicated that not only Tregs express FOXP3. Further studies should investigate the role of FOXP3 on MDSCs and how this marker could possibly influence MDSC function. Also intriguing was the observed up-regulation of CXCR3 expression in Mo-MDSCs during Ls infection, since this chemokine receptor is mainly expressed on Th1 cells. Similar observations have been noticed with the up-regulation of TBX21 (T-bet), the key regulator of the Th1 phenotype differentiation system, in Mo-MDSCs during Ls infection. The down-regulation of RORC, a transcription factor of Th17 cells, was noted in Mo-MDSCs in the current model of Ls infection. This is not supported by recent findings which have attributed a role for RORC1 in MDSC expansion. Indeed, mice lacking this nuclear transcriptor failed to induce

MDSC differentiation (Strauss et al., 2015). Interestingly, the gene responsible for the expression of STAT3 is up-regulated in PMN-MDSCs, corroborating with previous findings. In fact, a study has reported that STAT3 played a main role in PMN-MDSC-mediated function (Albeituni et al., 2013). Furthermore, PMN-MDSCs have been shown to facilitate immunotolerance in pregnant mice and have been found to differentiate and be activated through STAT3 signalling (Pan et al., 2016). In contrast, authors have suggested that STAT3 activation promoted Mo-MDSCs in a murine model of pancreatic cancer (Panni et al., 2014).

NF-kB is required for both innate and adaptive immune responses and using BMP4 which causes a defect in NF-kB signalling authors generated a reduced amount of MDSCs that showed impaired immunosuppressive abilities (Cao et al., 2014). Consistent with these findings, data of this thesis showed an up-regulation of NFKB1 (NF-kB) in the two subsets of MDSCs isolated during Ls infection and in PMN-MDSCs this up-regulation was supported by a down-regulation of NFKBIA: an inhibitor of NF-kB. This was followed by high expression levels of TLR8 and Lymphocyte antigen 96 (Ly96) (also known as MD2 a protein which binds to TLR4 and is associated with responsiveness to lipopolysaccharide (LPS)) in Mo-MDSCs. In support with this, studies by Shirota *et al.*, have shown the presence of TLR7, 8 and 9 on MDSCs (Shirota et al., 2012). Furthermore, an elevated expression of MYD88 the adaptor protein was observed, providing evidence for potent activities in Mo-MDSCs during Ls infection. However, TNF receptor associated factor-6 (TRAF6), a receptor induced in response to proinflammatory cytokines and MAPK1, both involved in MYD88-dependent and TRIF-dependent pathways (Liu and Cao, 2016) are also down-regulated in Mo-MDSCs, suggesting an overall reduced inflammation driven by the presence of these cells.

An up-regulation of Fas ligand (FasL) was markedly displayed in the PCR array results of Mo-MDSCs isolated during Ls infection. Conflicting data have shown the expansion of Mo-MDSCs,

Tregs and PD-1/PD-L1 expression which led to lower survival, during FasL deficiency in mice bearing Lewis lung carcinoma tumors (Peyvandi et al., 2015). With regards to the capacity of MDSCs for antigen presentation, H2-T23 exhibited a down-regulation in Mo-MDSCs during Ls infection which could possibly not enable the cells to present antigens. Inversely, CD86 a costimulatory molecule is up-regulated in PMN-MDSCs. In line with this, recent findings have indicated up-regulation of CD86 in MDSCs in a mouse model of hepetocelluler carcinoma (Lacotte et al., 2016).

It is well known that MDSCs express CD11b and Gr-1 (Gabrilovich et al., 2007; Ostrand-Rosenberg and Sinha, 2009). Here data from PCR array indicated a down-regulation of ITGAM in Mo-MDSCs isolated from Ls-infected compared to those of naive mice. In contrast, data have been provided by Sun *et al.* in human colorectal carcinoma and have found an up-regulation of CD11b (ITGAM)/CD18 expression in patients when compared with the MDSCs from healthy donors (Sun et al., 2012). More in depth examination of Mo-MDSCs are needed to clarify such down-regulation of genes and thus potential functional pathways.

4.7 Conclusion

Using the Ls model, this study aimed to explore the impact of MDSCs on immune responses during filariasis and specifically to examine whether MDSC subsets evolve during ongoing infection. Moreover, it was determined whether they affect specific-filarial responses and another goal of the study was to assess molecular mechanisms implicated in MDSC activities. Current knowledge on MDSCs indicates that, by means of receptors and/or cytokines pathways, MDSCs display a detrimental role in cancer and other pathological conditions, where they impair the defense system of the host whereas in some others conditions such as graft transplantation, understanding and enhancing MDSC capacities may represent a tool to improve such conditions.

In this view, parasitological analyses, flow cytometry and culture assays were used to address diverse aspects of MDSC abilities. The results revealed that during Ls infection, MDSC subsets expanded in the TC which is the site of infection, whereas only very few MDSCs were found in naive mice and this expansion positively correlated with worm burden (strongly) and MF count (weakly), at the site of infection but no correlation was found between MDSC infiltration and MF count in blood. Interestingly, although large numbers of PMN-MDSCs with no consistent suppressive activities were observed, Mo-MDSCs amounts were low but these cells showed high suppressive abilities on the production of IL-13 and IFN-γ, but not IL-5 by infection-derived $CD4^+$ T cells upon re-stimulation with Ls-antigen. Further analyses demonstrated that Mo-MDSCs used distinct functional mechanisms such as NO and TGF-β to impair the production of IL-13 and IFN-γ, respectively. Surprisingly, infection-derived Mo-MDSCs displayed an up-regulation of IFN-γ, IL-13 and T-bet among many other genes and a down-regulation of RORC in a PCR array. However, both subsets were found to down-regulate IL-18 and up-regulate FOXP3 gene. The summary of the mechanisms used by Mo-MDSCs is depicted in Figure 4.1. In addition, using mice simultaneously deficient in IL-4Rα and IL-5, data showed that in the absence of Th2 responses, dramatically increased numbers of worms and MF were observed followed by high levels of IFN-γ produced by $CD4^+$ T cells and also higher amounts of Mo-MDSCs were found at the site of infection during Ls infection. Nevertheless, lack of this receptor and thus recognition of Th2 cytokines was not required for the suppression of $CD4^+$ T cell responses *in vitro*. In conclusion, the involvement of MDSCs during Ls infection offered a favorable milieu for parasite development, impairing the host immunity and therefore targeting MDSCs may supply a key for therapy in order to eliminate filariasis.

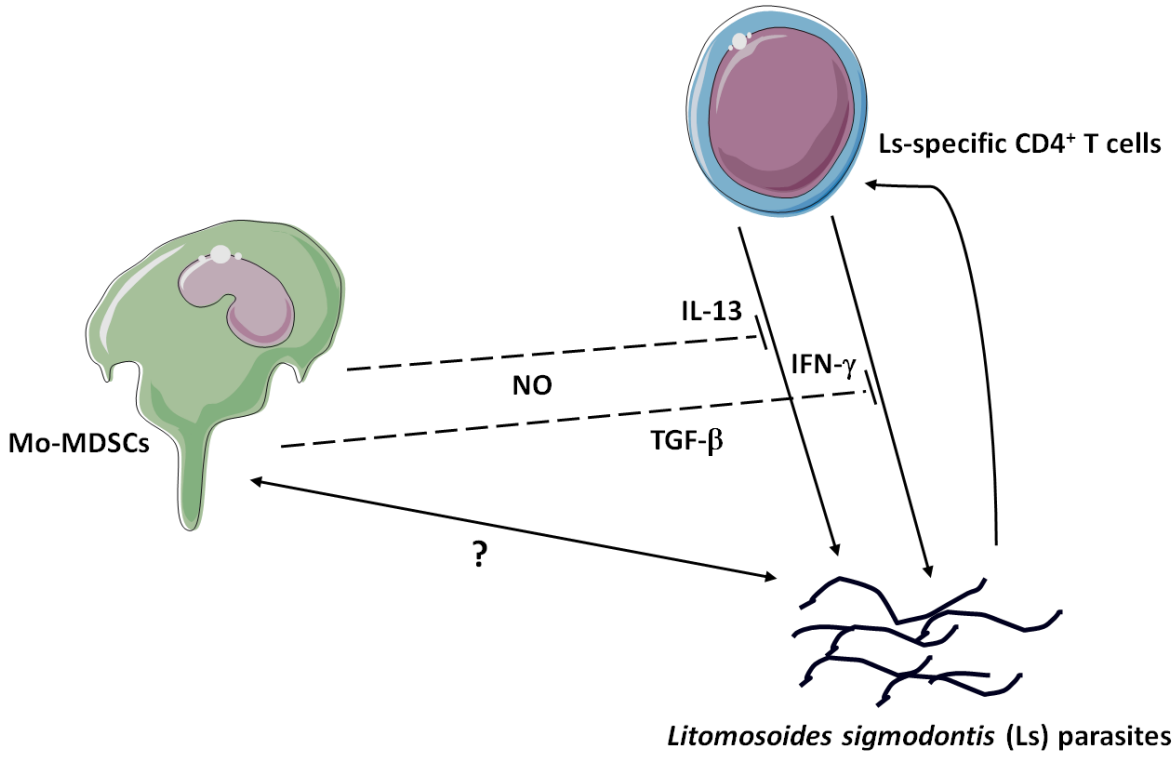

Figure 4.1: Hypothetical mechanisms of Mo-MDSCs on Ls-specific $CD4^+$ T cells during Ls infection

5. REFERENCES

Ajendra, J., Specht, S., Neumann, A.L., Gondorf, F., Schmidt, D., Gentil, K., Hoffmann, W.H., Taylor, M.J., Hoerauf, A., and Hubner, M.P. (2014). ST2 Deficiency Does Not Impair Type 2 Immune Responses during Chronic Filarial Infection but Leads to an Increased Microfilaremia Due to an Impaired Splenic Microfilarial Clearance. PloS one *9*.

Ajendra, J., Specht, S., Ziewer, S., Schiefer, A., Pfarr, K., Parcina, M., Kufer, T.A., Hoerauf, A., and Hubner, M.P. (2016). NOD2 dependent neutrophil recruitment is required for early protective immune responses against infectious Litomosoides sigmodontis L3 larvae. Sci Rep-Uk *6*.

Al-Qaoud, K.M., Fleischer, B., and Hoerauf, A. (1998). The Xid defect imparts susceptibility to experimental murine filariosis - association with a lack of antibody and IL-10 production by B cells in response to phosphorylcholine. Int Immunol *10*, 17-25.

Al-Qaoud, K.M., Pearlman, E., Hartung, T., Klukowski, J., Fleischer, B., and Hoerauf, A. (2000). A new mechanism for IL-5-dependent helminth control: neutrophil accumulation and neutrophil-mediated worm encapsulation in murine filariasis are abolished in the absence of IL-5. Int Immunol *12*, 899-908.

Al-Qaoud, K.M., Taubert, A., Zahner, H., Fleischer, B., and Hoerauf, A. (1997). Infection of BALB/c mice with the filarial nematode Litomosoides sigmodontis: Role of CD4(+) T cells in controlling larval development. Infect Immun *65*, 2457-2461.

Albeituni, S.H., Ding, C., and Yan, J. (2013). Hampering immune suppressors: therapeutic targeting of myeloid-derived suppressor cells in cancer. Cancer journal *19*, 490-501.

Alexander, N.D., and Grenfell, B.T. (1999). The effect of pregnancy on Wuchereria bancrofti microfilarial load in humans. Parasitology *119 (Pt 2)*, 151-156.

Almand, B., Resser, J.R., Lindman, B., Nadaf, S., Clark, J.I., Kwon, E.D., Carbone, D.P., and Gabrilovich, D.I. (2000). Clinical significance of defective dendritic cell differentiation in cancer. Clinical cancer research : an official journal of the American Association for Cancer Research *6*, 1755-1766.

Amaral, F., Dreyer, G., Figueredosilva, J., Noroes, J., Cavalcanti, A., Samico, S.C., Santos, A., and Coutinho, A. (1994). Live Adult Worms Detected by Ultrasonography in Human Bancroftian Filariasis. Am J Trop Med Hyg *50*, 753-757.

Anitha, K., and Shenoy, R.K. (2001). Treatment of lymphatic filariasis: current trends. Indian journal of dermatology, venereology and leprology *67*, 60-65.

Arihara, F., Mizukoshi, E., Kitahara, M., Takata, Y., Arai, K., Yamashita, T., Nakamoto, Y., and Kaneko, S. (2013). Increase in CD14(+)HLA-DR-/low myeloid-derived suppressor cells in hepatocellular carcinoma patients and its impact on prognosis. Cancer Immunol Immun *62*, 1421-1430.

Arndts, K., Deininger, S., Specht, S., Klarmann, U., Mand, S., Adjobimey, T., Debrah, A.Y., Batsa, L., Kwarteng, A., Epp, C.*, et al.* (2012). Elevated Adaptive Immune Responses Are Associated with Latent Infections of Wuchereria bancrofti. Plos Neglect Trop D *6*.

Arora, M., Poe, S.L., Oriss, T.B., Krishnamoorthy, N., Yarlagadda, M., Wenzel, S.E., Billiar, T.R., Ray, A., and Ray, P. (2010). TLR4/MyD88-induced CD11b+Gr-1int F4/80+ non-migratory myeloid cells suppress Th2 effector function in the lung. Mucosal Immunol *3*, 578–593.

Atretkhany, K.S., Nosenko, M.A., Gogoleva, V.S., Zvartsev, R.V., Qin, Z., Nedospasov, S.A., and Drutskaya, M.S. (2016). TNF Neutralization Results in the Delay of Transplantable Tumor Growth and Reduced MDSC Accumulation. Front Immunol *7*, 147.

Attout, T., Martin, C., Babayan, S.A., Kozek, W.J., Bazzocchi, C., Oudet, F., Gallagher, I.J., Specht, S., and Bain, O. (2008). Pleural cellular reaction to the filarial infection Litomosoides sigmodontis is determined by the moulting process, the worm alteration, and the host strain. Parasitology International *57*, 201-211.

Babayan, S., Ungeheuer, M.N., Martin, C., Attout, T., Belnoue, E., Snounou, G., Renia, L., Korenaga, M., and Bain, O. (2003). Resistance and susceptibility to filarial infection with Litomosoides

sigmodontis are associated with early differences in parasite development and in localized immune reactions. Infect Immun *71*, 6820-6829.
Babu, S., Bhat, S.Q., Kumar, N.P., Lipira, A.B., Kumar, S., Karthik, C., Kumaraswami, V., and Nutman, T.B. (2009). Filarial Lymphedema Is Characterized by Antigen-Specific Th1 and Th17 Proinflammatory Responses and a Lack of Regulatory T Cells. Plos Neglect Trop D *3*.
Babu, S., Blauvelt, C.P., Kumaraswami, V., and Nutman, T.B. (2006). Regulatory networks induced by live parasites impair both Th1 and Th2 pathways in patent lymphatic filariasis: Implications for parasite persistence. Journal of Immunology *176*, 3248-3256.
Babu, S., Blauvelt, C.P., and Nutman, T.B. (2007). Filarial parasites induce NK cell activation, type 1 and type 2 cytokine secretion, and subsequent apoptotic cell death. Journal of Immunology *179*, 2445-2456.
Bain, O., and Babayan, S. (2003). Behaviour of filariae: morphological and anatomical signatures of their life style within the arthropod and vertebrate hosts. Filaria Journal *2*.
Ballbach, M., Hall, T., Brand, A., Neri, D., Singh, A., Schaefer, I., Herrmann, E., Hansmann, S., Handgretinger, R., Kuemmerle-Deschner, J.*, et al.* (2016). Induction of Myeloid-Derived Suppressor Cells in Cryopyrin-Associated Periodic Syndromes. Journal of innate immunity *8*, 493-506.
Bhumiratana, A., Koyadun, S., Suvannadabba, S., Karnjanopas, K., Rojanapremsuk, J., Buddhirakkul, P., and Tantiwattanasup, W. (1999). Field trial of the ICT filariasis for diagnosis of Wuchereria bancrofti infections in an endemic population of Thailand. The Southeast Asian journal of tropical medicine and public health *30*, 562-568.
Bobe, P., Benihoud, K., Grandjon, D., Opolon, P., Pritchard, L.L., and Huchet, R. (1999). Nitric oxide mediation of active immunosuppression associated with graft-versus-host reaction. Blood *94*, 1028-1037.
Boyd, A., Killoran, K., Mitre, E., and Nutman, T.B. (2015). Pleural cavity type 2 innate lymphoid cells precede Th2 expansion in murine Litomosoides sigmodontis infection. Exp Parasitol *159*, 118-126.
Brandau, S., Trellakis, S., Bruderek, K., Schmaltz, D., Steller, G., Elian, M., Suttmann, H., Schenck, M., Welling, J., Zabel, P., and Lang, S. (2011). Myeloid-derived suppressor cells in the peripheral blood of cancer patients contain a subset of immature neutrophils with impaired migratory properties. J Leukoc Biol *89*, 311-317.
Brimnes, M.K., Vangsted, A.J., Knudsen, L.M., Gimsing, P., Gang, A.O., Johnsen, H.E., and Svane, I.M. (2010). Increased Level of both CD4+FOXP3+ Regulatory T Cells and CD14+HLA-DR-/low Myeloid-Derived Suppressor Cells and Decreased Level of Dendritic Cells in Patients with Multiple Myeloma. Scand J Immunol *72*, 540-547.
Bronte, V., Chappell, D.B., Apolloni, E., Cabrelle, A., Wang, M., Hwu, P., and Restifo, N.P. (1999). Unopposed production of granulocyte-macrophage colony-stimulating factor by tumors inhibits CD8+ T cell responses by dysregulating antigen-presenting cell maturation. J Immunol *162*, 5728-5737.
Bunt, S.K., Clements, V.K., Hanson, E.M., Sinha, P., and Ostrand-Rosenberg, S. (2009). Inflammation enhances myeloid-derived suppressor cell cross-talk by signaling through Toll-like receptor 4. J. Leukoc. Biol. *85*, 996-1004.
Bunt, S.K., Sinha, P., Clements, V.K., Leips, J., and Ostrand-Rosenberg, S. (2006). Inflammation induces myeloid-derived suppressor cells that facilitate tumor progression. Journal of Immunology *176*, 284-290.
Cano, J., Rebollo, M.P., Golding, N., Pullan, R.L., Crellen, T., Soler, A., Kelly-Hope, L.A., Lindsay, S.W., Hay, S.I., Bockarie, M.J., and Brooker, S.J. (2014). The global distribution and transmission limits of lymphatic filariasis: past and present. Parasites & vectors *7*, 466.
Cao, Y., Slaney, C.Y., Bidwell, B.N., Parker, B.S., Johnstone, C.N., Rautela, J., Eckhardt, B.L., and Anderson, R.L. (2014). BMP4 inhibits breast cancer metastasis by blocking myeloid-derived suppressor cell activity. Cancer research *74*, 5091-5102.

Cardillo, F., de Pinho, R.T., Antas, P.R.Z., and Mengel, J. (2015). Immunity and immune modulation in Trypanosoma cruzi infection. Pathog Dis *73*.
Carme, B., Boulesteix, J., Boutes, H., and Puruehnce, M.F. (1991). Five cases of encephalitis during treatment of loiasis with diethylcarbamazine. Am J Trop Med Hyg *44*, 684-690.
Cauley, L.S., Miller, E.E., Yen, M., and Swain, S.L. (2000). Superantigen-induced CD4 T cell tolerance mediated by myeloid cells and IFN-gamma. Journal of Immunology *165*, 6056-6066.
Chalmin, F., Ladoire, S., Mignot, G., Vincent, J., Bruchard, M., Remy-Martin, J.P., Boireau, W., Rouleau, A., Simon, B., Lanneau, D.*, et al.* (2010). Membrane-associated Hsp72 from tumor-derived exosomes mediates STAT3-dependent immunosuppressive function of mouse and human myeloid-derived suppressor cells. J Clin Invest *120*, 457-471.
Chamaillard, M., Hashimoto, M., Horie, Y., Masumoto, J., Qiu, S., Saab, L., Ogura, Y., Kawasaki, A., Fukase, K., Kusumoto, S.*, et al.* (2003). An essential role for NOD1 in host recognition of bacterial peptidoglycan containing diaminopimelic acid. Nat Immunol *4*, 702-707.
Chandy, A., Thakur, A.S., Singh, M.P., and Manigauha, A. (2011). A review of neglected tropical diseases: filariasis. Asian Pacific journal of tropical medicine *4*, 581-586.
Charo, I.F., and Ransohoff, R.M. (2006). The many roles of chemokines and chemokine receptors in inflammation. The New England journal of medicine *354*, 610-621.
Condamine, T., and Gabrilovich, D.I. (2011). Molecular mechanisms regulating myeloid-derived suppressor cell differentiation and function. Trends Immunol *32*, 19-25.
Corzo, C.A., Cotter, M.J., Cheng, P.Y., Cheng, F.D., Kusmartsev, S., Sotomayor, E., Padhya, T., McCaffrey, T.V., McCaffrey, J.C., and Gabrilovich, D.I. (2009). Mechanism Regulating Reactive Oxygen Species in Tumor-Induced Myeloid-Derived Suppressor Cells. Journal of Immunology *182*, 5693-5701.
Cripps, J.G., Wang, J., Maria, A., Blumenthal, I., and Gorham, J.D. (2010). Type 1 T helper cells induce the accumulation of myeloid-derived suppressor cells in the inflamed Tgfb1 knockout mouse liver. Hepatology *52*, 1350-1359.
Crook, K.R., Jin, M., Weeks, M.F., Rampersad, R.R., Baldi, R.M., Glekas, A.S., Shen, Y., Esserman, D.A., Little, P., Schwartz, T.A., and Liu, P. (2015). Myeloid-derived suppressor cells regulate T cell and B cell responses during autoimmune disease. J Leukoc Biol *97*, 573-582.
Cui, T.X., Kryczek, I., Zhao, L., Zhao, E., Kuick, R., Roh, M.H., Vatan, L., Szeliga, W., Mao, Y., Thomas, D.G.*, et al.* (2013). Myeloid-derived suppressor cells enhance stemness of cancer cells by inducing microRNA101 and suppressing the corepressor CtBP2. Immunity *39*, 611-621.
De-Jian, S., Xu-Li, D., and Ji-Hui, D. (2013). The history of the elimination of lymphatic filariasis in China. Infectious diseases of poverty *2*, 30.
Debrah AY , Batsa L , Albers A , Mand S , Toliat MR , Nürnberg P , Adjei O , Hoerauf A , and K, P. (2011). Transforming growth factor-beta 1 variant Leu 10 Pro is associated with both lack of microfilariae and differential microfilarial loads in the blood of persons infected with lymphatic filariasis. Human Immunology *72*, 1143-1148.
Desjardins, C.A., Cerqueira, G.C., Goldberg, J.M., Dunning Hotopp, J.C., Haas, B.J., Zucker, J., Ribeiro, J.M., Saif, S., Levin, J.Z., Fan, L.*, et al.* (2013). Genomics of Loa loa, a Wolbachia-free filarial parasite of humans. Nature genetics *45*, 495-500.
Devaney, E., Gillan, V., Wheatley, I., Jenson, J., O'Connor, R., and Balmer, P. (2002). Interleukin-4 influences the production of microfilariae in a mouse model of Brugia infection. Parasite Immunol *24*, 29-37.
Dittrich, A.M., Erbacher, A., Specht, S., Diesner, F., Krokowski, M., Avagyan, A., Stock, P., Ahrens, B., Hoffmann, W.H., Hoerauf, A., and Hamelmann, E. (2008). Helminth infection with Litomosoides sigmodontis induces regulatory T cells and inhibits allergic sensitization, airway inflammation, and hyperreactivity in a murine asthma model. J Immunol *180*, 1792-1799.
Dolcetti, L., Peranzoni, E., Ugel, S., Marigo, I., Gomez, A.F., Mesa, C., Geilich, M., Winkels, G., Traggiai, E., Casati, A.*, et al.* (2010). Hierarchy of immunosuppressive strength among myeloid-derived suppressor cell subsets is determined by GM-CSF. Eur J Immunol *40*, 22-35.

Dreyer, G., Addiss, D., Roberts, J., and Noroes, J. (2002). Progression of lymphatic vessel dilatation in the presence of living adult Wuchereria bancrofti. Transactions of the Royal Society of Tropical Medicine and Hygiene *96*, 157-161.
Dreyer, G., Medeiros, Z., Netto, M.J., Leal, N.C., de Castro, L.G., and Piessens, W.F. (1999). Acute attacks in the extremities of persons living in an area endemic for bancroftian filariasis: differentiation of two syndromes. Transactions of the Royal Society of Tropical Medicine and Hygiene *93*, 413-417.
Dubinski, D., Wolfer, J., Hasselblatt, M., Schneider-Hohendorf, T., Bogdahn, U., Stummer, W., Wiendl, H., and Grauer, O.M. (2016). CD4(+) T effector memory cell dysfunction is associated with the accumulation of granulocytic myeloid-derived suppressor cells in glioblastoma patients. Neuro-Oncology *18*, 807-818.
Egelston, C., Kurko, J., Besenyei, T., Tryniszewska, B., Rauch, T.A., Glant, T.T., and Mikecz, K. (2012). Suppression of dendritic cell maturation and T cell proliferation by synovial fluid myeloid cells from mice with autoimmune arthritis. Arthritis Rheum-Us *64*, 3179-3188.
Fiorucci, S., Santucci, L., Antonelli, E., Distrutti, E., Del Sero, G., Morelli, O., Romani, L., Federici, B., Del Soldato, P., and Morelli, A. (2000). NO-aspirin protects from T cell-mediated liver injury by inhibiting caspase-dependent processing of Th1-like cytokines. Gastroenterology *118*, 404-421.
Fischer, P., Supali, T., and Maizels, R.M. (2004). Lymphatic filariasis and Brugia timori: prospects for elimination. Trends Parasitol *20*, 351-355.
Foster, J., Ganatra, M., Kamal, I., Ware, J., Makarova, K., Ivanova, N., Bhattacharyya, A., Kapatral, V., Kumar, S., Posfai, J.*, et al.* (2005). The Wolbachia genome of Brugia malayi: Endosymbiont evolution within a human pathogenic nematode. Plos Biol *3*, 599-614.
Fujita, M., Kohanbash, G., Fellows-Mayle, W., Hamilton, R.L., Komohara, Y., Decker, S.A., Ohlfest, J.R., and Okada, H. (2011). COX-2 blockade suppresses gliomagenesis by inhibiting myeloid-derived suppressor cells. Cancer research *71*, 2664-2674.
Gabitass, R.F., Annels, N.E., Stocken, D.D., Pandha, H.A., and Middleton, G.W. (2011). Elevated myeloid-derived suppressor cells in pancreatic, esophageal and gastric cancer are an independent prognostic factor and are associated with significant elevation of the Th2 cytokine interleukin-13. Cancer immunology, immunotherapy : CII *60*, 1419-1430.
Gabrilovich, D.I., Bronte, V., Chen, S.H., Colombo, M.P., Ochoa, A., Ostrand-Rosenberg, S., and Schreiber, H. (2007). The terminology issue for myeloid-derived suppressor cells. Cancer research *67*, 425; author reply 426.
Gabrilovich, D.I., and Nagaraj, S. (2009). Myeloid-derived suppressor cells as regulators of the immune system. Nat Rev Immunol *9*, 162-174.
Gallina, G., Dolcetti, L., Serafini, P., De Santo, C., Marigo, I., Colombo, M.P., Basso, G., Brombacher, F., Borrello, I., Zanovello, P.*, et al.* (2006). Tumors induce a subset of inflammatory monocytes with immunosuppressive activity on CD8(+) T cells. J Clin Invest *116*, 2777-2790.
Gao, J.J., Wu, Y.M., Su, Z.L., Barnie, P.A., Jiao, Z.J., Bie, Q.L., Lu, L.W., Wang, S.J., and Xu, H.X. (2014). Infiltration of Alternatively Activated Macrophages in Cancer Tissue Is Associated with MDSC and Th2 Polarization in Patients with Esophageal Cancer. PloS one *9*.
Geary, T.G., and Moreno, Y. (2012). Macrocyclic lactone anthelmintics: spectrum of activity and mechanism of action. Current pharmaceutical biotechnology *13*, 866-872.
Gebhardt, C., Nemeth, J., Angel, P., and Hess, J. (2006). S100A8 and S100A9 in inflammation and cancer. Biochem Pharmacol *72*, 1622-1631.
Gehad, A.E., Lichtman, M.K., Schmults, C.D., Teague, J.E., Calarese, A.W., Jiang, Y., Watanabe, R., and Clark, R.A. (2012). Nitric Oxide-Producing Myeloid-Derived Suppressor Cells Inhibit Vascular E-Selectin Expression in Human Squamous Cell Carcinomas. J Invest Dermatol *132*, 2642-2651.
Gershon, D. (2002). Microarray technology: an array of opportunities. Nature *416*, 885-891.
Giallongo, C., Romano, A., Parrinello, N.L., La Cava, P., Brundo, M.V., Bramanti, V., Stagno, F., Vigneri, P., Chiarenza, A., Palumbo, G.A.*, et al.* (2016). Mesenchymal Stem Cells (MSC) Regulate Activation of

Granulocyte-Like Myeloid Derived Suppressor Cells (G-MDSC) in Chronic Myeloid Leukemia Patients. PloS one *11*.
Girardin, S.E., Boneca, I.G., Carneiro, L.A., Antignac, A., Jehanno, M., Viala, J., Tedin, K., Taha, M.K., Labigne, A., Zahringer, U.*, et al.* (2003). Nod1 detects a unique muropeptide from gram-negative bacterial peptidoglycan. Science *300*, 1584-1587.
Goedegebuure, P., Mitchem, J.B., Porembka, M.R., Tan, M.C.B., Belt, B.A., Wang-Gillam, A., Gillanders, W.E., Hawkins, W.G., and Linehan, D.C. (2011). Myeloid-Derived Suppressor Cells: General Characteristics and Relevance to Clinical Management of Pancreatic Cancer. Curr Cancer Drug Tar *11*, 734-751.
Gorgun, G.T., Whitehill, G., Anderson, J.L., Hideshima, T., Maguire, C., Laubach, J., Raje, N., Munshi, N.C., Richardson, P.G., and Anderson, K.C. (2013). Tumor-promoting immune-suppressive myeloid-derived suppressor cells in the multiple myeloma microenvironment in humans. Blood *121*, 2975-2987.
Graham, A.L., Taylor, M.D., Le Goff, L., Lamb, T.J., Magennis, M., and Allen, J.E. (2005). Quantitative appraisal of murine filariasis confirms host strain differences but reveals that BALB/c females are more susceptible than males to Litomosoides sigmodontis. Microbes and infection *7*, 612-618.
Gray, C.A., and Lawrence, R.A. (2002). Interferon-gamma and nitric oxide production are not required for the immune-mediated clearance of Brugia malayi microfilariae in mice. Parasite Immunol *24*, 329-336.
Green, K.A., Cook, W.J., and Green, W.R. (2013). Myeloid-Derived Suppressor Cells in Murine Retrovirus-Induced AIDS Inhibit T- and B-Cell Responses In Vitro That Are Used To Define the Immunodeficiency. J Virol *87*, 2058-2071.
Greenhough, A., Smartt, H.J., Moore, A.E., Roberts, H.R., Williams, A.C., Paraskeva, C., and Kaidi, A. (2009). The COX-2/PGE2 pathway: key roles in the hallmarks of cancer and adaptation to the tumour microenvironment. Carcinogenesis *30*, 377-386.
Gross, O., Yazdi, A.S., Thomas, C.J., Masin, M., Heinz, L.X., Guarda, G., Quadroni, M., Drexler, S.K., and Tschopp, J. (2012). Inflammasome Activators Induce Interleukin-1 alpha Secretion via Distinct Pathways with Differential Requirement for the Protease Function of Caspase-1. Immunity *36*, 388-400.
Guilliams, M., Movahedi, K., Bosschaerts, T., VandenDriessche, T., Chuah, M., K., H., M., Acosta-Sanchez, A., Ma, L., Moser, M., Van Ginderachter, J., A.*, et al.* (2009). IL-10 dampens TNF/inducible nitric oxide synthase-producing dendritic cells-mediated pathogenicity during parasite infection. Journal of Immunology *182*, 1107-1118.
Haben, I., Hartmann, W., Specht, S., Hoerauf, A., Roers, A., Muller, W., and Breloer, M. (2013). T-cell-derived, but not B-cell-derived, IL-10 suppresses antigen-specific T-cell responses in Litomosoides sigmodontis-infected mice. Eur J Immunol *43*, 1799-1805.
Haile, L.A., Gamrekelashvili, J., Manns, M.P., Korangy, F., and Greten, T.F. (2010). CD49d Is a New Marker for Distinct Myeloid-Derived Suppressor Cell Subpopulations in Mice. Journal of Immunology *185*, 203-210.
Hale, M., Itani, F., Buchta, C.M., Wald, G., Bing, M., and Norian, L.A. (2015). Obesity triggers enhanced MDSC accumulation in murine renal tumors via elevated local production of CCL2. PloS one *10*, e0118784.
Ham, B., Wang, N., D'Costa, Z., Fernandez, M.C., Bourdeau, F., Auguste, P., Illemann, M., Eefsen, R.L., Hoyer-Hansen, G., Vainer, B.*, et al.* (2015). TNF Receptor-2 Facilitates an Immunosuppressive Microenvironment in the Liver to Promote the Colonization and Growth of Hepatic Metastases. Cancer research *75*, 5235-5247.
Hanson, E.M., Clements, V.K., Sinha, P., Ilkovitch, D., and Ostrand-Rosenberg, S. (2009). Myeloid-Derived Suppressor Cells Down-Regulate L-Selectin Expression on CD4(+) and CD8(+) T Cells. Journal of Immunology *183*, 937-944.

Hartmann, W., Marsland, B.J., Otto, B., Urny, J., Fleischer, B., and Korten, S. (2011). A Novel and Divergent Role of Granzyme A and B in Resistance to Helminth Infection. Journal of Immunology *186*, 2472-2481.
Hartmann, W., Schramm, C., and Breloer, M. (2015). Litomosoides sigmodontis induces TGF-beta receptor responsive, IL-10-producing T cells that suppress bystander T-cell proliferation in mice. Eur J Immunol *45*, 2568-2581.
Hegde, V.L., Tomar, S., Jackson, A., Rao, R., Yang, X., Singh, U.P., Singh, N.P., Nagarkatti, P.S., and Nagarkatti, M. (2013). Distinct microRNA expression profile and targeted biological pathways in functional myeloid-derived suppressor cells induced by Δ9-tetrahydrocannabinol in vivo: regulation of CCAAT/enhancer-binding protein α by microRNA-690. Journal of Biological Chemistry *288*, 36810-36826.
Heim, C.E., Vidlak, D., and Kielian, T. (2015). Interleukin-10 production by myeloid-derived suppressor cells contributes to bacterial persistence during Staphylococcus aureus orthopedic biofilm infection. J Leukocyte Biol *98*, 1003-1013.
Highfill, S.L., Rodriguez, P.C., Zhou, Q., Goetz, C.A., Koehn, B.H., Veenstra, R., Taylor, P.A., Panoskaltsis-Mortari, A., Serody, J.S., Munn, D.H.*, et al.* (2010). Bone marrow myeloid-derived suppressor cells (MDSCs) inhibit graft-versus-host disease (GVHD) via an arginase-1-dependent mechanism that is up-regulated by interleukin-13. Blood *116*, 5738-5747.
Hise, A.G., Gillette-Ferguson, I., and Pearlman, E. (2004a). The role of endosymbiotic Wolbachia bacteria in filarial disease. Cell Microbiol *6*, 97-104.
Hise, A.G., Gillette-Ferguson, I., and Pearlman, E. (2004b). The role of endosymbiotic Wolbachia bacteria in filarial disease. Cell Microbiol *6*, 97-104.
Ho, V., Lim, T.S., Lee, J., Steinberg, J., Szmyd, R., Tham, M., Yaligar, J., Kaldis, P., Abastado, J.P., and Chew, V. (2015). TLR3 agonist and Sorafenib combinatorial therapy promotes immune activation and controls hepatocellular carcinoma progression. Oncotarget *6*, 27252-27266.
Hochst, B., Mikulec, J., Baccega, T., Metzger, C., Welz, M., Peusquens, J., Tacke, F., Knolle, P., Kurts, C., Diehl, L., and Ludwig-Portugall, I. (2015). Differential induction of Ly6G and Ly6C positive myeloid derived suppressor cells in chronic kidney and liver inflammation and fibrosis. PloS one *10*, e0119662.
Hoerauf, A. (2003). Control of filarial infections: not the beginning of the end, but more research is needed. Current opinion in infectious diseases *16*, 403-410.
Hoerauf, A., Nissen-Pahle, K., Schmetz, C., Henkle-Duhrsen, K., Blaxter, M.L., Buttner, D.W., Gallin, M.Y., Al-Qaoud, K.M., Lucius, R., and Fleischer, B. (1999). Tetracycline therapy targets intracellular bacteria in the filarial nematode Litomosoides sigmodontis and results in filarial infertility. J Clin Invest *103*, 11-17.
Hoerauf, A., Satoguina, J., Saeftel, M., and Specht, S. (2005). Immunomodulation by filarial nematodes. Parasite Immunol *27*, 417-429.
Hoffmann, W.H., Petit, G., Schulz-Key, H., Taylor, D.W., Bain, O., and Le Goff, L. (2000). Litomosoides sigmodontis in mice: Reappraisal of an old model for filarial research. Parasitol Today *16*, 387-389.
Hoffmann, W.H., Pfaff, A.W., Schulz-Key, H., and Soboslay, P.T. (2001). Determinants for resistance and susceptibility to microfilaraemia in Litomosoides sigmodontis filariasis. Parasitology *122*, 641-649.
Horton, J. (2002). Albendazole: a broad spectrum anthelminthic for treatment of individuals and populations. Current opinion in infectious diseases *15*, 599-608.
Hossain, D.M., Pal, S.K., Moreira, D., Duttagupta, P., Zhang, Q., Won, H., Jones, J., D'Apuzzo, M., Forman, S., and Kortylewski, M. (2015). TLR9-Targeted STAT3 Silencing Abrogates Immunosuppressive Activity of Myeloid-Derived Suppressor Cells from Prostate Cancer Patients. Clinical cancer research : an official journal of the American Association for Cancer Research *21*, 3771-3782.

Hsieh, C.C., Chou, H.S., Yang, H.R., Lin, F., Bhatt, S., Qin, J., Wang, L.F., Fung, J.J., Qian, S.G., and Lu, L. (2013). The role of complement component 3 (C3) in differentiation of myeloid-derived suppressor cells. Blood *121*, 1760-1768.
Hu, X., Li, B., Xiaoyan, L., Zhao, X., Wan, L., Lin, G., Yu, M., Wang, J., Jiang, X., Feng, W., Zhihai, Q.*, et al.* (2014). Transmembrane TNF-a promotes suppressive activities of myeloid-derived suppressor cells via TNFR2. Jounal of Immunology *192*, 1320-1331.
Huang, A., Zhang, B., Wang, B., Zhang, F., Fan, K.X., and Guo, Y.J. (2013). Increased CD14(+)HLA-DR-/low myeloid-derived suppressor cells correlate with extrathoracic metastasis and poor response to chemotherapy in non-small cell lung cancer patients. Cancer Immunol Immun *62*, 1439-1451.
Huang, B., Lei, Z., Zhao, J., Gong, W., Liu, J., Chen, Z., Liu, Y., Li, D., Yuan, Y., Zhang, G.M., and Feng, Z.H. (2007). CCL2/CCR2 pathway mediates recruitment of myeloid suppressor cells to cancers. Cancer letters *252*, 86-92.
Huang, B., Pan, P.Y., Li, Q.S., Sato, A.I., Levy, D.E., Bromberg, J., Divino, C.M., and Chen, S.H. (2006). Gr-1(+)CD115(+) immature myeloid suppressor cells mediate the development of tumor-induced T regulatory cells and T-cell anergy in tumor-bearing host. Cancer research *66*, 1123-1131.
Hubner, M.P., Stocker, J.T., and Mitre, E. (2009). Inhibition of type 1 diabetes in filaria-infected non-obese diabetic mice is associated with a T helper type 2 shift and induction of FoxP3(+) regulatory T cells. Immunology *127*, 512-522.
Hussain, R., Hamilton, R.G., Kumaraswami, V., Adkinson, N.F., Jr., and Ottesen, E.A. (1981). IgE responses in human filariasis. I. Quantitation of filaria-specific IgE. J Immunol *127*, 1623-1629.
Hussein, O., El Setouhy, M., Ahmed, E.S., Kandil, A.M., Ramzy, R.M.R., Helmy, H., and Weil, G.J. (2004). Duplex Doppler sonographic assessment of the effects of diethylcarbamazine and albendazole therapy on adult filarial worms and adjacent host tissues in bancroftian filariasis. Am J Trop Med Hyg *71*, 471-477.
Idorn, M., Kollgaard, T., Kongsted, P., Sengelov, L., and Straten, P.T. (2014). Correlation between frequencies of blood monocytic myeloid-derived suppressor cells, regulatory T cells and negative prognostic markers in patients with castration-resistant metastatic prostate cancer. Cancer Immunol Immun *63*, 1177-1187.
Ignarro, L.J., Napoli, C., and Loscalzo, J. (2002). Nitric oxide donors and cardiovascular agents modulating the bioactivity of nitric oxide - An overview. Circ Res *90*, 21-28.
Ivoke, N., Ezeabikwa, B.O., Ivoke, O.N., Ekeh, F.N., Ezenwaji, N.E., Odo, G.E., Onoja, U.S., and Eyo, J.E. (2015). Wuchereria bancrofti infection in rural tropical guinea-savannah communities: Rapid epidemiological assessment using immunochromatographic card test and prevalence of hydrocoele. Trop Biomed *32*, 365-375.
Jain, S.P., and Singh, J. (2010). Traditional medicinal practice among the tribal people of Raigarh (Chattishgarh), India. Ind J Nat Product Resources *1*, 109-115.
Jenkins, S.J., and Allen, J.E. (2010). Similarity and Diversity in Macrophage Activation by Nematodes, Trematodes, and Cestodes. J Biomed Biotechnol.
Jiang, J.W., Guo, W.J., and Liang, X.H. (2014). Phenotypes, accumulation, and functions of myeloid-derived suppressor cells and associated treatment strategies in cancer patients. Human Immunology *75*, 1128-1137.
Kamari, Y., Shaish, A., Shemesh, S., Vax, E., Grosskopf, I., Dotan, S., White, M., Voronov, E., Dinarello, C.A., Apte, R.N., and Harats, D. (2011). Reduced atherosclerosis and inflammatory cytokines in apolipoprotein-E-deficient mice lacking bone marrow-derived interleukin-1 alpha. Biochem Bioph Res Co *405*, 197-203.
Kapanadze, T., Gamrekelashvili, J., Ma, C., Chan, C., Zhao, F., Hewitt, S., Zender, L., Kapoor, V., Felsher, D.W., Manns, M.P.*, et al.* (2013). Regulation of accumulation and function of myeloid derived suppressor cells in different murine models of hepatocellular carcinoma. J Hepatol *59*, 1007-1013.

Katawa, G., Layland, L.E., Debrah, A.Y., von Horn, C., Batsa, L., Kwarteng, A., Arriens, S., Taylor, D.W., Specht, S., Hoerauf, A., and Adjobimey, T. (2015). Hyperreactive Onchocerciasis is Characterized by a Combination of Th17-Th2 Immune Responses and Reduced Regulatory T Cells. Plos Neglect Trop D *9*.
Kennedy, D.E., and Knight, K.L. (2015). Inhibition of B Lymphopoiesis by Adipocytes and IL-1-Producing Myeloid-Derived Suppressor Cells. Journal of Immunology *195*, 2666-2674.
Keskinov, A.A., and Shurin, M.R. (2015). Myeloid regulatory cells in tumor spreading and metastasis. Immunobiology *220*, 236-242.
King, C.L., Mahanty, S., Kumaraswami, V., Abrams, J.S., Regunathan, J., Jayaraman, K., Ottesen, E.A., and Nutman, T.B. (1993). Cytokine Control of Parasite-Specific Anergy in Human Lymphatic Filariasis - Preferential Induction of a Regulatory T-Helper Type-2 Lymphocyte Subset. J Clin Invest *92*, 1667-1673.
Knaul, J.K., Jorg, S., Oberbeck-Mueller, D., Heinemann, E., Scheuermann, L., Brinkmann, V., Mollenkopf, H.J., Yeremeev, V., Kaufmann, S.H.E., and Dorhoi, A. (2014). Lung-Residing Myeloid-derived Suppressors Display Dual Functionality in Murine Pulmonary Tuberculosis. Am J Resp Crit Care *190*, 1053-1066.
Kochin, B.F., Bull, J.J., and Antia, R. (2010). Parasite evolution and life history theory. Plos Biol *8*, e1000524.
Kohanbash, G., McKaveney, K., Sakaki, M., Ueda, R., Mintz, A.H., Amankulor, N., Fujita, M., Ohlfest, J.R., and Okada, H. (2013). GM-CSF Promotes the Immunosuppressive Activity of Glioma-Infiltrating Myeloid Cells through Interleukin-4 Receptor-alpha. Cancer research *73*, 6413-6423.
Korten, S., Volkmann, L., Saeftel, M., Fischer, K., Taniguchi, M., Fleischer, B., and Hoerauf, A. (2002). Expansion of NK cells with reduction of their inhibitory Ly-49A, Ly-49C, and Ly-49G2 receptor-expressing subsets in a murine helminth infection: Contribution to parasite control. Journal of Immunology *168*, 5199-5206.
Kozek, W.J. (1977). Transovarially-transmitted intracellular microorganisms in adult and larval stages of Brugia malayi. The Journal of parasitology *63*, 992-1000.
Kurko, J., Vida, A., Glant, T.T., Scanzello, C.R., Katz, R.S., Nair, A., Mikecz, K., and Szekanecz, Z. (2014). Identification of myeloid-derived suppressor cells in the synovial fluid of patients with rheumatoid arthritis: a pilot study. Bmc Musculoskel Dis *15*.
Kurniawan, A., Yazdanbakhsh, M., Vanree, R., Aalberse, R., Selkirk, M.E., Partono, F., and Maizels, R.M. (1993). Differential Expression of Ige and Igg4 Specific Antibody-Responses in Asymptomatic and Chronic Human Filariasis. Journal of Immunology *150*, 3941-3950.
Lacotte, S., Slits, F., Orci, L.A., Meyer, J., Oldani, G., Delaune, V., Gonelle-Gispert, C., Morel, P., and Toso, C. (2016). Impact of myeloid-derived suppressor cell on Kupffer cells from mouse livers with hepatocellular carcinoma. Oncoimmunology *5*, e1234565.
Lammie, P.J., Hitch, W.L., Allen, E.M.W., Hightower, W., and Eberhard, M.L. (1991). Maternal Filarial Infection as Risk Factor for Infection in Children. Lancet *337*, 1005-1006.
Lawrence, R.A., and Devaney, E. (2001). Lymphatic filariasis: parallels between the immunology of infection in humans and mice. Parasite Immunol *23*, 353-361.
Layland, L.E., Ajendra, J., Ritter, M., Wiszniewsky, A., Hoerauf, A., and Hubner, M.P. (2015). Development of patent Litomosoides sigmodontis infections in semi-susceptible C57BL/6 mice in the absence of adaptive immune responses. Parasites & vectors *8*.
Le Goff L, Lamb TJ, Graham AL, Harcus Y, and JE., A. (2002). IL-4 is required to prevent filarial nematode development in resistant but not susceptible strains of mice. Int J Parasitol *32*, 1277-1284.
Lee, C.R., Kwak, Y., Yang, T., Han, J.H., Park, S.H., Ye, M.B., Lee, W., Sim, K.Y., Kang, J.A., Kim, Y.C.*, et al.* (2016). Myeloid-Derived Suppressor Cells Are Controlled by Regulatory T Cells via TGF-beta during Murine Colitis. Cell Rep *17*, 3219-3232.
Lei, G.S., Zhang, C., and Lee, C.H. (2015). Myeloid-Derived Suppressor Cells Impair Alveolar Macrophages through PD-1 Receptor Ligation during Pneumocystis Pneumonia. Infect Immun *83*, 572-582.

Lesokhin, A.M., Hohl, T.M., Kitano, S., Cortez, C., Hirschhorn-Cymerman, D., Avogadri, F., Rizzuto, G.A., Lazarus, J.J., Pamer, E.G., Houghton, A.N.*, et al.* (2012). Monocytic CCR2(+) Myeloid-Derived Suppressor Cells Promote Immune Escape by Limiting Activated CD8 T-cell Infiltration into the Tumor Microenvironment. Cancer research *72*, 876-886.
Lim, H.X., Hong, H.J., Cho, D., and Kim, T.S. (2014). IL-18 Enhances Immunosuppressive Responses by Promoting Differentiation into Monocytic Myeloid-Derived Suppressor Cells. Journal of Immunology *193*, 5453-5460.
Liu, J., and Cao, X. (2016). Cellular and molecular regulation of innate inflammatory responses. Cell Mol Immunol *13*, 711-721.
Ludwig-Portugall, I., and Layland, L.E. (2012). TLRs, Treg, and B cells, an interplay of regulation during helminth infection. Front Immunol *3*.
Mace, T.A., Ameen, Z., Collins, A., Wojcik, S., Mair, M., Young, G.S., Fuchs, J.R., Eubank, T.D., Frankel, W.L., Bekaii-Saab, T.*, et al.* (2013). Pancreatic cancer-associated stellate cells promote differentiation of myeloid-derived suppressor cells in a STAT3-dependent manner. Cancer research *73*, 3007-3018.
Mahalingashetti, P.B., Subramanian, R.A., Jayker, S.S., and Vijay, A. (2014). Lymphatic filariasis: A view at pathological diversity. Trop Parasitol *4*, 128-132.
Mahanty, S., Mollis, S.N., Ravichandran, M., Abrams, J.S., Kumaraswami, V., Jayaraman, K., Ottesen, E.A., and Nutman, T.B. (1996). High levels of spontaneous and parasite antigen-driven interleukin-10 production are associated with antigen-specific hyporesponsiveness in human lymphatic filariasis. J Infect Dis *173*, 769-773.
Mahanty, S., and Nutman, T.B. (1995). Immunoregulation in Human Lymphatic Filariasis - the Role of Interleukin-10. Parasite Immunol *17*, 385-392.
Maizels, R.M., Sartono, E., Kurniawan, A., Partono, F., Selkirk, M.E., and Yazdanbakhsh, M. (1995). T-Cell Activation and the Balance of Antibody Isotypes in Human Lymphatic Filariasis. Parasitol Today *11*, 50-56.
Mand, S., Debrah, A., Batsa, L., Adjei, O., and Hoerauf, A. (2004). Reliable and frequent detection of adult Wuchereria bancrofti in Ghanaian women by ultrasonography. Tropical medicine & international health : TM & IH *9*, 1111-1114.
Mandruzzato, S., Solito, S., Falisi, E., Francescato, S., Chiarion-Sileni, V., Mocellin, S., Zanon, A., Rossi, C.R., Nitti, D., Bronte, V., and Zanovello, P. (2009). IL4Ralpha+ myeloid-derived suppressor cell expansion in cancer patients. J Immunol *182*, 6562-6568.
Mao, Y.M., Poschke, I., Wennerberg, E., de Coana, Y.P., Brage, S.E., Schultz, I., Hansson, J., Masucci, G., Lundqvist, A., and Kiessling, R. (2013). Melanoma-Educated CD14(+) Cells Acquire a Myeloid-Derived Suppressor Cell Phenotype through COX-2-Dependent Mechanisms. Cancer research *73*, 3877-3887.
Markiewski, M.M., DeAngelis, R.A., Benencia, F., Ricklin-Lichtsteiner, S.K., Koutoulaki, A., Gerard, C., Coukos, G., and Lambris, J.D. (2008). Modulation of the antitumor immune response by complement. Nat Immunol *9*, 1225-1235.
Marshall, M.A., Jankovic, D., Maher, V.E., Sher, A., and Berzofsky, J.A. (2001). Mice infected with Schistosoma mansoni develop a novel non-T-lymphocyte suppressor population which inhibits virus-specific CTL induction via a soluble factor. Microbes and infection *3*, 1051-1061.
Martin C, Saeftel M, Vuong PN, S, B., Fischer K, Bain O, and A, H. (2001). B-cell deficiency suppresses vaccine-induced protection against murine filariasis but does not increase the recovery rate for primary infection. INFECTION AND IMMUNITY *69*, 7067-7073.
Masumoto, J., Yang, K., Varambally, S., Hasegawa, M., Tomlins, S.A., Qiu, S., Fujimoto, Y., Kawasaki, A., Foster, S.J., Horie, Y.*, et al.* (2006). Nod1 acts as an intracellular receptor to stimulate chemokine production and neutrophil recruitment in vivo. J Exp Med *203*, 203-213.
McLaren, D.J., Worms, M.J., Laurence, B.R., and Simpson, M.G. (1975). Micro-organisms in filarial larvae (Nematoda). Transactions of the Royal Society of Tropical Medicine and Hygiene *69*, 509-514.

Melrose, W., and Rahmah, N. (2006). Use of Brugia Rapid dipstick and ICT test to map distribution of lymphatic filariasis in the Democratic Republic of Timor-Leste. The Southeast Asian journal of tropical medicine and public health *37*, 22–25.
Mencacci, A., Montagnoli, C., Bacci, A., Cenci, E., Pitzurra, L., Spreca, A., Kopf, M., Sharpe, A.H., and Romani, L. (2002). CD80(+)Gr-1(+) myeloid cells inhibit development of antifungal Th1 immunity in mice with candidiasis. Journal of Immunology *169*, 3180-3190.
Movahedi, K., Guilliams, M., Van den Bossche, J., Van den Bergh, R., Gysemans, C., Beschin, A., De Baetselier, P., and Van Ginderachter, J.A. (2008). Identification of discrete tumor-induced myeloid-derived suppressor cell subpopulations with distinct T cell-suppressive activity. Blood *111*, 4233-4244.
Mundy-Bosse, B.L., Young, G.S., Bauer, T., Binkley, E., Bloomston, M., Bill, M.A., Bekaii-Saab, T., Carson, W.E., 3rd, and Lesinski, G.B. (2011). Distinct myeloid suppressor cell subsets correlate with plasma IL-6 and IL-10 and reduced interferon-alpha signaling in CD4(+) T cells from patients with GI malignancy. Cancer immunology, immunotherapy : CII *60*, 1269-1279.
Muthuswamy, R., Corman, J.M., Dahl, K., Chatta, G.S., and Kalinski, P. (2016). Functional reprogramming of human prostate cancer to promote local attraction of effector CD8(+) T cells. The Prostate *76*, 1095-1105.
Nagaraj, S., Gupta, K., Pisarev, V., Kinarsky, L., Sherman, S., Kang, L., Herber, D., Schneck, J., and Gabrilovich, D.I. (2007). Altered recognition of antigen is a mechanism of CD8+ T cell tolerance in cancer. Nature Medicine *13*, 828-835.
Nagaraj, S., Youn, J.I., and Gabrilovich, D.I. (2013). Reciprocal Relationship between Myeloid-Derived Suppressor Cells and T Cells. Journal of Immunology *191*, 17-23.
O'Connor, R.A., and Devaney, E. (2002). Nitric oxide limits the expansion of antigen-specific T cells in mice infected with the microfilariae of Brugia pahangi. Infect Immun *70*, 5997-6004.
O'Connor, R.A., Jenson, J.S., and Devaney, E. (2000). NO contributes to proliferative suppression in a murine model of filariasis. Infect Immun *68*, 6101-6107.
Obermajer, N., Muthuswamy, R., Lesnock, J., Edwards, R.P., and Kalinski, P. (2011). Positive feedback between PGE2 and COX2 redirects the differentiation of human dendritic cells toward stable myeloid-derived suppressor cells. Blood *118*, 5498-5505.
Ostrand-Rosenberg, S., and Sinha, P. (2009). Myeloid-derived suppressor cells: linking inflammation and cancer. J Immunol *182*, 4499-4506.
Pak, A.S., Wright, M.A., Matthews, J.P., Collins, S.L., Petruzzelli, G.J., and Young, M.R.I. (1995). Mechanisms of Immune Suppression in Patients with Head and Neck-Cancer - Presence of Cd34(+) Cells Which Suppress Immune Functions within Cancers That Secrete Granulocyte-Macrophage Colony-Stimulating Factor. Clinical Cancer Research *1*, 95-103.
Pan, T., Liu, Y., Zhong, L.M., Shi, M.H., Duan, X.B., Wu, K., Yang, Q., Liu, C., Wei, J.Y., Ma, X.R., *et al.* (2016). Myeloid-derived suppressor cells are essential for maintaining feto-maternal immunotolerance via STAT3 signaling in mice. J Leukoc Biol *100*, 499-511.
Pan, W., Shen, Y.J., Liu, H., Hu, Y., Jiang, Y.Y., Zhou, H.J., Xu, Y.X., Yuan, Z.Y., Wang, Y.J., and Cao, J.P. (2014). [Accumulation of myeloid-derived suppressor cells in the spleen and peripheral blood of Schistosoma japonicum-infected mice]. Zhongguo ji sheng chong xue yu ji sheng chong bing za zhi = Chinese journal of parasitology & parasitic diseases *32*, 6-11.
Pan, W., Zhou, H.J., Shen, Y.J., Wang, Y., Xu, Y.X., Hu, Y., Jiang, Y.Y., Yuan, Z.Y., Ugwu, C.E., and Cao, J.P. (2013). Surveillance on the status of immune cells after Echinococcus granulosus protoscoleces infection in Balb/c mice. PloS one *8*, e59746.
Panni, R.Z., Sanford, D.E., Belt, B.A., Mitchem, J.B., Worley, L.A., Goetz, B.D., Mukherjee, P., Wang-Gillam, A., Link, D.C., Denardo, D.G., *et al.* (2014). Tumor-induced STAT3 activation in monocytic myeloid-derived suppressor cells enhances stemness and mesenchymal properties in human pancreatic cancer. Cancer immunology, immunotherapy : CII *63*, 513-528.

Pearlman, E., Saint Andre, A., Blackwell, N., and Lass, J.H. (2002). A critical role for endosymbiotic wolbachia bacteria and Tlr4 signaling in the pathogenesis of onchocerca volvulus - Induced corneal inflammation (river Blindness). Invest Ophth Vis Sci *43*, U208-U208.
Peng, D.J., Tanikawa, T., Li, W., Zhao, L.L., Vatan, L., Szeliga, W., Wan, S.S., Wei, S., Wang, Y., Liu, Y., *et al.* (2016). Myeloid-Derived Suppressor Cells Endow Stem-like Qualities to Breast Cancer Cells through IL6/STAT3 and NO/NOTCH Cross-talk Signaling. Cancer research *76*, 3156-3165.
Peranzoni, E., Zilio, S., Marigo, I., Dolcetti, L., Zanovello, P., Mandruzzato, S., and Bronte, V. (2010). Myeloid-derived suppressor cell heterogeneity and subset definition. Current opinion in immunology *22*, 238-244.
Petit, G., Diagne, M., Marechal, P., Owen, D., Taylor, D., and Bain, O. (1992). Maturation of the Filaria Litomosoides-Sigmodontis in Balb/C Mice - Comparative Susceptibility of 9 Other Inbred Strains. Ann Parasit Hum Comp *67*, 144-150.
Peyvandi, S., Buart, S., Samah, B., Vetizou, M., Zhang, Y., Durrieu, L., Polrot, M., Chouaib, S., Benihoud, K., Louache, F., and Karray, S. (2015). Fas Ligand Deficiency Impairs Tumor Immunity by Promoting an Accumulation of Monocytic Myeloid-Derived Suppressor Cells. Cancer research *75*, 4292-4301.
Pfaff, A.W., Schulz-Key, H., Soboslay, P.T., Geiger, S.M., and Hoffmann, W.H. (2000). The role of nitric oxide in the innate resistance to microfilariae of Litomosoides sigmodontis in mice. Parasite Immunol *22*, 397-405.
Pfarr, K.M., Debrah, A.Y., Specht, S., and Hoerauf, A. (2009). Filariasis and lymphoedema. Parasite Immunol *31*, 664-672.
Phantana, S., Sensathein, S., Songtrus, J., Klagrathoke, S., and Phongnin, K. (1999). ICT filariasis test: a new screening test for Bancroftian filariasis. The Southeast Asian journal of tropical medicine and public health *30*, 47-51.
Pinton, L., Solito, S., Damuzzo, V., Francescato, S., Pozzuoli, A., Berizzi, A., Mocellin, S., Rossi, C.R., Bronte, V., and Mandruzzato, S. (2016). Activated T cells sustain myeloid-derived suppressor cell-mediated immune suppression. Oncotarget *7*, 1168-1184.
Polz, J., Remke, A., Weber, S., Schmidt, D., Weber-Steffens, D., Pietryga-Krieger, A., Muller, N., Ritter, U., Mostbock, S., and Mannel, D.N. (2014). Myeloid suppressor cells require membrane TNFR2 expression for suppressive activity. Immunity, inflammation and disease *2*, 121-130.
Prata, M.M., Havt, A., Bolick, D.T., Pinkerton, R., Lima, A., and Guerrant, R.L. (2016). Comparisons between myeloperoxidase, lactoferrin, calprotectin and lipocalin-2, as fecal biomarkers of intestinal inflammation in malnourished children. J Transl Sci *2*, 134-139.
Prokopowicz, Z., Marcinkiewicz, J., Katz, D.R., and Chain, B.M. (2012). Neutrophil Myeloperoxidase: Soldier and Statesman. Arch Immunol Ther Ex *60*, 43-54.
Qin, J., Arakawa, Y., Morita, M., Fung, J.J., Qian, S., and Lu, L. (2016). C-C Chemokine Receptor type 2 (CCR2)-Dependent Migration of Myeloid-Derived Suppressor Cells in Protection of Islet Transplants. Transplantation.
Raber, P.L., Thevenot, P., Sierra, R., Wyczechowska, D., Halle, D., Ramirez, M.E., Ochoa, A.C., Fletcher, M., Velasco, C., Wilk, A., *et al.* (2014). Subpopulations of myeloid-derived suppressor cells impair T cell responses through independent nitric oxide-related pathways. Int J Cancer *134*, 2853-2864.
Ramaiah, K.D., and Ottesen, E.A. (2014). Progress and Impact of 13 Years of the Global Programme to Eliminate Lymphatic Filariasis on Reducing the Burden of Filarial Disease. Plos Neglect Trop D *8*.
Ramzy, R.M.R., El Setouhy, M., Helmy, H., Ahmed, E.S., Abd Elaziz, K.M., Farid, H.A., Shannon, W.D., and Weil, G.J. (2006). Effect of yearly mass drug administration with diethylcarbamazine and albendazole on bancroftian filariasis in Egypt: a comprehensive assessment. Lancet *367*, 992-999.
Rastad, J.L., and Green, W.R. (2016). Myeloid-derived suppressor cells in murine AIDS inhibit B-cell responses in part via soluble mediators including reactive oxygen and nitrogen species, and TGF-beta. Virology *499*, 9-22.

Ray, A., Chakraborty, K., and Ray, P. (2013). Immunosuppressive MDSCs induced by TLR signaling during infection and role in resolution of inflammation. Front Cell Infect Mi *3*.
Rayamajhi, M., Humann, J., Penheiter, K., Andreasen, K., and Lenz, L.L. (2010). Induction of IFN-alpha beta enables Listeria monocytogenes to suppress macrophage activation by IFN-gamma. J Exp Med *207*, 327-337.
Ren, J.P., Zhao, J., Dai, J., Griffin, J.W.D., Wang, L., Wu, X.Y., Morrison, Z.D., Li, G.Y., El Gazzar, M., Ning, S.B*., et al.* (2016). Hepatitis C virus-induced myeloid-derived suppressor cells regulate T-cell differentiation and function via the signal transducer and activator of transcription 3 pathway. Immunology *148*, 377-386.
Ristimaki, A., Narko, K., Enholm, B., Joukov, V., and Alitalo, K. (1998). Proinflammatory cytokines regulate expression of the lymphatic endothelial mitogen vascular endothelial growth factor-C. The Journal of biological chemistry *273*, 8413-8418.
Ritter, M., Gross, O., Kays, S., Ruland, J., Nimmerjahn, F., Saijo, S., Tschopp, J., Layland, L.E., and da Costa, C.P. (2010). Schistosoma mansoni triggers Dectin-2, which activates the Nlrp3 inflammasome and alters adaptive immune responses. Proceedings of the National Academy of Sciences of the United States of America *107*, 20459-20464.
Ritter, M., Tamadaho, R.S., Feid, J., Vogel, W., Wiszniewsky, K., Perner, S., Hoerauf, A., and Layland, L.E. (2017). IL-4/5 signalling plays an important role during Litomosoides sigmodontis infection, influencing both immune system regulation and tissue pathology in the thoracic cavity. International Journal for Parasitology *47*, 951-960.
Robinson, M.W., Harmon, C., and O'Farrelly, C. (2016). Liver immunology and its role in inflammation and homeostasis. Cell Mol Immunol *13*, 267-276.
Rodrigo, M.B., Schulz, S., Krupp, V., Ritter, M., Wiszniewsky, K., Arndts, K., Tamadaho, R.S.E., Endl, E., Hoerauf, A., and Layland, L.E. (2016). Patency of Litomosoides sigmodontis infection depends on Toll-like receptor 4 whereas Toll-like receptor 2 signalling influences filarial-specific CD4(+) T-cell responses. Immunology *147*, 429-442.
Rose, S., Misharin, A., and Perlman, H. (2012). A novel Ly6C/Ly6G-based strategy to analyze the mouse splenic myeloid compartment. Cytom Part A *81A*, 343-+.
Rudolph, B.M., Loquai, C., Gerwe, A., Bacher, N., Steinbrink, K., Grabbe, S., and Tuettenberg, A. (2014). Increased frequencies of CD11b(+) CD33(+) CD14(+) HLA-DR(low) myeloid-derived suppressor cells are an early event in melanoma patients. Experimental dermatology *23*, 202-204.
Saeftel, M., Volkmann, L., Korten, S., Brattig, N., Al-Qaoud, K., Fleischer, B., and Hoerauf, A. (2001). Lack of interferon-gamma confers impaired neutrophil granulocyte function and imparts prolonged survival of adult filarial worms in murine filariasis. Microbes and infection *3*, 203-213.
Sahare, K.N., Anandharaman, V., Meshram, V.G., Meshram, S.U., Gajalakshmi, D., Goswami, K., and Reddy, M.V. (2008). In vitro effect of four herbal plants on the motility of Brugia malayi microfilariae. The Indian journal of medical research *127*, 467-471.
Saint Andre, A.V., Blackwell, N.M., Hall, L.R., Hoerauf, A., Brattig, N.W., Volkmann, L., Taylor, M.J., Ford, L., Hise, A.G., Lass, J.H*., et al.* (2002). The role of endosymbiotic Wolbachia bacteria in the pathogenesis of river blindness. Science *295*, 1892-1895.
Sander, L.E., Sackett, S.D., Dierssen, U., Beraza, N., Linke, R.P., Muller, M., Blander, J.M., Tacke, F., and Trautwein, C. (2010). Hepatic acute-phase proteins control innate immune responses during infection by promoting myeloid-derived suppressor cell function. J Exp Med *207*, 1453-1464.
Satapathy, A.K., Sartono, E., Sahoo, P.K., Dentener, M.A., Michael, E., Yazdanbakhsh, M., and Ravindran, B. (2006). Human bancroftian filariasis: immunological markers of morbidity and infection. Microbes and infection *8*, 2414-2423.
Sauer, H., Wartenberg, M., and Hescheler, J. (2001). Reactive oxygen species as intracellular messengers during cell growth and differentiation. Cell Physiol Biochem *11*, 173-186.

Schilling, B., Sucker, A., Griewank, K., Zhao, F., Weide, B., Gorgens, A., Giebel, B., Schadendorf, D., and Paschen, A. (2013). Vemurafenib reverses immunosuppression by myeloid derived suppressor cells. Int J Cancer *133*, 1653-1663.
Schlecker, E., Stojanovic, A., Eisen, C., Quack, C., Falk, C.S., Umansky, V., and Cerwenka, A. (2012). Tumor-infiltrating monocytic myeloid-derived suppressor cells mediate CCR5-dependent recruitment of regulatory T cells favoring tumor growth. J Immunol *189*, 5602-5611.
Schmid, M., Zimara, N., Wege, A.K., and Ritter, U. (2014). Myeloid-derived suppressor cell functionality and interaction with Leishmania major parasites differ in C57BL/6 and BALB/c mice. Eur J Immunol *44*, 3295-3306.
Schumak, B., Klocke, K., Kuepper, J.M., Biswas, A., Djie-Maletz, A., Limmer, A., van Rooijen, N., Mack, M., Hoerauf, A., and Dunay, I.R. (2015). Specific Depletion of Ly6C(hi) Inflammatory Monocytes Prevents Immunopathology in Experimental Cerebral Malaria. PloS one *10*.
Semnani, R.T., and Nutman, T.B. (2004). Toward an understanding of the interaction between filarial parasites and host antigen-presenting cells. Immunol Rev *201*, 127-138.
Shime, H., Kojima, A., Maruyama, A., Saito, Y., Oshiumi, H., Matsumoto, M., and Seya, T. (2014). Myeloid-derived suppressor cells confer tumor-suppressive functions on natural killer cells via polyinosinic:polycytidylic acid treatment in mouse tumor models. Journal of innate immunity *6*, 293-305.
Shirota, Y., Shirota, H., and Klinman, D.M. (2012). Intratumoral Injection of CpG Oligonucleotides Induces the Differentiation and Reduces the Immunosuppressive Activity of Myeloid-Derived Suppressor Cells. Journal of Immunology *188*, 1592-1599.
Simonsen, P.E., Derua, Y.A., Magesa, S.M., Pedersen, E.M., Stensgaard, A.S., Malecela, M.N., and Kisinza, W.N. (2014a). Lymphatic filariasis control in Tanga Region, Tanzania: status after eight rounds of mass drug administration. Parasites & vectors *7*, 507.
Simonsen, P.E., Fischer, P.U., Hoerauf, A., and Weil, G.J. (2014b). The filariases. Manson's Tropical Diseases, 737-765.
Simonsen, P.E., Magesa, S.M., Meyrowitsch, D.W., Malecela-Lazaro, M.N., Rwegoshora, R.T., Jaoko, W.G., and Michael, E. (2005). The effect of eight half-yearly single-dose treatments with DEC on Wuchereria bancrofti circulating antigenaemia. Transactions of the Royal Society of Tropical Medicine and Hygiene *99*, 541-547.
Simonsen, P.E., Niemann, L., and Meyrowitsch, D.W. (1997). Wuchereria bancrofti in Tanzania: microfilarial periodicity and effect of blood sampling time on microfilarial intensities. Tropical medicine & international health : TM & IH *2*, 153-158.
Sinha, P., Parker, K.H., Horn, L., and Ostrand-Rosenberg, S. (2012). Tumor-induced myeloid-derived suppressor cell function is independent of IFN-gamma and IL-4R alpha. Eur J Immunol *42*, 2052-2059.
Skabytska, Y., Wolbing, F., Gunther, C., Koberle, M., Kaesler, S., Chen, K.M., Guenova, E., Demircioglu, D., Kempf, W.E., Volz, T.*, et al.* (2014). Cutaneous Innate Immune Sensing of Toll-like Receptor 2-6 Ligands Suppresses T Cell Immunity by Inducing Myeloid-Derived Suppressor Cells. Immunity *41*, 762-775.
Sodahlon, Y.K., Dorkenoo, A.M., Morgah, K., Nabiliou, K., Agbo, K., Miller, R., Datagni, M., Seim, A., and Mathieu, E. (2013). A Success Story: Togo Is Moving toward Becoming the First Sub-Saharan African Nation to Eliminate Lymphatic Filariasis through Mass Drug Administration and Countrywide Morbidity Alleviation. Plos Neglect Trop D *7*.
Solito, S., Marigo, I., Pinton, L., Damuzzo, V., Mandruzzato, S., and Bronte, V. (2014). Myeloid-derived suppressor cell heterogeneity in human cancers. Ann Ny Acad Sci *1319*, 47-65.
Song, J., Lee, J., Kim, J., Jo, S., Kim, Y.J., Baek, J.E., Kwon, E.S., Lee, K.P., Yang, S., Kwon, K.S.*, et al.* (2016). Pancreatic adenocarcinoma up-regulated factor (PAUF) enhances the accumulation and functional activity of myeloid-derived suppressor cells (MDSCs) in pancreatic cancer. Oncotarget.

Specht, S., Frank, J.K., Alferink, J., Dubben, B., Layland, L.E., Denece, G., Bain, O., Forster, I., Kirschning, C.J., Martin, C., and Hoerauf, A. (2011). CCL17 Controls Mast Cells for the Defense against Filarial Larval Entry. Journal of Immunology *186*, 4845-4852.
Specht, S., Saeftel, M., Arndt, M., Endl, E., Dubben, B., Lee, N.A., Lee, J.J., and Hoerauf, A. (2006). Lack of eosinophil peroxidase or major basic protein impairs defense against murine filarial infection. Infect Immun *74*, 5236-5243.
Specht, S., Taylor, M.D., Hoeve, M.A., Allen, J.E., Lang, R., and Hoerauf, A. (2012). Over expression of IL-10 by macrophages overcomes resistance to murine filariasis. Exp Parasitol *132*, 90-96.
Specht, S., Volkmann, L., Wynn, T., and Hoerauf, A. (2004). Interleukin-10 (IL-10) counterregulates IL-4-dependent effector mechanisms in murine filariasis. Infect Immun *72*, 6287-6293.
Spencer, L.A., and Weller, P.F. (2010). Eosinophils and Th2 immunity: contemporary insights. Immunology and cell biology *88*, 250-256.
Srivastava, M.K., Sinha, P., Clements, V.K., Rodriguez, P., and Ostrand-Rosenberg, S. (2010). Myeloid-derived suppressor cells inhibit T-cell activation by depleting cystine and cysteine. Cancer research *70*, 68-77.
Steel, C., Guinea, A., and Ottesen, E.A. (1996). Evidence for protective immunity to bancroftian filariasis in the Cook Islands. J Infect Dis *174*, 598-605.
Strauss, L., Sangaletti, S., Consonni, F.M., Szebeni, G., Morlacchi, S., Totaro, M.G., Porta, C., Anselmo, A., Tartari, S., Doni, A.*, et al.* (2015). RORC1 Regulates Tumor-Promoting "Emergency" Granulo-Monocytopoiesis. Cancer cell *28*, 253-269.
Su, H., Cong, X., and Liu, Y.L. (2013). Transplantation of granulocytic myeloid-derived suppressor cells (G-MDSCs) could reduce colitis in experimental murine models. J Digest Dis *14*, 251-258.
Sun, H.L., Zhou, X., Xue, Y.F., Wang, K., Shen, Y.F., Mao, J.J., Guo, H.F., and Miao, Z.N. (2012). Increased frequency and clinical significance of myeloid-derived suppressor cells in human colorectal carcinoma. World J Gastroenterol *18*, 3303-3309.
Svoronos, N., Perales-Puchalt, A., Allegrezza, M.J., Rutkowski, M.R., Payne, K.K., Tesone, A.J., Nguyen, J.M., Curiel, T.J., Cadungog, M.G., Singhal, S.*, et al.* (2016). Tumor cell-independent estrogen signaling drives disease progression through mobilization of myeloid-derived supressor cells. Cancer Discovery.
Tada, I. (2011). Lymphatic filariasis and its control in Japan -the background of success. Tropical medicine and health *39*, 15-20.
Tamadaho, R.S.E., Hoerauf, A., and Layland, L.E. (2018). Immunomodulatory effects of myeloid-derived suppressor cells in diseases: Role in cancer and infections. Immunobiology *223*, 432-442.
Tamarozzi, F., Halliday, A., Gentil, K., Hoerauf, A., Pearlman, E., and Taylor, M.J. (2011). Onchocerciasis: the role of Wolbachia bacterial endosymbionts in parasite biology, disease pathogenesis, and treatment. Clinical microbiology reviews *24*, 459-468.
Taylor, M.D., Harris, A., Nair, M.G., Maizels, R.M., and Allen, J.E. (2006). F4/80(+) alternatively activated macrophages control CD4(+) T cell hyporesponsiveness at sites peripheral to filarial infection. Journal of Immunology *176*, 6918-6927.
Taylor, M.D., LeGoff, L., Harris, A., Malone, E., Allen, J.E., and Maizels, R.M. (2005). Removal of regulatory T cell activity reverses hyporesponsiveness and leads to filarial parasite clearance in vivo. Journal of Immunology *174*, 4924-4933.
Taylor, M.D., van der Werf, N., Harris, A., Graham, A.L., Bain, O., Allen, J.E., and Maizels, R.M. (2009). Early recruitment of natural CD4+ Foxp3+ Treg cells by infective larvae determines the outcome of filarial infection. Eur J Immunol *39*, 192-206.
Taylor, M.J., Cross, H.F., and Bilo, K. (2000). Inflammatory responses induced by the filarial nematode Brugia malayi are mediated by lipopolysaccharide-like activity from endosymbiotic Wolbachia bacteria. J Exp Med *191*, 1429-1435.
Taylor, M.J., Cross, H.F., Mohammed, A.A., Trees, A.J., and Bianco, A.E. (1996). Susceptibility of Brugia malayi and Onchocerca lienalis microfilariae to nitric oxide and hydrogen peroxide in cell-free culture and from IFN gamma-activated macrophages. Parasitology *112*, 315-322.

Taylor, M.J., Hoerauf, A., and Bockarie, M. (2010). Lymphatic filariasis and onchocerciasis. Lancet *376*, 1175-1185.
Tendongfor, N., Wanji, S., Ngwa, J.C., Esum, M.E., Specht, S., Enyong, P., Matthaei, K.I., and Hoerauf, A. (2012). The human parasite Loa loa in cytokine and cytokine receptor gene knock out BALB/c mice: survival, development and localization. Parasites & vectors *5*.
Torrero, M.N., Hübner, M.P., Larson, D., Karasuyama, H., and Mitre, E. (2010). Basophils amplify type 2 immune responses, but do not serve a protective role, during chronic infection of mice with the filarial nematode Litomosoides sigmodontis. J Immunol *185*, 7426-7434.
Trellakis, S., Bruderek, K., Hutte, J., Elian, M., Hoffmann, T.K., Lang, S., and Brandau, S. (2013). Granulocytic myeloid-derived suppressor cells are cryosensitive and their frequency does not correlate with serum concentrations of colony-stimulating factors in head and neck cancer. Innate Immunology *19*, 328-336.
Tu, S., Bhagat, G., Cui, G., Takaishi, S., Kurt-Jones, E.A., Rickman, B., Betz, K.S., Penz-Oesterreicher, M., Bjorkdahl, O., Fox, J.G., and Wang, T.C. (2008). Overexpression of interleukin-1beta induces gastric inflammation and cancer and mobilizes myeloid-derived suppressor cells in mice. Cancer cell *14*, 408-419.
Turner, P., Copeman, B., Gerisi, D., and Speare, R. (1993). A Comparison of the Og4c3 Antigen Capture Elisa, the Knott Test, an Igg4 Assay and Clinical Signs, in the Diagnosis of Bancroftian Filariasis. Trop Med Parasitol *44*, 45-48.
Valanparambil, R.M., Tam, M., Jardim, A., Geary, T.G., and Stevenson, M.M. (2017). Primary Heligmosomoides polygyrus bakeri infection induces myeloid-derived suppressor cells that suppress CD4(+) Th2 responses and promote chronic infection. Mucosal Immunology *10*, 238-249.
Voisin, M.-B., Buzoni-Gatel, D., Bout, D., and Velge-Roussel, F. (2004). Both expansion of regulatory Gr1+CD11b+ myeloid cells and anergy of T lymphocytes participate in hyporesponsiveness of the lung-associated immune system during acute toxoplasmosis. Infection and Immunology *72*, 5487-5492.
Volkmann, L., Bain, O., Saeftel, M., Specht, S., Fischer, K., Brombacher, F., Matthaei, K.I., and Hoerauf, A. (2003). Murine filariasis: interleukin 4 and interleukin 5 lead to containment of different worm developmental stages. Med Microbiol Immun *192*, 23-31.
Volkmann, L., Saeftel, M., Bain, O., Fischer, K., Fleischer, B., and Hoerauf, A. (2001). Interleukin-4 is essential for the control of microfilariae in murine infection with the filaria Litomosoides sigmodontis. Infect Immun *69*, 2950-2956.
Vollbrecht, T., Stirner, R., Tufman, A., Roider, J., Huber, R.M., Bogner, J.R., Lechner, A., Bourquin, C., and Draenert, R. (2012). Chronic progressive HIV-1 infection is associated with elevated levels of myeloid-derived suppressor cells. Aids *26*, F31-F37.
Vonk, A.G., Netea, M.G., van Krieken, J.H., Iwakura, Y., van der Meer, J.W., and Kullberg, B.J. (2006). Endogenous interleukin (IL)-1 alpha and IL-1 beta are crucial for host defense against disseminated candidiasis. J Infect Dis *193*, 1419-1426.
Wabo Pone, J., Bilong Bilong, C.F., and Mpoame, M. (2010). In vitro nematicidal activity of extracts of Canthium mannii (Rubiaceae), on different life-cycle stages of Heligmosomoides polygyrus (Nematoda, Heligmosomatidae). Journal of helminthology *84*, 156-165.
Wagner, M., Peterson, C.G.B., Ridefelt, P., Sangfelt, P., and Carlson, M. (2008). Fecal markers of inflammation used as surrogate markers for treatment outcome in relapsing inflammatory bowel disease. World J Gastroentero *14*, 5584-5589.
Wang, L., Chang, E.W.Y., Wong, S.C., Ong, S.M., Chong, D.Q.Y., and Ling, K.L. (2013). Increased Myeloid-Derived Suppressor Cells in Gastric Cancer Correlate with Cancer Stage and Plasma S100A8/A9 Proinflammatory Proteins. Journal of Immunology *190*, 794-804.
Wang, W., Jiao, Z., Duan, T., Liu, M., Zhu, B., Zhang, Y., Xu, Q., Wang, R., Xiong, Y., Xu, H., and Lu, L. (2015). Functional characterization of myeloid-derived suppressor cell subpopulations during the development of experimental arthritis. Eur J Immunol *45*, 464-473.

Wanji, S., Amvongo-Adjia, N., Koudou, B., Njouendou, A.J., Ndongmo, P.W.C., Kengne-Ouafo, J.A., Datchoua-Poutcheu, F.R., Fovennso, B.A., Tayong, D.B., Fombad, F.F., *et al.* (2015). Cross-Reactivity of Filariais ICT Cards in Areas of Contrasting Endemicity of Loa loa and Mansonella perstans in Cameroon: Implications for Shrinking of the Lymphatic Filariasis Map in the Central African Region. Plos Neglect Trop D *9*.

Wanji, S., Amvongo-Adjia, N., Njouendou, A.J., Kengne-Ouafo, J.A., Ndongmo, W.P.C., Fombad, F.F., Koudou, B., Enyong, P.A., and Bockarie, M. (2016). Further evidence of the cross-reactivity of the Binax NOW (R) Filariasis ICT cards to non-Wuchereria bancrofti filariae: experimental studies with Loa loa and Onchocerca ochengi. Parasites & vectors *9*.

Webber, R.H. (1979). Eradication of Wuchereria-Bancrofti Infection through Vector Control. Transactions of the Royal Society of Tropical Medicine and Hygiene *73*, 722-724.

WHO (2015). Weekly epidemiological record. *90*, 489–504.

Wu, L., Yan, C., Czader, M., Foreman, O., Blum, J.S., Kapur, R., and Du, H. (2012). Inhibition of PPAR gamma in myeloid-lineage cells induces systemic inflammation, immunosuppression, and tumorigenesis. Blood *119*, 115-126.

Xu, X., Meng, Q., Erben, U., Wang, P., Glauben, R., Kuhl, A.A., Wu, H., Ma, C.W., Hu, M., Wang, Y., *et al.* (2016). Myeloid-derived suppressor cells promote B-cell production of IgA in a TNFR2-dependent manner. Cell Mol Immunol.

Yang Q, Li X, Chen H, Cao Y, Xiao Q, He Y, Wei J, and J, Z. (2017). IRF7 regulates the development of granulocytic myeloid-derived suppressor cells through S100A9 transrepression in cancer. Oncogene, 1-12.

Yazdi, A.S., and Drexler, S.K. (2013). Regulation of interleukin 1alpha secretion by inflammasomes. Annals of the rheumatic diseases *72 Suppl 2*, ii96-99.

Yazdi, A.S., Guarda, G., Riteau, N., Drexler, S.K., Tardivel, A., Couillin, I., and Tschopp, J. (2010). Nanoparticles activate the NLR pyrin domain containing 3 (Nlrp3) inflammasome and cause pulmonary inflammation through release of IL-1 alpha and IL-1 beta. Proceedings of the National Academy of Sciences of the United States of America *107*, 19449-19454.

Youn, J.I., Kumar, V., Collazo, M., Nefedova, Y., Condamine, T., Cheng, P.Y., Villagra, A., Antonia, S., McCaffrey, J.C., Fishman, M., *et al.* (2013). Epigenetic silencing of retinoblastoma gene regulates pathologic differentiation of myeloid cells in cancer. Nat Immunol *14*, 211-220.

Youn, J.I., Nagaraj, S., Collazo, M., and Gabrilovich, D.I. (2008). Subsets of myeloid-derived suppressor cells in tumor-bearing mice. Journal of Immunology *181*, 5791-5802.

Young, M.R., Petruzzelli, G.J., Kolesiak, K., Achille, N., Lathers, D.M., and Gabrilovich, D.I. (2001). Human squamous cell carcinomas of the head and neck chemoattract immune suppressive CD34(+) progenitor cells. Hum Immunol *62*, 332-341.

Young, M.R., Wright, M.A., Lozano, Y., Prechel, M.M., Benefield, J., Leonetti, J.P., Collins, S.L., and Petruzzelli, G.J. (1997). Increased recurrence and metastasis in patients whose primary head and neck squamous cell carcinomas secreted granulocyte-macrophage colony-stimulating factor and contained CD34+ natural suppressor cells. Int J Cancer *74*, 69-74.

Zhang, Y.L., Luan, B., Wang, X.F., Qiao, J.Y., Song, L., Lei, R.R., Gao, W.X., and Liu, Y. (2013). Peripheral Blood MDSCs, IL-10 and IL-12 in Children with Asthma and Their Importance in Asthma Development. PloS one *8*.

Zhao, F., Hoechst, B., Duffy, A., Gamrekelashvili, J., Fioravanti, S., Manns, M.P., Greten, T.F., and Korangy, F. (2012). S100A9 a new marker for monocytic human myeloid-derived suppressor cells. Immunology *136*, 176-183.

Zhu, K., Zhang, N., Guo, N., Yang, J., Wang, J., Yang, C., Yang, C., Zhu, L., Xu, C., Deng, Q., *et al.* (2014). SSC(high)CD11b(high)Ly-6C(high)Ly-6G(low) myeloid cells curtail CD4 T cell response by inducible nitric oxide synthase in murine hepatitis. The international journal of biochemistry & cell biology *54*, 89-97.

Ziewer, S., Hubner, M.P., Dubben, B., Hoffmann, W.H., Bain, O., Martin, C., Hoerauf, A., and Specht, S. (2012). Immunization with L. sigmodontis Microfilariae Reduces Peripheral Microfilaraemia after Challenge Infection by Inhibition of Filarial Embryogenesis. Plos Neglect Trop D *6*.

6. APPENDIX

APPENDIX A: EQUIPMENTS

Equipments	Compagny and location
5 ml Polystyrene Round Bottom Tube	Falcon
Automatic pipettes (10-1000µl)	Eppendorf AG, Hamburg, Germany
BD FACS Diva flow cytometer	BD Biosciences, Heidelberg, Germany
BD FACSAria III Cell Sorter	BD Biosciences, Heidelberg, Germany
BD FACSCanto™ I flow cytometer	BD Biosciences, Heidelberg, Germany
Bench (for PCR pipetting)	Peqlab, Erlangen, Germany
Bench (human lab)	HeraSafe
Cell scraper	Sartedt, Inc., Newton, USA
Cellstar 96-Well Cell Culture Plate, sterile, U-bottom, with lid	Greiner bio-one, Frickenhausen, Germany
Cellstar serological pipette, 5mL, 10mL	Greiner bio-one, Frickenhausen, Germany
Centrifuge (Eppendorf 5417 R) for RNA extraction	Eppendorf AG, Hamburg, Germany
Centrifuge (Multifuge 4KR)	Heraeus Holding GmbH, Hanau, Germany
ELISA plate	greiner bio-one, Frickenhausen, Germany
ELISA Plate reader (Spectra Max 340pc384	Molecular Devices, Sunnyvale, USA
Experion	BioRad, Hercules, USA
Falcon serological pipette, 15 mL	Becton Dickinson Labware, Franklin Lakes, NJ. USA
Falcon serological pipette, 50 mL	Becton Dickinson Labware, Franklin Lakes, NJ. USA
Filter (Whatman Nucleopore, 5 µm)	Carl Roth, Karlsruhe, Germany
Freezer (-20°C)	Bosch GmbH, Stuttgart, Germany
Freezer (-80°C)	Heraeus Holding GmbH, Hanau, Germany
Fridge	Bosch GmbH, Stuttgart, Germany
Glass mortar	VWR, Langenfeld, Germany
Glass Pasteur Pipette	Brand GmbH + CO, Wertheim, Germany

Glass pipettes (1-20 ml)	Brand GmbH & Co KG, Wertheim, Germany
Glass plates (1.5 mm)	Bio-Rad, Munich, Germany
Glassware	Schott AG, Mainz, Germany
Gloves	Meditrade GmbH, Kiefersfelden, Germany
Heating Block (Thermomixer comfort)	Eppendorf AG, Hamburg, Germany
HTS Transwell 96 Permeable Support	Corning GmbH Life Sciences, Wiesbaden, Germany
Ice machine (Scotsman AF 80)	Gastro Handel GmbH, Wien, Austria
iCycler	Bio-rad, Munich, Germany
Incubator	Binder GmbH, Tuttlingen, Germany
MACS multistand separator	Miltenyi BiotecGmbH, Bergisch Gladbach, Germany
MACS columns (MS) Germany	Miltenyi Biotech GmbH, Bergisch Gladbach
MACS separator Germany	Miltenyi Biotech GmbH, Bergisch Gladbach, Germany
Microscope (Leica DM IL)	Leica Microsystems GmbH, Wetzlar, Germany
Multichannel pipette (300 µl)	Biohit, Göttingen, Germany
NanoVue	GE Lifescience, Chalfont St Giles, Great Britain
Needles (BD Microlance™, 21G)	BD™ Biosciences, Heidelberg, Germany
Neubauer counting chamber	LO Laboroptik GmbH, Bad Homburg, Germany
Petri dish	VWR, Langenfeld, Germany
PH meter	Mettler Toledo GmbH, Giessen, Germany
Pipetboy (pipetus®-akku)	Hirschmann Laborgeräte, Eberstadt, Germany
Power supply	Bio-Rad, Munich, Germany
Qiagility	Qiagen, Hilden, Germany
Rotor-Gene Q	Qiagen, Hilden, Germany
Round-Bottom Tubes (5mL)	Becton Dickinson Labware, Franklin Lakes, NJ. USA
Sandwich-ELISA: 96well flat bottom	Maxisorp
Syringes (5 ml, 10 ml)	BD™ Biosciences, Heidelberg, Germany
Thermo magnetic stirrer	IKA® GmbH & Co.KG, Staufen, Germany
Thermocycler	Biometra GmbH, Göttingen, Germany

Vortex mixer (Minishaker)	IKA® GmbH & Co.KG, Staufen, Germany
Water bath	VWR, Langenfeld, Germany
Water purifier Milli-Q plus	Millipore, Schwalbach, Germany
Weighing machine	Sartorius AG, Göttingen, Germany

APPENDIX B: SOFTWARE

Software	**Compagny and location**
BD FACS Diva	BD Biosciences, Heidelberg, Germany
FlowJo VX	Tree Star, Inc, Ashland, Oregon, USA
GraphPad PRISM 5.02	GraphPad Software, Inc., La Jolla, USA
Microsoft	Redmond, Washington, USA
RT2 profiler PCR Array data analysis 3.5	Qiagen, Hilden, Germany
SoftMax Pro 5.0	Molecular Devices, Sunnyvale, USA

APPENDIX C: CHEMICALS AND REAGENTS

Chemicals and reagents	**Compagny and location**
1-Bromo-3-chloropropane (BCP)	Sigma-Aldrich GmbH, Munich, Germany
Advanced RPMI 1640 (1x)	Life Technologies Corporation, Grand Island, NY, USA
autoMACS running buffer	Miltenyi Biotec GmbH, Bergisch Gladbach, Germany
BSA	PAA Laboratories GmbH, Pasching, Austria
Dimethyl sulfoxide (DMSO)	Sigma-Aldrich, Steinheim, Germany
DNA-free Dulbecco's PBS	Life Technologies Corporation, Grand Island, NY, USA
eBioscience coktail (plus inhibitor)	Thermo Fisher Scientific, Inc., Waltham, MA, USA
ELISA kits (IL-5, IL-6, IL-10, IL-13, IL-17, IFN-	R&D, Wiesbaden-Nordenstadt, Germany

alpha, TNF)	
ELISA kits Ready-SET-Go (IL-6, IL-10, IFN-alpha, TNF)	Thermo Fisher Scientific, Inc., Waltham, MA, USA
Ethanol	Merck KGAA, Darmstadt, Germany
Experion kit	BioRad, Hercules, USA
Fetal Calf Serum, Standard Quality	PAA Laboratories GmbH, Pasching, Austria
Fixation/Permeabilization Concentrate	ebioscience, San Diego, USA
Gentamycin (50 mg mL-1)	PAA Laboratories GmbH, Pasching, Austria
Griess Reagent Kit for Nitrite Determination (G-7921)	Molecular Probes, Inc, Eugene Oregon, USA
Hydrogen peroxide (H_2O_2)	Sigma-Aldrich GmbH, Munich, Germany
Isofluran	Prima Healthcare, Northumberland, UK
Isopropanol	Merck KGAA, Darmstadt, Germany
L-Glutamine 200 mM (100x)	Life Technologies Corporation, Grand Island, NY, USA
L-NMMA	Abcam, Cambridge, UK
LPS	Sigma-Aldrich GmbH, Munich, Germany
miRNeasy Kit	Qiagen, Hilden, Germany
Monosodium phosphate	Merck KGAA, Darmstadt, Germany
Paraformaldehyde	Merck KGAA, Darmstadt, Germany
Penicillin Streptomycin	Life Technologies Corporation, Grand Island, NY, USA
Permeabilization Buffer (10x)	Ebioscience, San Diego, USA
Stop solution 2N H_2SO_4	Merck KGAA, Darmstadt, Germany
Streptavidin-Peroxidase	Roche Diagnostics GmbH, Mannheim, Germany
TMB	Sigma-Aldrich GmbH, Munich, Germany
Trizol	Invitrogen GmbH, Darmstadt, Germany
Trypan blue 2 % in PBS	Sigma-Aldrich GmbH, Munich, Germany
Tween 20	Sigma-Aldrich GmbH, Munich, Germany

APPENDIX D: BUFFERS AND SOLUTIONS

eBioscience ELISA

Coating Buffer: dilute 10x coating buffer with DI water to 1x

Capture Ab: 1:250, for 1 plate 20 µl of Ab solution to 5 ml coating buffer

Wash buffer: 1x PBS, 0.05 % Tween 20

Blocking buffer (1x Assay diluent): add 10 ml of 5x Assay diluent to 40 ml of DI water

Detection Ab: 1:250, for 1 plate add 20 µl of Ab solution to 5 ml of assay diluent

Enzyme: Avidin-HRP: 1:250, for 1 plate add 20 µl of enzyme solution to 5 ml of assay diluent

Substrate: 1x TMB solution (provided)

Stop Solution: 2N H_2SO_4 (½ Liter: 26.6 ml H_2SO_4 +473 ml DI water)

R&D Duo Set ELISA

Washing buffer: 1 M PBS + 0.05 % Tween 20 pH 7.0-7.3

Blocking buffer: 1x PBS / 1 % BSA

Solution 4: 0.1 M NaH_2PO_4 in DI water, pH 5.5

TMB: 60 mg 3,3`,5,5`Tetramethylenbenzidine in 10 ml DMSO

Developer: 10 ml Solution 4 + 200 µl TMB + 2 µl H_2O_2

Stopping reagent: 2 M H_2SO_4 (½ Liter: 26.6ml H_2SO_4 +473 ml DI water)

BD ELISA

Coating buffer: 0.1 M Na_2HPO_4 in DI water, pH 9.0

Washing buffer: 1 M PBS + 0.05 % Tween 20 pH 7.0-7.3

Blocking buffer: 1x PBS / 1 % BSA

Solution 4: 0.1 M NAH2PO4 in DI water, pH 5.5

TMB: 60 mg 3,3`,5,5`Tetramethylenbenzidine in 10 ml DMSO

Developer: 10 ml Solution 4 + 200 µl TMB + 2 µl H_2O_2

Stopping reagent: 2 M H_2SO_4 (½ Liter: 26.6 ml H_2SO_4 +473 ml DI water)

Cell culture medium

500ml RPMI 1640 medium

5ml Penicillin (100µg/ml)/Streptomycin (100µg/ml)

0.5 ml Gentamycin (50µg/ml)

5ml L-glutamine (292.3µg/ml)

10% FCS

FACS Buffer

1xPBS with 2 % FCS

PFA 4% solution (FACS)

40g of PFA dissolved while heating (max 60°C) in 900ml 1x PBS. The solubility was increased by adding NaOH dropwise, top to 1 liter with 1x PBS. The Solution was then cooled and filtered and adjusted pH to 6.9 using dilute HCl.

Permeabilization Buffer

1:10 dilution with DI water

Hinkelmann solution

0.5% [wt/vol] eosin Y, 0.5% [wt/vol] phenol (both Merck) and 0.185% [vol/vol] formaldehyde (Sigma-Aldrich) in DI water.

APPENDIX E: GENE TABLE FOR PCR ARRAY

Number of sorted cells from TC for PCR array

Sorted cells	**Ly6C$^+$**	**Ly6G$^+$**
Naive	76,000	15,000
Naive_a	107,000	7,000
Naive_b	191,000	2,000
Group 1	1,200,000	7,100,000
Group 2	1,100,000	4,400,000
Group 3	1,400,000	7,600,000

Position	**Symbol**	**Description**	**Gene name**
A01	Apcs	Serum amyloid P-component	Sap
A02	C3	Complement component 3	AI255234/ASP/HSE-MSF/Plp
A03	C5ar1	Complement component 5a receptor 1	C5aR/C5r1/Cd88/D7Msu1
A04	Casp1	Caspase 1	ICE/Il1bc
A05	Ccl12	Chemokine (C-C motif) ligand 12	MCP-5/Scya12

A06	Ccl5	Chemokine (C-C motif) ligand 5	MuRantes/RANTES/SISd/Scya5/TCP228
A07	Ccr4	Chemokine (C-C motif) receptor 4	C-C CKR-4/CHEMR1/Cmkbr4/LESTR/Sdf1r
A08	Ccr5	Chemokine (C-C motif) receptor 5	AM4-7/CD195/Cmkbr5
A09	Ccr6	Chemokine (C-C motif) receptor 6	CC-CKR-6/CCR-6/Cmkbr6/KY411
A10	Ccr8	Chemokine (C-C motif) receptor 8	C-C/C-C CKR-8/CC-CKR-8/CCR-8/CKR-8/Cmkbr8/mCCR8
A11	Cd14	CD14 antigen	-
A12	Cd4	CD4 antigen	L3T4/Ly-4
B01	Cd40	CD40 antigen	AI326936/Bp50/GP39/HIGM1/IGM/IMD3/T-BAM/TRAP/Tnfrsf5/p50
B02	Cd40lg	CD40 ligand	CD154/CD40-L/Cd40l/HIGM1/IGM/IMD3/Ly-62/Ly62/T-BAM/TRAP/Tnfsf5/gp39
B03	Cd80	CD80 antigen	B71/Cd28l/Ly-53/Ly53/MIC17/TSA1
B04	Cd86	CD86 antigen	B7/B7-2/B7.2/B70/CLS1/Cd28l2/ETC-1/Ly-58/Ly58/MB7/MB7-2/TS/A-2
B05	Cd8a	CD8 antigen, alpha chain	BB154331/Ly-2/Ly-35/Ly-B/Lyt-2
B06	Crp	C-reactive protein, pentraxin-related	AI255847
B07	Csf2	Colony stimulating factor 2 (granulocyte-macrophage)	Csfgm/GMCSF/Gm-CSf/MGI-IGM

B08	Cxcl10	Chemokine (C-X-C motif) ligand 10	C7/CRG-2/INP10/IP-10/IP10/Ifi10/Scyb10/gIP-10/mob-1
B09	Cxcr3	Chemokine (C-X-C motif) receptor 3	Cd183/Cmkar3
B10	Ddx58	DEAD (Asp-Glu-Ala-Asp) box polypeptide 58	6430573D20Rik/C330021E21/RIG-I/RLR-1
B11	Fasl	Fas ligand (TNF superfamily, member 6)	APT1LG1/CD178/CD95-L/CD95L/Fas-L/Faslg/Tnfsf6/gld
B12	Foxp3	Forkhead box P3	JM2/scurfin/sf
C01	Gata3	GATA binding protein 3	Gata-3/jal
C02	H2-Q10	Histocompatibility 2, Q region locus 10	H-2Q10/Q10/Qa10
C03	H2-T23	Histocompatibility 2, T region locus 23	37b/37c/H-2T23/H2-Qa1/Qa-1/Qa-1(b)/Qa1/Qed-1/T18c/T18c(37)/T23b/T23d
C04	Icam1	Intercellular adhesion molecule 1	CD54/Icam-1/Ly-47/MALA-2
C05	Ifna2	Interferon alpha 2	Ifa2
C06	Ifnar1	Interferon (alpha and beta) receptor 1	CD118/Ifar/Ifnar/Ifrc/Infar
C07	Ifnb1	Interferon beta 1, fibroblast	IFN-beta/IFNB/Ifb
C08	Ifng	Interferon gamma	IFN-g/Ifg

C09	Ifngr1	Interferon gamma receptor 1	CD119/IFN-gammaR/Ifgr/Ifngr/Nktar
C10	Il10	Interleukin 10	CSIF/Il-10
C11	Il13	Interleukin 13	Il-13
C12	Il17a	Interleukin 17A	Ctla-8/Ctla8/IL-17/IL-17A/Il17
D01	Il18	Interleukin 18	Igif/Il-18
D02	Il1a	Interleukin 1 alpha	Il-1a
D03	Il1b	Interleukin 1 beta	IL-1beta/Il-1b
D04	Il1r1	Interleukin 1 receptor, type I	CD121a/CD121b/IL-1R1/IL-iR/Il1r-1
D05	Il2	Interleukin 2	Il-2
D06	Il23a	Interleukin 23, alpha subunit p19	IL-23/p19
D07	Il4	Interleukin 4	BSF-1/Il-4
D08	Il5	Interleukin 5	Il-5
D09	Il6	Interleukin 6	Il-6
D10	Irak1	Interleukin-1 receptor-associated kinase 1	AA408924/IRAK/IRAK-1/IRAK1-S/IRAK1b/Il1rak/Plpk/mPLK
D11	Irf3	Interferon regulatory factor 3	C920001K05Rik/IRF-3
D12	Irf7	Interferon regulatory factor 7	-
E01	Itgam	Integrin alpha M	CD11b/CD18/CR3/CR3A/Cd11b/F730045J24Rik/Ly-40/MAC1/Mac-1/Mac-1a
E02	Jak2	Janus kinase 2	Fd17
E03	Ly96	Lymphocyte antigen 96	ESOP-1/MD-2/MD2

E04	Lyz2	Lysozyme 2	AI326280/Lys/Lysm/Lyzs/Lzm/Lzm-s1/Lzp
E05	Mapk1	Mitogen-activated protein kinase 1	9030612K14Rik/AA407128/AU018647/C78273/ERK/Erk2/MAPK2/PRKM2/Prkm1/p41mapk/p42mapk
E06	Mapk8	Mitogen-activated protein kinase 8	AI849689/JNK/JNK1/Prkm8/SAPK1
E07	Mbl2	Mannose-binding lectin (protein C) 2	L-MBP/MBL/MBL-C/MBP-C
E08	Mpo	Myeloperoxidase	mKIAA4033
E09	Mx1	Myxovirus (influenza virus) resistance 1	AI893580/Mx/Mx-1
E10	Myd88	Myeloid differentiation primary response gene 88	-
E11	Nfkb1	Nuclear factor of kappa light polypeptide gene enhancer in B-cells 1, p105	NF-KB1/NF-kappaB/NF-kappaB1/p105/p50/p50/p105
E12	Nfkbia	Nuclear factor of kappa light polypeptide gene enhancer in B-cells inhibitor, alpha	AI462015/Nfkbi
F01	Nlrp3	NLR family, pyrin domain containing 3	AGTAVPRL/AII/AVP/Cias1/FCAS/FCU/MWS/Mmig1/NALP3/Pypaf1
F02	Nod1	Nucleotide-binding	C230079P11/Card4/F830007N14Rik/Nlrc1

		oligomerization domain containing 1	
F03	Nod2	Nucleotide-binding oligomerization domain containing 2	ACUG/BLAU/CD/Card15/F830032C23Rik/IBD1/Nlrc2
F04	Rag1	Recombination activating gene 1	Rag-1
F05	Rorc	RAR-related orphan receptor gamma	Nr1f3/RORgamma/TOR/Thor
F06	Slc11a1	Solute carrier family 11 (proton-coupled divalent metal ion transporters), member 1	Bcg/Ity/Lsh/Nramp/Nramp1/ity
F07	Stat1	Signal transducer and activator of transcription 1	2010005J02Rik/AA408197
F08	Stat3	Signal transducer and activator of transcription 3	1110034C02Rik/AW109958/Aprf
F09	Stat4	Signal transducer and activator of transcription 4	-
F10	Stat6	Signal transducer and activator of transcription 6	-

F11	Tbx21	T-box 21	TBT1/Tbet/Tblym
F12	Ticam1	Toll-like receptor adaptor molecule 1	AW046014/AW547018/TICAM-1/TRIF
G01	Tlr1	Toll-like receptor 1	-
G02	Tlr2	Toll-like receptor 2	Ly105
G03	Tlr3	Toll-like receptor 3	AI957183
G04	Tlr4	Toll-like receptor 4	Lps/Ly87/Ran/M1/Rasl2-8
G05	Tlr5	Toll-like receptor 5	-
G06	Tlr6	Toll-like receptor 6	-
G07	Tlr7	Toll-like receptor 7	-
G08	Tlr8	Toll-like receptor 8	-
G09	Tlr9	Toll-like receptor 9	-
G10	Tnf	Tumor necrosis factor	DIF/TNF-a/TNF-alpha/TNFSF2/TNFalpha/Tnfa/Tnfsf1a
G11	Traf6	Tnf receptor-associated factor 6	2310003F17Rik/AI851288/C630032O20Rik
G12	Tyk2	Tyrosine kinase 2	JTK1
H01	Actb	Actin, beta	Actx/E430023M04Rik/beta-actin
H02	B2m	Beta-2 microglobulin	Ly-m11/beta2-m/beta2m
H03	Gapdh	Glyceraldehyde-3-phosphate dehydrogenase	Gapd
H04	Gusb	Glucuronidase, beta	AI747421/Gur/Gus/Gus-r/Gus-s/Gus-t/Gus-u/Gut/asd/g

H05	Hsp90ab1	Heat shock protein 90 alpha (cytosolic), class B member 1	90kDa/AL022974/C81438/Hsp84/Hsp84-1/Hsp90/Hspcb
H06	MGDC	Mouse Genomic DNA Contamination	MIGX1B
H07	RTC	Reverse Transcription Control	RTC
H08	RTC	Reverse Transcription Control	RTC
H09	RTC	Reverse Transcription Control	RTC
H10	PPC	Positive PCR Control	PPC
H11	PPC	Positive PCR Control	PPC
H12	PPC	Positive PCR Control	PPC

7. ERKLÄRUNG

Hiermit erkläre ich dass, ich die vorgelegte Dissertation eigenständig und ohne unerlaubte Hilfsmittel angefertigt habe. Die Dissertation wurde in der vorgelegten oder in ähnlicher Form noch bei keiner anderen Institution eingereicht.

Bonn, 15.05.2018

Ruth Shalom Emilie Tamadaho

Poster presentations

Date	Conferences/Schools
05-10.03.2017	13th Spring School on immunology, Ettal-Germany *Title*: Role of myeloid-derived suppressor cells (MDSCs) during *Litomosoides sigmodontis* infection
09-14.10.2016	8th Autumn School "Current concepts in immunology", Merseburg-Germany *Title*: Identification and functional responses of myeloid-derived suppressor cells (MDSCs) during *Litomosoides sigmodontis* infection *Updated results*
27-30.09.2016	46th Annual meeting of the german society for immunology, Hamburg-Germany *Title*: Identification and functional responses of myeloid-derived suppressor cells (MDSCs) during *Litomosoides sigmodontis* infection *Updated results*
03-04.11.2014	Cluster science days, Bonn-Germany *Title*: Identification and functional responses of myeloid-derived suppressor cells (MDSCs) during *Litomosoides sigmodontis* infection. *Initial results*

Acknowledgements

I acknowledge Prof. Dr. med. Achim Hörauf, director of the Institute for Medical Microbiology, Immunology and Parasitology (IMMIP), for giving me the opportunity to do and successfully complete my PhD in the institute and for his unconditional support.

I also address my gratitude to Prof. Dr. Irmgard Förster for accepting to supervise my thesis. My regards are extended to PD Dr. Gerhild van Echten-Deckert and Prof. Dr. Dorothea Bartels for being part of my committee board.

I am very grateful to Dr. Laura E. Layland for thoughtfully directing my thesis. She has been available since the beginning of my work and cared for my ideas and doing so, she has contributed to my scientific growth. Many thanks for the exchange of ideas, the time she invested in me and the extraordinary help.

Many thanks to the group leaders: Dr. Kenneth Pfarr, Dr. Tomabu Adjobimey, Dr. Beatrix Schumak and Dr. Marc Hübner for their advice and input into the success of this work and especially Dr. Hübner for providing us with the anti-TGF-β Ab.

I thank Prof.Dr. Matthias Mack (University of Regensburg) for providing us with the anti-mCCR2 Ab.

I thank Dr. Manuel Ritter for nicely supporting me, for the time he has invested in my project and for critically helping to correct my thesis and I also thank Dr. Kathrin Arndts for her contribution. I would like to extend my gratitude to the former and current members of AG Layland (Özlem Mutluer, Katharina Wiszniewsky, Anna Filz, Vanessa Krupp, Sandy Schulz, Marc Bläser, Melanie Becker, Nils Jelden and Judith Feid) for their technical assistance and the nice time we had together in the laboratory and at gatherings.

I acknowledge the current members of the IMMIP especially the members of AG Adjobimey, AG Hübner, AG Pfarr and AG Schumak, for their technical assistance and for being of great help.

A special thanks to Dr. Jesuthas Ajendra for helping me for the optimization of the Griess reaction and for his advice concerning the PCR array. I also thank Julia Schulz for the special help and attention during the whole process of the PCR array.

I thank the former members of the IMMIP institute including Dr. Gnatoulma Katawa, Dr. Fabien Prodjinotho, Dr. Alexander Kwarteng, Dr. Patrica Korir, Dr. Janina Küpper and Dr. Afiat Berbudi whose advice have been priceless.

I extend my gratitude to the Flow Cytometry Core Facility (FCCF) for helping with the FACS.

I address my warmest regards to my dear Dèhogbé Noulèkoun for his encouragement and moral support and to Michael Ethan Noulèkoun for the joy and hope he brings to my heart.

I acknowledge my family and friends for their loving support, affection and prayers.

I thank Dr. Judith Gbenoudon for supporting my application for the DAAD scholarship and for helping me during the registration process at the faculty at the University of Bonn.

I address my warm regards to the Deutscher Akademischer Austauschdienst (DAAD) and Bonfor for the financial support.

"Bless and affectionately praise the Lord, O my soul, and all that is within me, bless His holy name. Bless and affectionately praise the Lord, O my soul and do not forget any of His benefits" Ps 103: 1-2